Sofia Raquel Paulo Rebelo

Mestre em Biologia Evolutiva e do Desenvolvimento

Development of 3D *in vitro* models for prediction of hepatic metabolism and toxicity

Dissertação para obtenção do Grau de Doutor em Bioengenharia

Orientador: Paula M. Alves, PhD, ITQB-UNL
Co-orientador: Catarina Brito, PhD, ITQB-UNL

FACULDADE DE CIÊNCIAS E TECNOLOGIA
UNIVERSIDADE NOVA DE LISBOA

2015

Development of 3D *in vitro* models for prediction of hepatic metabolism and toxicity

Sofia Raquel Paulo Rebelo

Faculdade de Ciências e Tecnologia – Universidade Nova de Lisboa

ACKNOWLEDGMENTS

I would like to express my gratitude to all the people who have contributed directly or indirectly to this thesis.

To my supervisor Dr. Paula Alves for the opportunity to join the animal cell technology unit and for the scientific support, knowledge and experience shared with me throughout these years. Also for the challenges, which have prompted me to go further, and the example of commitment to the group, that builds an environment of excellence.

To my co-supervisor Dr. Catarina Brito for engaging in this journey with me and for the support through it. Thanks for promoting my independence and broadening my scientific perspectives, which made me grow as a scientist. Also, for supporting the 3D team, understanding our needs and potentiating our skills.

To Professor Manuel Carrondo for truly being an entrepreneur and creating iBET, for the inspiring attitude and good advices concerning science and beyond.

To Dr. Paulo Marcelino and Dr. Sílvia Silva from Hospital Curry Cabral and Dr. Henrique Alexandrino and Prof. José Tralhão from Hospitais Universitários de Coimbra for making the work with human hepatocytes possible. Also, for the effort of bridging the gap between clinics and research, despite all the difficulties.

To Dr. Valery Shevchenko, Dr. Ruoya Li and Dr. Christophe Chesné from Biopredic for providing tools to perform some of the work developed in this thesis and for sharing knowledge.

To the MIT-Portugal program for a year of intense learning and experiences, which stimulated my interest in engineering. Thanks to my professors and colleagues.

To the financial support provided by Fundação para a Ciência e Tecnologia (SFRH/BD/70264/ 2010 and PTDC/EBB-BIO/112786/2009).

To my animal cell technology unit colleagues, from whom I learned from different fields and for the help provided; in particular to Marcos Sousa for the support with bioprocess operations.

To Rita Costa for sharing with me the hurdles and joys of working with human hepatocytes.

To the 3D team, Marta E., Catarina P., Daniel, Marta S. Ana Paula, Rita, Francisca A. and Vítor for truly being a team. For the discussions and critical suggestions, ideas and excitement shared and also for being supportive and making my daily life in the lab happier. You are much more than coworkers!

To all the people who contributed to the great environment in (and outside) the lab, especially to João Vidigal, Mafalda, Tiago, Fabiana, João Sá, Ana Oliveira, Paulo and Francisca. Thanks for all the great moments!

Pessoalmente gostaria de agradecer,

Aos meus amigos Maria João, Emília, Mara, Neto por estarem sempre por perto.

Ao Miguel pela partilha, por me fazer rir e por estimular a minha criatividade.

À Jus e ao Jerónimo, pelo exemplo e pelo vosso papel na minha formação, que é muito maior do que imaginam.

À minha família, porque são a base de tudo. À minha mãe, cuja bondade e generosidade são inigualáveis, e ao meu pai por nos apoiarem. Às minhas irmãs Ana e Carla, irmão Pedro, aos meus cunhados Adérito, Eduardo e Paula e às minhas sobrinhas Catarina e Inês, que me enchem de alegria. Obrigada pela força e união, que fazem de mim quem sou hoje e me dão coragem para fazer tudo, sabendo que tenho apoio para o que precisar. Também pelo exemplo e pela confiança, que me dão vontade de ser melhor pessoa e profissional.

RESUMO

O uso de modelos celulares humanos para prever a função hepática em culturas *in vitro* permite compreender os mecanismos metabólicos de toxicidade e doença. A sua relevância biológica, benefícios económicos e fácil manipulação para múltiplos testes pode contribuir para aumentar a eficiência do desenvolvimento de novos fármacos na indústria farmacêutica.

A mimetização da função hepática em cultura é o maior desafio associado ao uso de modelos celulares hepáticos e requer a aplicação de estratégias de cultura avançadas, como cultura 3D, co-culturas e biomateriais. Contudo, estas etratégias estão muitas vezes associados a baixa robustez e baixa compatilidade com plataformas de ensaios celulares e com escalas maiores. Neste trabalho, foram usadas várias estratégias para desenvolver modelos celulares avançados baseados em esferóides de hepatócitos humanos e de células HepaRG, usando sistemas de cultura agitados.

No **capítulo 2**, o isolamento de hepatócitos humanos a partir de tecido proveniente de hepatectomias foi implementado e o método de perfusão do tecido foi optimizado, resultando num protocolo de isolamento compatível com cultura 3D, com melhoria da eficiência do isolamento e agregação de hepatócitos. No **capítulo 3**, os hepatócitos humanos foram co-cultivados com células estaminais mesenquimais e o fenótipo dos dois tipos celulares foi caracterizado, mostrando que as células estaminais mesenquimais adquirem um papel de suporte de função hepática, funcionando como estroma. Os hepatócitos têm maior viabilidade em co-cultura e mantêm as funções diferenciadas, com elevada actividade das enzimas de detoxificação. No **capítulo 4**, foi implementada uma estratégia para a diferenciação das células HepaRG baseada em cultura 3D e microencapsulação em alginato, resultando numa maior eficiência de diferenciação em hepatócitos, com elevada actividade das enzimas de detoxificação e aumento da actividade biossintética.

O trabalho desenvolvido nesta tese resultou em novas estratégias para a cultura de modelos hepáticos humanos em 3D que são reprodutíveis, escaláveis e compatíveis com métodos de caracterização, tendo estes permitido ganhar conhecimento do fenótipo dos modelos desenvolvidos. Os modelos celulares hepáticos de origem humana podem contribuir para aumentar a eficiência da fase pré-clinica de desenvolvimento de fármacos, estudar doenças hepáticas e para desenvolver terapias celulares para a falência hepática.

Palavras-chave: 3D, microencapsulação, co-cultura, bioreactor, HepaRG, hepatócitos humanos

ABSTRACT

The development of human cell models that recapitulate hepatic functionality allows the study of metabolic pathways involved in toxicity and disease. The increased biological relevance, cost-effectiveness and high-throughput of cell models can contribute to increase the efficiency of drug development in the pharmaceutical industry.

Recapitulation of liver functionality *in vitro* requires the development of advanced culture strategies to mimic *in vivo* complexity, such as 3D culture, co-cultures or biomaterials. However, complex 3D models are typically associated with poor robustness, limited scalability and compatibility with screening methods. In this work, several strategies were used to develop highly functional and reproducible spheroid-based *in vitro* models of human hepatocytes and HepaRG cells using stirred culture systems.

In **chapter 2**, the isolation of human hepatocytes from resected liver tissue was implemented and a liver tissue perfusion method was optimized towards the improvement of hepatocyte isolation and aggregation efficiency, resulting in an isolation protocol compatible with 3D culture. In **chapter 3**, human hepatocytes were co-cultivated with mesenchymal stem cells (MSC) and the phenotype of both cell types was characterized, showing that MSC acquire a supportive stromal function and hepatocytes retain differentiated hepatic functions, stability of drug metabolism enzymes and higher viability in co-cultures. In **chapter 4**, a 3D alginate microencapsulation strategy for the differentiation of HepaRG cells was evaluated and compared with the standard 2D DMSO-dependent differentiation, yielding higher differentiation efficiency, comparable levels of drug metabolism activity and significantly improved biosynthetic activity.

The work developed in this thesis provides novel strategies for 3D culture of human hepatic cell models, which are reproducible, scalable and compatible with screening platforms. The phenotypic and functional characterization of the *in vitro* systems performed contributes to the state of the art of human hepatic cell models and can be applied to the improvement of pre-clinical drug development efficiency of the process, model disease and ultimately, development of cell-based therapeutic strategies for liver failure.

Keywords: 3D, hepatic, microencapsulation, bioreactor, co-culture, HepaRG, human hepatocytes

TABLE OF CONTENTS

LIST OF FIGURES

LIST OF TABLES

LIST OF ABBREVIATIONS

Abbreviation	Full form
2D	Two-dimensional
3D	Three-dimensional
ALB	Albumin
ALF	Acute liver failure
APAP	Acetaminophen
BAL	Bioartificial liver
BLC	Biliary-like cells
BNF	β-Naphthoflavone
BRs	Bioreactors
CDFDA	5-(and-6)-carboxy-2'-7'-dichlorofluorescein diacetate
CK18	Cytokeratin 18
COL I	Collagen type I
CPS1	Carbamoyl phosphate synthase 1
CYP1A2	cytochrome P450 Family 1- Subfamily A- Polypeptide 2
CYP2C9	cytochrome P450 Family 2- Subfamily C- Polypeptide 9
CYP3A4	cytochrome P450 Family 3- Subfamily A- Polypeptide 4
CYP450	Cytochrome P450
DMSO	Dimethyl Sulfoxide
ECM	Extracellular Matrix
G6PC	Glucose-6-phosphatase
GAPDH	Glyceraldehyde 3- phosphate dehydrogenase
GS	Glutamine Synthase
GSTA1	Glutathione S- transferase A1
HH	Human hepatocytes
HLC	Hepatocyte-like cells
HNF3β	Hepatocyte nuclear factor 3 beta
HNF4α	Hepatocyte nuclear factor 4 alpha
HSC	Hepatic stellate cell
IL6	Interleukin 6
KC	Kupffer cell
LSECs	Liver sinusoidal endothelial cell
MRP2	Multidrug resistance protein 2
MSC	Mesenchymal stem cell
NPLC	Non parenchymal liver cells
PC	Pericentral
PFA	Paraformaldehyde
PP	Periportal
PSC	Pluripotent stem cells
PXR	Pregnane X receptor
qRT-PCR	Quantitative real time polymerase chain reaction
Rif	Rifampicin
UGT	Uridine 5'-diphospho-glucuronosyltransferase
VC	Vehicle control
VIM	Vimentin
ZO-1	Zonnula occludens protein 1

À minha família,

CHAPTER 1

Introduction

TABLE OF CONTENTS

1. Introduction

1.1 The need for human hepatic cell models

The liver is a central organ in body homeostasis, comprising functions related with nutrient level maintenance, protein, bile and hormone synthesis and an important role in xenobiotic metabolism and detoxification. Due to the plethora of liver functions and, particularly, to the hepatic drug clearance, modeling the liver *in vitro* has applications in multiple areas, ranging from drug development to clinical applications.

The stringent pipelines of drug development and high costs associated with drug failure during clinical trials drive the need for an efficient prediction of efficacy and safety in pre-clinical development. It is estimated that approximately only 10% of the development paths that enter clinical development in phase I advance to market approval (Hay et al., 2014), resulting in a high R&D expenditure per drug approved. Although the use of animal models is essential to assess toxicity at the systemic level, the interspecies variability in drug metabolic mechanisms, the ethical issues associated with animal testing and the low throughput that animal testing allows are accountable for the inefficiency observed. Thus, the use of human liver models to evaluate safety at the pre-clinical stage could contribute to reduce the attrition rates observed in the industry, by improving predictability and therefore reducing costs throughout the drug development process.

A relevant feature of hepatic *in vitro* models is the potential to mimic liver disease, allowing to depict cellular mechanisms in a more simplistic approach and higher relevance than alternative animal models. Disease modeling is not only important in the context of drug development, but also for basic and translational research, being particularly relevant for the study of liver damage (*e.g.* fibrosis, steatosis, cholestasis) caused by severe hepatic malignancies including drug induced liver injury (DILI), alcoholic liver disease, hepatitis B (HBV) and C (HCV), which may ultimately lead to acute liver failure (ALF).

Liver disease represents a heavy burden for the healthcare system, affecting over 600 million people worldwide and causing over 1 million deaths per year, either due to acute or chronic liver disease (Gonzalez and Keeffe, 2011). The only treatment currently available is orthotypic transplantation, which is severely limited by the number of available donors and adverse immune reactions. Cell-based therapies with hepatocytes or other cell types (Forbes et al., 2015), engineered tissue transplantation or the bio-artificial liver system, in which the biocomponent is provided extracellularly, are some of the methods aiming to extend survival and overcome the shortage of liver donors (Bañares et al., 2013). Despite the advances in the development of extracorporeal devices to support liver function and to engineer liver tissues for transplantation, these are still a promise up to date and new technologies still need to be developed.

1.2 *In vivo* liver microenvironment

The design of hepatic tissues ex-vivo requires the comprehension of the liver microenvironment to ultimately seek its recreation. The liver is organized in hepatic lobules, which consist of microunits of extensively vascularized and compact layers of hepatocytes arranged radially around the central vein towards the portal triad, which comprises the portal vein, hepatic artery and bile duct (Figure 1.1). The liver parenchyma is composed of hepatocytes, which account for 60% of the cellular components of the liver and 80% of its total volume (LeCluyse et al., 2012). The remaining non-parenchymal liver cells (NPLC) include the biliary epithelial cells or cholangiocytes, the liver sinusoidal endothelial cells (LSECs), hepatic stellate cells (HSC), kupffer cells (KC) and pit cells.

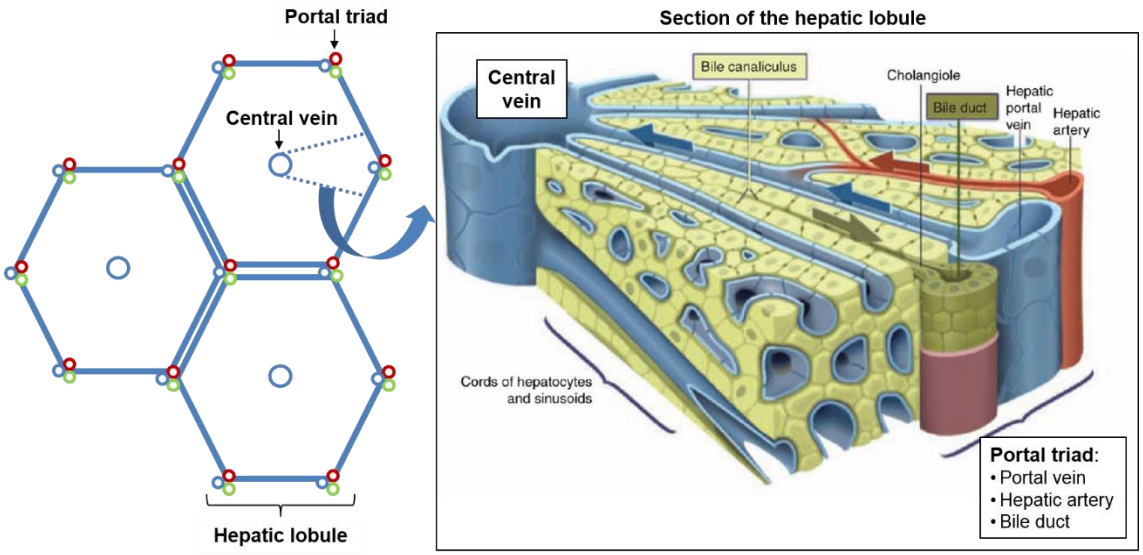

Figure 1.1 Schematic representation of the hexagonal-shaped liver lobules, with the central vein and portal triad. Amplification of the lobule segment, showing the stratified parenchyma and the countercurrent flows of the bile and blood circulation. Adapted from Treyer and Müsch (2013).

Hepatocytes perform most of the hepatic functions, constituting metabolic active cells which unique cytoarchitecture is closely linked to their specific functions. The hepatocytes cuboidal shape and disposition in plates along the liver lobule and the exposure to countercurrent flows – bile secretion to the canaliculi and sinusoidal blood circulation (Figure 1.1) – result in a unique polarization. Thus, hepatocytes have an apical pole, with tight junctions surrounding the bile canaliculi, and a basolateral domain, in contact the sinusoidal endothelium (Figure 1.2). The cellular organelles and protein trafficking routes are polarized and the membrane proteins, mainly transporters, are assembled either at the apical or basolateral membranes and their function depends on the polarized status of the cell (Treyer and Müsch, 2013). Furthermore, along the liver lobule there is a structural and functional zonation, according to the oxygen availability throughout the lobule generated by the distance to the central vein or hepatic artery (Figure 1.3). This zonation, first depicted by Jungermann et al (1982), describes the existence of periportal (PP) hepatocytes, which have oxidative metabolism and are responsible for gluconeogenesis, ureagenesis and cholesterol synthesis, and pericentral (PC) hepatocytes, which have glycolytic metabolism, synthesize the bile and perform most detoxification reactions (Jungermann and Kietzmann, 2000).

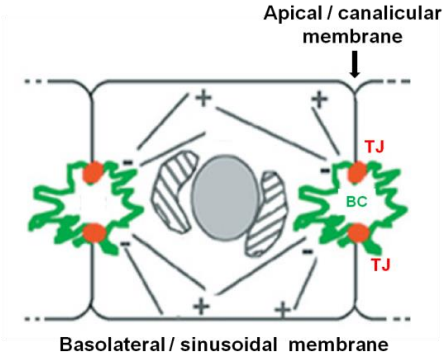

Figure 1.2 Schematic representation of hepatocyte polarity. The apical or canalicular membrane is separated from the basolateral or sinusoidal membrane by the tight junctions (red), which surround the bile canaliculi (green). The organelle polarization is represented by the golgi apparatus which is involved in vesicular transport and the minus-end of the microtubules facing the apical poles. Adapted from Decaens et al (2008).

Although previously not accounted to the hepatic functions, it is now widely accepted that the NPLC play an important role in supporting hepatocyte functionality and proliferation (Godoy et al., 2013). The cholangiocytes are epithelial cells which line the biliary ducts and are derived from the hepatoblasts, a common hepatocyte progenitor. They are involved in the bile secretion process, multiple liver diseases and have been implied in immunoregulation (Huang et al., 2006; Masyuk, Masyuk, & LaRusso, 2008). The LSECs are the fenestrated endothelial cells that compose the liver sinusoids. More than a barrier between blood and hepatocytes, LSECs actively participate in hepatic clearance, as the fenestrated endothelium acts as a selective barrier between the parenchyma and the circulatory system. LSECs can also act as scavengers due to the high receptor-mediated endocytic activity, clearing an array of physiological or foreign macromolecules from the blood (Braet & Wisse, 2002). Moreover, they are involved in inflammatory response and in the regeneration of hepatocytes after injury (DeLeve, 2013). Hepatic stellate cells (HSC) are perisinusoidal cells located between the endothelium and the liver parenchyma, in the space of Disse (Figure 1.3). These cells are responsible for the storage of vitamin A, control the production and homeostasis of extra-cellular matrix (ECM), regulate contractility of the sinusoids and secrete cytokines, thereby mediating the inflammatory response. Upon activation, HSC acquire a miofibroblastic phenotype, which impairs ECM regulation and ultimately leads to fibrosis (Puche et al., 2013). The Kupffer cells are the resident liver macrophages, with high endocytic and phagocytic activity and important mediators of the local and systemic inflammatory response through cytokine secretion (Dixon et al., 2013). The immune response is further mediated by the pit cells, which are intrahepatic leucocytes or natural killer cells.

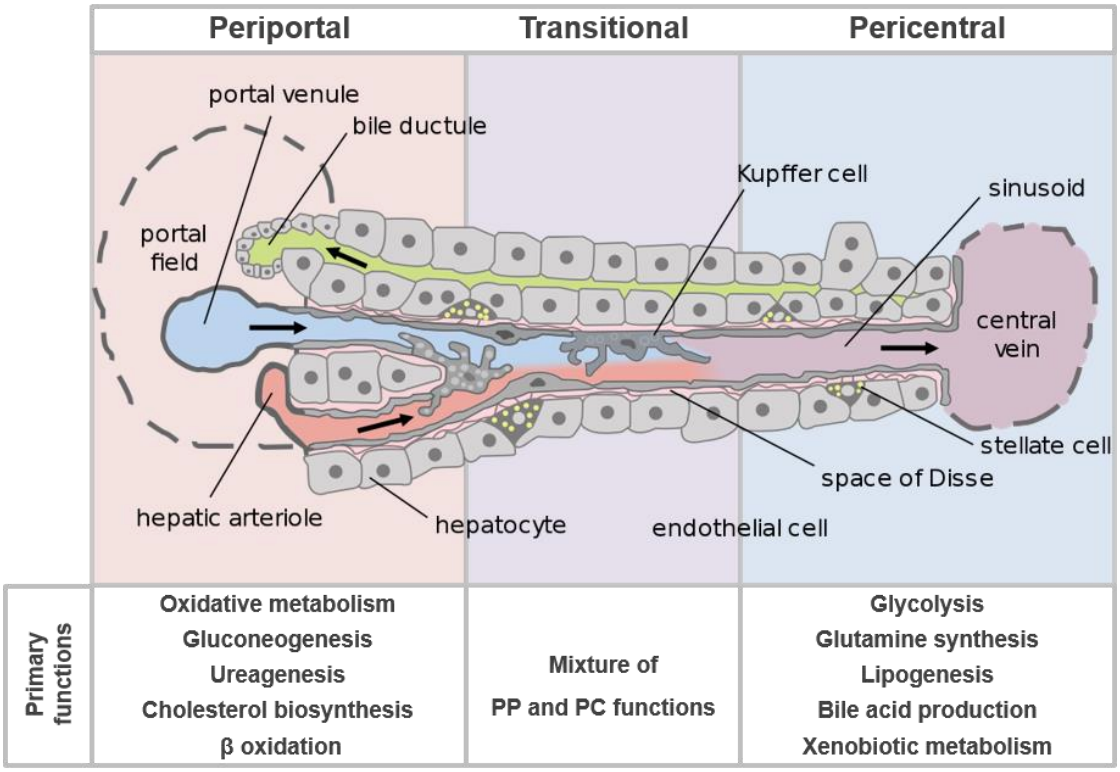

Figure 1.3 Schematic representation of the liver acinus, with the major cell types of the liver and the periportal to pericentral zones represented. The hepatocyte functions are listed in the figure, according to the position in the liver acinus. Adapted from Frevert et al. (2005).

While the normal liver is not particularly rich in ECM, its composition, topography and biomechanical properties strongly affect hepatocyte and NPLC phenotypes. ECM alterations are associated with severe pathologies such as fibrosis or cirrhosis. Matrix proteins are mostly present in the portal tracts, central veins and in the sinusoid walls, lining the frontier between the liver parenchyma and the blood (space of Disse). In the liver parenchyma, the most abundant ECM proteins are collagen type I and fibronectin whilst collagen type III, IV and laminin, are mostly present in the portal and central regions (Godoy et al., 2013). More than the ECM components *per se*, the matrix stiffness exerts a strong influence on the hepatocyte phenotype. The biomechanical forces are sensed by the hepatocytes through cell-surface receptors (*e.g.* integrins) and cytoskeleton, affecting intracellular signaling cascades (LeCluyse et al., 2012).

Overall, the tissue architecture, homotypic and heterotypic interactions, matrix composition, and biomechanical stimuli have effects on signal transduction and gene regulation, affecting the hepatocytic phenotype. These factors need to be accounted when engineering an *in vitro* model.

1.3 *In vitro* evaluation of liver function

One of the challenges of applying *in vitro* models is to evaluate their performance and outlook its relevance to other models and, importantly, to the existent *in vivo* data. The standardization of methodologies and endpoints to assess functionality (*e.g.* activity levels, measurement units, etc.) and biomarkers would allow a more straightforward comparison of differentiation protocols, culture strategies and cell sources for a specific application. The parameters evaluated when characterizing a liver cell model include hepatic phenotype, xenobiotic metabolism and biosynthetic activity. In Table 1.1 an overview of the existent tools to evaluate *in vitro* models performance based on multiple parameters of liver functionality is presented.

Hepatic xenobiotic metabolism is a biotransformation process that encompasses 3 phases: I - modification, II - conjugation and III – excretion. Phase I is mostly performed by CYP450 complex, localized in the membrane of the endoplasmic reticulum, and includes reactions such as oxidation, reduction, hydrolysis, cyclization or decyclization. After modification, xenobiotics undergo conjugation with functional groups through methylation, sulphation, acetylation, glucoronidation, etc. to transform xenobiotics into hydrophilic metabolites that are actively transported towards the cell exterior. In phase III, metabolites may be further modified and are then excreted by specialized membrane transporters (*e.g*. MRP, ATP). Phase I enzymes are considered the most critical step of the biotransformation process, as they account for approximately 75% of the total drug metabolism and originate a high diversity of metabolites. The efflux activity is severely affected by hepatocyte polarization, which is required for the correct assembly of membrane transporters (Guengerich, 2008; Hewitt et al., 2007).

Regarding biosynthesis, one of the major hallmarks of hepatic functionality is albumin production. Other proteins such as Alpha 1-antitrypsin (A1AT) and the enzymes Aspartate aminotransferase (AST) and Alanine transaminase (ALT) are also biosyntethized in the liver and are a reference of liver activity, particularly as *in vivo* biochemical markers. Moreover, the conversion of glucose into glycogen, cholesterol synthesis, bile acid production and ammonia detoxification into urea occur in the liver and may be assessed to evaluate hepatic function.

Table 1.1 List of hepatic parameters that may be applied to evaluate the hepatic functionality of an *in vitro* model.

Hepatic function	Parameter	Method	References
Hepatic phenotype	*Polarity*	ICC of apical (MRP2, BSEP, HA4) and basolateral markers (ASGP, HA321)	(Abu-Absi et al., 2002; Hoffmaster et al., 2004) (Tostões et al., 2012)
	Presence of hepatic nuclear factors	ICC of HNF4α	
	Cytoskeletal markers	Localization of F-actin, ICC CK18	
Xenobiotic metabolism	*Phase I - modification*	Gene expression of CYP450 isoforms (1A2, 3A4, 2C9, 2B6)	(Anthérieu et al., 2010; Wolf et al., 2008; Zamek-Gliszczynski et al., 2003)
		Drug induction studies: Omeprazole (CYP1A2, CYP2B6, CYP3A4) , Rifampicin (CYP2A6, CYP2B6, CYP3A4), B-Naphthloflavone (CYP1A2, CYP2B6)	
		Functional activity with substrates for specific isoforms: Bupropion (CYP2B6), Midazolan, testosterone (CYP3A4), Phenacetin (CYP1A2)	
	Phase II - conjugation	Gene expression (UGT, GST)	
		Functional activity with substrates: 7-Hydroxycoumarin (Glucuronidation/sulfation)	
	Phase III - transport (influx, efflux)	Functional assays: MRP2 (CDFDA efflux) , BSEP (H-taurcholate efflux)	
Ammonia detoxification	*Glutamine synthesis Urea production*	NH_4Cl feeding, Urea nitrogen kit, GC-MS detection	(Du et al., 2008; Hofmann et al., 2008)
Blood protein production	*AAT, ALT, Albumin*	Immunodetection by ELISA	(Tostões et al., 2012)
Lipid metabolism	*Cholesterol, LDL*	LDL uptake and secretion,	(Cayo et al., 2012)
Bile synthesis	*Uptake and secretion of bile acids*	Bilirrubin conjugation, uptake of fluorescent bile acids	(Hoekstra et al., 2013; Murray et al., 2011)
Carbohydrate metabolism	*Gluconeogenesis, glycogen storage*	Gene expression: G6PD; Periodic acid Schiff staining; Lactate/pyruvate [U-^{14}C] or glutamine feeding [U-^{14}C]; G6PD activity	(Khuu et al., 2011; El Manoubi et al., 1983)

ICC: Immunocytochemistry

1.4 Hepatic cell sources

The available hepatic cell sources can be globally divided into three categories – primary cultures, immortalized cell lines and hepatocyte-like cells derived from pluripotent stem cells. The characteristics, applications and recent developments are summarized in Table 1.2.

Table 1.2. Available cell sources for development of cell hepatic models and their inherent advantages and disadvantages.

Cell source	Advantages	Disadvantages
Human hepatocytes	Maintain hepatic functionality, highly predictable Representative of population heterogeneity Recommended by the regulatory agencies	Scarce and unpredictable availability Complex isolation process; batch to batch variability Rapid dediferentiation *in vitro* Limited lifespan
Immortalized cell lines	Availability Easy maintenance and manipulation Reproducibility	Clonal origin, not representative of population variability Low expression of drug metabolic enzymes
Hepatocyte-like cells derived from pluripotent stem cells	Availability Representative of population heterogeneity Applicability in disease modelling & cell therapy	Immature hepatic phenotype (fetal-like) Low differentiation yields

1.4.1 Human hepatocytes

Human hepatocytes isolated from liver tissue are the cell source with higher resemblance to *in vivo* in terms of hepatic functions, thus it is considered the gold standard for toxicity testing in pre-clinical drug development by the regulatory agencies (Guguen-Guillouzo and Guillouzo, 2010). Human hepatocytes express all the major enzymes and transporters and exhibit xenobiotic metabolic functions comparable to the liver tissue (Hart et al., 2010). Importantly, primary cultures are representative of the population variability caused by genetic polymorphisms or pathophysiology. Therefore, hepatotoxicity testing with primary cultures in pre-clinical phase may prevent idiosyncratic drug reactions and consequent drug retrieval from the market (Hewitt et al., 2007).

The major caveat of primary cultures is that the differentiated hepatic features are only maintained for few days in monolayer cultures. Thus, the challenge has long been to retain the adult phenotype and associated functions for longer periods, by elaborating advanced culture strategies, as described below. Moreover, the lack of proliferative ability *in vitro*, the scarce and irregular availability of human liver tissue as well as the complex isolation process and resultant

batch-to-batch variability hamper its widespread adoption and drive the need for alternative cellular sources.

1.4.2 Immortalized cell lines

The availability, stable phenotype and unlimited life span that generally characterize immortalized cell lines make them a convenient alternative to primary cultures to model liver function *in vitro*. However, hepatic cell lines, either derived from human hepatomas or obtained by oncolytic immortalization, generally lack or have downregulated expression of metabolic enzyme families and fail to recapitulate liver metabolism at physiological levels, particularly regarding phase I enzymes. HepG2, the best characterized hepatic cell line, carries out most biosynthetic functions of the liver (e.g. albumin, plasminogen secretion) but has low activity of phase I and II enzymes (Westerink and Schoonen, 2007). Fa2N-4 is a non-tumorigenic immortalized cell line, which has been proposed to assess drug inducing mechanisms and has been applied by the industry. Nevertheless, direct comparison with human hepatocyte in terms of expression and activity levels of CYP450 have identified limitations of Fa2N-4 as a predictive hepatic model (Hariparsad et al., 2008).

HepaRG differs from other existent cell lines since it is a bipotent progenitor cell line that can be differentiated into hepatocyte-like cells (HLC) and biliary-like cells (BLC). Nevertheless, the 2D protocol to attain differentiated metabolic functions requires the supplementation of high Dimethyl sulfoxide (DMSO) concentrations. At the differentiated state, HLC exhibit activity of the CYP450 complex, phase II enzymes and express the gene regulatory proteins and liver specific proteins (Anthérieu et al., 2010; Le Vee et al., 2006). Moreover, the expression of phase I enzymes, particularly CYP3A4, was comparable to primary hepatocytes (Hart et al., 2010) and have been shown to express most of the hepatobiliary transporters (phase III) expressed in cultured human hepatocytes (Bachour-El Azzi et al., 2015), therefore it has been used to assess hepatotoxicity. Despite the unique characteristics and potential of HepaRG to be applied for hepatotoxicity studies, the high concentration of DMSO may interfere with detoxification pathways due to effects such as anti-apoptotic activity (Cerec et al., 2007) and limit its application for cell transplantation or extracorporeal liver support due to toxicity.

Overall, among the existent lines, HepaRG is the best candidate to be applied for hepatotoxicity studies due to the expression and function of detoxification enzymes and transporters. However, due to the clonal origin of the cell line, additional models for toxicity testing are required to enclose the population variability in the drug response. For cell therapy purposes, immortalized cell lines are hampered by their genomic instability and potential tumorigenesis.

1.4.3 Hepatocyte-like cells derived from pluripotent stem cells

The limited availability of primary hepatocytes and the lack of functional immortalized cell lines make the use of renewable cell sources such as pluripotent stem cells (PSC) extremely attractive, with potential to cover cell therapy, disease modeling, developmental studies and *in vitro* toxicological research. PSC are capable of self-renewal, can be differentiated into all cell lineages of the three germ layers of the body and may be of embryonic origin such as human embryonic stem cells (hESC) or derived from adult tissue such as induced pluripotent stem cells (iPSC). The use of iPSC is particularly attractive, due to the potential to obtain cells from virtually any adult tissue which may be applied to model and study liver diseases *in vitro* and, importantly, to use patient-specific cell types for personalized therapies, minimizing adverse immune reactions.

A large number of protocols to differentiate either hESC or iPSC into hepatocyte-like cells have arisen in the past years. Most of these protocols are step-wise protocols that use soluble factors to recapitulate the *in vivo* differentiation process, from pluripotent cells to endoderm cells, hepatic specification into hepatoblasts and finally maturation into hepatocyte-like terminally differentiated cells (Amour et al., 2006; Spence et al., 2011). The differentiation protocols and strategies developed so far have not yet yielded hepatocyte-like cells with functional hepatic activity comparable to adult hepatocytes or liver tissue, displaying hepatic morphology and expression of differentiation markers comparable to fetal rather than adult hepatocytes (Schwartz et al., 2014). Moreover, the efficiency of differentiation with the current protocols is still low, with the best protocols achieving 50 to 60% of differentiation efficiency (Chistiakov and Chistiakov, 2012). The low yields of HLC obtained associated with expensive and inefficient purification procedures are far from the necessary to meet the scalability demands of cell-based therapies. The development of novel culture strategies based on co-cultures or 3D, the improvement of knowledge on the mechanisms of maturation from fetal to adult liver and the standardization of endpoint differentiation markers will be key to improve the efficiency and maturity of the hepatocyte-like cells differentiated from pluripotent stem cells (Schwartz et al 2014).

1.5 Strategies for the culture of hepatic cell models

The use of 3D culture, biomaterials, co-cultures and bioreactors or all these strategies combined have provided advances in hepatic tissue engineering, which main methodologies and achievements are described below.

1.5.1 3D culture

Traditionally, hepatocytes were cultured as monolayers in adherent substrates coated with collagen. The rigidity of the substrate and the lack of cellular or 3D ECM support necessary to maintain the cuboidal shape and polarization resulted in dedifferentiation within 3 to 5 days, associated with downregulation of phase I enzymes and decrease of albumin production (Godoy et al., 2013). Media formulation (*e.g*. growth factor or DMSO supplementation; serum removal) has been used to improve cell survival and hepatic-specific functions (Hewitt et al., 2007). Moreover, 3D strategies that preserve the cuboidal shape achieve good outcomes in long-term functionality.

The collagen sandwich culture strategy, first implemented by Dunn and co-workers (1989), showed for the first time the impact of the ECM matrix in the culture of adult rat hepatocytes. The collagen sandwich consists in the culture of hepatocytes in between two gelled layers of collagen type I. Using this system, the cuboidal morphology of the hepatocytes is maintained and albumin secretion can be kept for several weeks, whereas hepatocytes without the collagen overlay cease albumin secretion within 1 week (Dunn et al., 1989).

The *ex-vivo* culture of liver tissue as precision cut slices is another 3D liver model, which principal advantage is the maintenance the original tissue architecture, ECM and cellular components. Thus, precision cut liver slices (PCLS) enable the study of multicellular processes, being applied in the study of liver physiology and in the metabolism and toxicity of xenobiotics. Despite the great advantage of sustaining liver architecture and microenvironment, PCLS often consist of several layers of cells and thick ECM, thus presenting diffusion problems, therefore cell viability can be maintained for short periods, typically up to 96h (de Graaf et al., 2010).

Hepatocytes may also be cultured as cell spheroids, which allow the establishment of extensive cell-cell contacts. Cell aggregation into spheroids can be obtained by different methods, including self-assembly in matrices (*e.g.* matrigel), low-adhesion conditions and hanging-drop platforms or using stirred conditions to promote aggregation (*e.g.* rotary shaker or stirred-tank bioreactors). Hepatic spheroids exhibit a polarized organization, with assembly of the actin cytoskeleton in the cell cortex and formation of bile canalicular-like structures. Moreover, the transcriptional program activated in hepatocyte spheroids is different from the genes expressed in 2D culture. In hepatic spheroids there is downregulation of mesenchymal and cytoskeletal genes, upregulation of the hepatic regulator HNF4α and its downstream target genes (Chang and Hughes-Fulford, 2014) and also genes related with metabolic and synthetic functions (Chang and Hughes-Fulford, 2009). The enhanced and long-term maintenance of hepatic functionality in spheroids has been

previously demonstrated by our group and others for rat (Miranda et al., 2009) and human (Tostões et al., 2012) primary cultures and also for immortalized hepatic cell lines (Chang and Hughes-Fulford, 2009). The effects of 3D culture in the differentiation of PSC are controversial: on one hand, it has been shown that 3D culture improves the efficiency of differentiation towards HLC, on the other hand, the 3D differentiation process may be more heterogenous which can be associated with unequal diffusion of soluble factors within spheroids (Schwartz et al., 2014).

1.5.2 Biomaterials

The use of biomaterials for the culture of hepatocytes has gained relevance in the past years, due to their capacity to elicit specific cellular functions, direct cell-cell interactions and support the 3D architecture. Biomaterials, either from natural or synthetic nature have inner characteristics such as chemical composition, porosity, permeability, degradability, biomechanical properties such as stiffness and elasticity and can be inert or biologically active, with adhesion motifs to ligands. Most of these characteristics can be used or tuned to suit the required architecture or composition of the liver (Jain et al., 2013).

The liver biomatrix is a natural type of biomaterial consisting of the native ECM recovered from decellularized livers, which can be used as a scaffold and re-populated. Importantly, the liver biomatrix is depleted of cellular components but ideally the original ECM composition remains intact as well as the tissue architecture and vasculature due to a sensitive decellularization procedure (Uygun and Yarmush, 2013). Liver decellularization was first described for rat livers, with rat hepatocytes maintaining viable and with high expression levels of albumin, urea and CYP450 genes up to 10 days after recellularization (Uygun et al., 2010). Baptista and coworkers, used the intact vasculature to reseed the scaffolds with human fetal liver and endothelial cells, which were capable of homing to their native niches within the scaffold (Baptista et al., 2011). The transplantation in rats after 90% hepatectomy has been successfully performed, despite the limited survival up to few days (Bao et al., 2011). Recellularization of porcine liver biomatrices using human fetal liver cells led to differentiated hepatic cells with high metabolic activity (Barakat et al., 2012), representing the major approach towards human liver transplantation with an engineered organ. Although the liver biomatrix represents the most promising solution for transplantation with engineered organs, its application for *in vitro* toxicity testing is hampered by the short-term survival (Uygun and Yarmush, 2013).

Other natural polymers are frequently applied as scaffolds in liver tissue engineering in different forms such as films, coatings, foams, nanofibers, hydrogels, sponges, and microcapsules. As previously mentioned, collagen is the principal component of the liver ECM and its use for hepatic cultures is widespread, from coating substrates to the sandwich culture system or incorporated in other matrices, making it the most used biomaterial for liver culture (Jain et al., 2013). Other polymers often used include hyaluronic acid, chitosan and alginate, as reviewed by Jain et al (2013).

Alginate, a linear polysaccharide copolymer of β-D-mannuronic acid and α-Lguluronic acid, is the most used biomaterial for cell immobilization and microencapsulation since it is inert, biocompatible and easy to use. Alginate crosslinking occurs upon addition of bivalent cations and all the procedure may be carried out in physiological conditions, with minimal effects to the cells (Lee and Mooney, 2012). The stiffness and porosity of alginate hydrogels may be tuned according to the composition of β-D-mannuronic acid, sequential structure, molecular size and calcium concentration (Martinsen et al., 1989). The hydrophilic porous network formed (approximately 90% of porosity) is compatible with 3D culture by allowing the establishment of cell-cell interactions. Moreover, alginate capsules are highly permeable, allowing the diffusion of oxygen, soluble factors and proteins (Lee and Mooney, 2012). The microencapsulation of rat hepatocyte spheroids allowed the long-term culture with maintenance of hepatic functions in stirred conditions for several weeks (Miranda et al., 2010; Tostões et al., 2011), denoting the role of alginate microencapsulation in the protection from shear stress. Moreover, alginate encapsulation of HepG2 C3A cells has been applied as a biocomponent for extracorporeal liver support (Yang et al., 2013). Importantly, alginate can be used in compliance with GMP guidelines and therefore potentially applied in cell-based therapy. Its potential use in cell transplantation has been shown in rats with ALF, that presented improved survival (Aoki et al 2005; Sgroi et al 2011; Jitraruch et al 2014)) with low immunogenicity when using ultrapure alginates. Nevertheless, the success after transplant differs substantially between studies due to the mechanical properties which may lead to capsule breakage (Santos et al., 2013). Thus, the improvement of the control on alginate mechanical properties may contribute to widespread the use of alginate for cell therapy applications.

The synthetic biomaterials most used for liver tissue engineering include poly L-lactic acid (PLLA), poly (lactide-coglycolide) (PLGA), poly(ethyleneglycol) (PEG), poly(N-isopropylacrylamide) and Polydimethylsiloxane (PDMS), extensively applied for microfabrication (Jain et al., 2013). The major advantage of synthetic biomaterials is the controllable physiochemical and biological properties, which modulation is easier than natural-derived biomaterials. Nevertheless, in general, synthetic biomaterials are more prone to poor biocompatibility and degradability properties for tissue engineering and cell-based therapies than natural derived biomaterials (Lutolf and Hubbell, 2005). The rapid advances in the development of bio and time-responsive materials may boost the application of synthetic biomaterials for liver engineering applications.

1.5.3 Co-cultures

As described in section 1.2, the functional compartment of the liver (liver parenchyma) is supported by the non-parenchymal (NPLC) fraction, which contributes to provide the environmental cues to maintain hepatocyte function. Thus, the co-culture of hepatocytes and NPLC or other types of stromal cells *ex-vivo* has gained relevance in the past years as a strategy to prolong and enhance the hepatocyte specific functions *in vitro* (Godoy et al., 2013).

LSECs have an important role in supporting hepatocytes *in vivo*. However, maintaining LSECs phenotype *in vitro* is challenging since these cells require tight microenvironmental regulation to maintain their characteristics, namely extensive fenestrae and high scavenger activity (March et al., 2009). Moreover, LSECs complex isolation and purification procedure from liver tissue has hampered major developments for human *in vitro* systems (Cheluvappa, 2014). Even so, co-cultures of LSECs and hepatocytes from rat origin either in collagen sandwich co-culture (Bale et al., 2014) and layered collagen culture in transwells (Kang et al., 2013) have demonstrated that endothelial and hepatic phenotypes can be maintained in long term cultures up to 4 weeks, with a significant increase in albumin production and CYP3A4 activity. For the development of human cell models, the immortalized Human Umbilical Vein Endothelial Cell (HUVEC) line is routinely used, enhancing hepatocyte function (Salerno et al., 2011). Hepatic spheroids covered with HUVECs have also been applied to establish vascularized liver tissue as biocomponents of BAL devices (Inamori et al., 2009) and transplantation of co-encapsulated hepatocytes and HUVECs has extended survival and improved the liver functional biomarkers in rats with ALF (Qiu et al., 2012).

Co-cultures with hepatic stellate cells (HSC) have mostly focused on the mechanisms underlying disease, such as fibrosis or fatty acid accumulation (Giraudi et al., 2015; Puche et al., 2013). Nevertheless, the effect of HSC has been demonstrated to be beneficial for hepatocyte spheroids, mostly by supporting hepatocyte architecture and tight junctions (Lee et al., 2013; Thomas et al., 2005). Kupffer cells (KC) have been co-cultured with hepatocytes to incorporate the role of inflammation on drug metabolism and it has been demonstrated that there is differential down-regulation of CYP450 in rat hepatocytes upon interaction of inflammatory drugs, which translates into differential sensitivity to drugs (Milosevic et al., 1999; Tukov et al., 2006). The modulation of inflammation in human systems has been rarely addressed, but studies using hepatic and monocytic cell lines have explored the sensitivity to drugs such as Troglitazone in a co-culture model (Edling et al., 2009).

All the studies referred show enhancement of hepatocyte functions in co-culture with NPLC types individually. The co-culture of the PC and all NPC types simultaneously, with recapitulation of the cellular proportions observed in the tissue, has been addressed with primary rat and human cells with the aim of prolonging and enhancing predictability of hepatotoxicity (Kostadinova et al., 2013). In this study, cultures were maintained long-term functions, were responsive to inflammatory stimuli and showed better correlation with *in vivo* data for drugs with idiosyncratic toxicity.

In alternative to primary NPLC, the use of stromal cells to support hepatocyte function has been widely explored through the co-culture with fibroblasts or mesenchymal stem cells. The availability and easy manipulation of fibroblasts are among the characteristics that make them suitable alternatives for NPLC. Data from rodent studies consistently demonstrated that fibroblasts contribute to the stability of hepatocytic phenotype, which has been attributed to the soluble factors secreted by fibroblasts such as HGF or cell surface proteins such as N-cadherin (Khetani et al., 2004; Leite et al., 2011). The co-culture of human hepatocytes and fibroblasts has been the basis for the establishment of microscale culture in a micropatterned system, for drug development applications (Khetani and Bhatia, 2008a). The use of mesenchymal cells in co-culture has been mostly explored for cell therapy in cases of liver fibrosis (Kim et al., 2014) or ALF (Jung et al., 2013; Zhang et al., 2012), either through cell transplantation or use of conditioned media, which has been shown to alleviate the symptoms in rodent models. Moreover, one of the most significant steps towards the development of vascularized tissues *in vitro* has been achieved with triple co-cultures of IPS-derived hepatocyte-like cells, endothelial and mesenchymal stem cells with successful engraftment and functional vascular network, thus denoting the importance of MSC in the development of organ buds and vascularization (Takebe et al., 2013).

1.5.4 Bioreactors

Bioreactors (BRs) are devices engineered to support biological processes for multiple applications, ranging from production of biopharmaceuticals to tissue engineering. The key feature of these systems is the high level of control over the bioprocesses, which is achieved by on-line monitorization and automated regulation of environmental culture parameters, such as temperature, pH, partial pressure of oxygen (pO_2), nutrient and metabolite concentration. Moreover, the dynamic conditions offered by bioreactors ensure efficient mass transfer in the culture vessel, which is a key factor to minimize oxygen and nutrient gradients and maintain a homogenous culture environment. The control, automation and efficient mass transfer simplify the transition from bench top bioreactors to larger scales, critical to meet the industrial requirements.

In the field of tissue engineering, bioreactors are developed to deliver a cell product that restores or improves organ-specific functions. For this purpose, the bioreactor and bioprocess are designed to recreate the tissue architecture and microenvironment by supporting 3D cellular interactions (mono or heterotypic), using biomaterials or modulating hydrodynamic forces and physiochemical parameters (Fennema et al. 2013; Martin et al. 2004; Griffith and Swartz 2006). An important aspect of bioreactors is the flexibility towards the operation mode applied. In perfusion operation mode, fresh medium is fed to a bioreactor containing cells that are retained within the system, with gradual replacement of culture medium. In contrast to batch and fed-batch, perfusion allows the removal of the toxic metabolic by-products and the constant replenishment

of nutrients and growth factors that contribute to elicit specific functions. It has previously been demonstrated that perfusion conditions elicit hepatic functions. In the MultiChamber Modular Bioreactor (McMB), primary cultures of human hepatocytes cultured in collagen-coated PDMS wells with constant perfusion had up-regulation of phase I, II and III enzymes and stable expression for longer periods than in static systems (Vinci et al. 2011). Several formats applying the same principle and presenting several adaptations are commercially available, such as the Minucell (Xia et al. 2009) which includes a collagen overlay to minimize the effects of shear stress. Although these represent the simplest formats of BRs, presenting an upgrade towards static culture by incorporating dynamic flow, they lack automated control and monitoring of culture parameters. Other monolayer-based BRs have been used to model physiological liver phenomena such as zonation. By controlling O_2 tension, the gradient of oxygen tensions sensed *in vivo* by pericentral and periportal hepatocytes was recapitulated (Allen et al., 2005).

Hollow-fiber bioreactors comprise an interwoven network of semipermeable membranes which are perfused by medium and oxygen, aiming to resemble blood capillaries *in vivo*. In between the capillary systems, the cells are arranged in compact 3D structures. Applying this principle, a number of bioreactors were designed for clinical application to support extracorporeal liver function in patients with liver failure: the Modular Extracorporeal Liver System (MELS), developed by Gerlach´s research group (Gerlach et al. 1994), and the AMC-bioreactor, by Chamuleau and coworkers (Flendrig et al. 1997). These systems have also been validated for pharmacological applications: in the miniaturized format of the MELS bioreactor, scaled down to 2 mL, major drug metabolizing P450 enzymes were preserved up to 23 days in primary cultures of human hepatocytes in co-culture with non-parenchymal cells (Zeilinger et al. 2011). More recently, this design has been applied for the differentiation of human pluripotent SC towards hepatocyte-like cells (Miki et al. 2011). The AMC-bioreactor has been validated using the hepatic cell line HepaRG, which presented phase I and II drug metabolism and production of bile salts (Nibourg et al. 2013). A major drawback of these systems is the inaccessibility to the cell compartment throughout the culture time, not allowing phenotypic monitoring and cell sampling. Furthermore, hollow fiber bioreactors fail to accurately control pH and pO_2 within the fibers.

For toxicological assessment, the possibility of miniaturizing and multiplexing bioreactor formats is a great advantage due to the minimization of expensive culture and scarce biological material and parallel testing of compounds of interest. The use of micro-electro mechanical systems (MEMS) has been applied with the development of dynamic micro-scale tissue culture devices, aiming to miniaturise *in vitro* organs to the smallest possible scale. These systems, based on microchannels for the flow of media and miniaturized cell culture compartments, support the replication of shear stress at physiological intracapillary or interstitial rates in order to maintain stable protein and oxygen gradient-based microenvironments. Several high throughput multiwell systems, applying microfluidics for somewhat complex *in vitro* models, have undergone validation for toxicological approaches. The Perfusion Array Liver System (PEARL), designed by Lee and co-workers (Lee et al., 2007) to mimic the liver acinus, constitutes an innovative approach to

design modular units with physiological relevance. With a design compatible with a 96 well plate, the system is composed of microunits of artificial liver acinus with an endothelial-like barrier, intended to simulate the mass transfer properties of the liver sinusoid. Primary cultures of human hepatocytes were maintained for 7 days in culture and were responsive to diclofenac toxicity at high concentrations (Lee et al. 2007). Khetani and Bhatia (Khetani and Bhatia, 2008b) developed a multiwell system containing micropatterned structures of PDMS for co-culture of fibroblasts and hepatocytes, which is compatible with robotic fluid handling and phenotypic screening tools. This co-culture system was validated for up to 6 weeks with maintenance of gene expression profile, phase I/II metabolism, canalicular transport, secretion of liver-specific products and susceptibility to hepatotoxins (Khetani and Bhatia 2008).

Stirred-tank bioreactors (STB), which have long been applied in industry for production of biopharmaceuticals, can also be used for *in vitro* cell models for pharmacological testing. In STB, cells are inoculated as cell suspension and the hydrodynamics of the bioreactor – determined by vessel, impeller type and agitation rate - is adjusted to elicit cell collisions and promote cell-cell contacts into aggregation. Dynamic parameters need to be balanced to guarantee diffusion through the aggregates, preventing the formation of necrotic centres, while the shear stress is minimized to avoid damage. Spheroid culture of rat hepatocytes has long been reported, resulting in increased albumin production and phase I-II activity (Abu-Absi et al. 2002) and maintenance of hepatocyte polarization (Miranda et al. 2009). More recently, primary cultures of human hepatocytes were maintained under physiological oxygen conditions and perfusion operation mode, extending culture viability and functionality for up to 3-4 weeks (Tostões et al. 2012). Hepatocytes in this system present a functional phenotype displaying bile canalicular networks, and inducible expression of CYP450. The use of biomaterials in STB has also been addressed, by alginate microencapsulation of rat hepatocyte (Miranda et al. 2010; Tostões et al. 2011), which represents a strategy to overcome eventual shear stress effects on stirred culture.

2. Scope of the thesis

The goal of this thesis was to develop culture strategies for the establishment of cellular models that recapitulate liver function *in vitro*, using human systems. These models made use of stirred conditions to promote cellular aggregation and were complemented with the use of biomaterials or co-cultures to overcome the existing caveats of hepatocyte culture by further enhancing the hepatic phenotype and/or long-term culture.

In **chapter 1** a review of the needs for human hepatic *in vitro* systems, existent cell sources and culture strategies as well as their applications and limitations is provided.

In **chapter 2**, the implementation and optimization of a protocol for isolation and 3D culture of hepatocytes isolated from resected liver tissue is described. The improvement of specific steps of hepatocyte isolation and its impact on the aggregation of hepatocytes is analysed, providing a novel protocol for the isolation of hepatocytes to be used in 3D culture.

In **chapter 3**, the co-culture of primary hepatocytes with bone marrow-derived mesenchymal stem cells as 3D spheroids is implemented. The results showed that the co-culture enhanced the hepatic phenotype and improved hepatocyte survival and functionality for long-term cultures, being the proof-of-concept of its application performed in repeated-dose toxicity testing with APAP.

In **chapter 4**, a strategy for the 3D culture of the hepatic cell line HepaRG is implemented, combining cell aggregation with alginate microencapsulation. The 3D strategy yielded a higher ratio of hepatocyte-like cells than the 2D DMSO-dependent protocol, with comparable levels of drug metabolic activity and enhanced biosynthetic metabolism.

In **chapter 5**, a general discussion about the work performed in this thesis is presented.

3. References

Abu-Absi SF, Friend JR, Hansen LK, Hu W-S. 2002. Structural polarity and functional bile canaliculi in rat hepatocyte spheroids. *Exp. Cell Res.* **274**:56–67.

Allen JW, Khetani SR, Bhatia SN. 2005. In vitro zonation and toxicity in a hepatocyte bioreactor. *Toxicol. Sci.* **84**:110–9.

Amour KAD, Bang AG, Eliazer S, Kelly OG, Agulnick AD, Smart NG, Moorman MA, Kroon E, Carpenter MK, Baetge EE, D'Amour K a. 2006. Production of pancreatic hormone-expressing endocrine cells from human embryonic stem cells. *Nat. Biotechnol.* **24**:1392–401.

Anthérieu S, Chesné C, Li R, Camus S, Lahoz A, Picazo L, Turpeinen M, Tolonen A, Uusitalo J, Guguen-Guillouzo C, Guillouzo A. 2010. Stable expression, activity, and inducibility of cytochromes P450 in differentiated HepaRG cells. *Drug Metab. Dispos.* **38**:516–525.

Aoki T, Jin Z, Nishino N, Kato H, Shimizu Y, Niiya T, Murai N, Enami Y, Mitamura K, Koizumi T, Yasuda D, Izumida Y, Avital I, Umehara Y, Demetriou AA, Rozga J, Kusano M. 2005. Intrasplenic transplantation of encapsulated hepatocytes decreases mortality and improves liver functions in fulminant hepatic failure from 90% partial hepatectomy in rats. *Transplantation* **79**:783–790.

Bachour-El Azzi P, Sharanek A, Burban A, Li R, Le Guével R, Abdel-Razzak Z, Stieger B, Guguen-Guillouzo C, Guillouzo A. 2015. Comparative localization and functional activity of the main hepatobiliary transporters in HepaRG cells and primary human hepatocytes. *Toxicol. Sci.*

Bale SS, Golberg I, Jindal R, McCarty WJ, Luitje M, Hegde M, Bhushan A, Usta OB, Yarmush ML. 2014. Long-Term Coculture Strategies for Primary Hepatocytes and Liver Sinusoidal Endothelial Cells. *Tissue Eng. Part C. Methods*.

Bañares R, Catalina M-V, Vaquero J. 2013. Liver support systems: will they ever reach prime time? *Curr. Gastroenterol. Rep.* **15**:312.

Bao J, Shi Y, Sun H, Yin X, Yang R, Li L, Chen X, Bu H. 2011. Construction of a portal implantable functional tissue-engineered liver using perfusion-decellularized matrix and hepatocytes in rats. *Cell Transplant.* **20**:753–766.

Baptista PM, Siddiqui MM, Lozier G, Rodriguez SR, Atala A, Soker S. 2011. The use of whole organ decellularization for the generation of a vascularized liver organoid. *Hepatology* **53**:604–617.

Barakat O, Abbasi S, Rodriguez G, Rios J, Wood RP, Ozaki C, Holley LS, Gauthier PK. 2012. Use of decellularized porcine liver for engineering humanized liver organ. *J. Surg. Res.* **173**.

Braet F, Wisse E. 2002. Structural and functional aspects of liver sinusoidal endothelial cell fenestrae: a review. *Comp. Hepatol.* **1**:1.

Cayo MA, Cai J, DeLaForest A, Noto FK, Nagaoka M, Clark BS, Collery RF, Si-Tayeb K, Duncan SA. 2012. JD induced pluripotent stem cell-derived hepatocytes faithfully recapitulate the pathophysiology of familial hypercholesterolemia. *Hepatology* **56**:2163–71.

Cerec V, Glaise D, Garnier D, Morosan S, Turlin B, Drenou B, Gripon P, Kremsdorf D, Guguen-Guillouzo C, Corlu A. 2007. Transdifferentiation of hepatocyte-like cells from the human hepatoma hepaRG cell line through bipotent progenitor. *Hepatology* **45**:957–967.

Chang TT, Hughes-Fulford M. 2009. Monolayer and spheroid culture of human liver hepatocellular carcinoma cell line cells demonstrate distinct global gene expression patterns and functional phenotypes. *Tissue Eng. Part A* **15**:559–567.

Chang TT, Hughes-Fulford M. 2014. Molecular mechanisms underlying the enhanced functions of three-dimensional hepatocyte aggregates. *Biomaterials* **35**:2162–71.

Cheluvappa R. 2014. Standardized isolation and culture of murine liver sinusoidal endothelial cells. *Curr. Protoc. Cell Biol.* **65**:2.9.1–8.

Chistiakov DA, Chistiakov PA. 2012. Strategies to produce hepatocytes and hepatocyte-like cells from pluripotent stem cells. *Hepatol. Res.*

Decaens C, Durand M, Grosse B, Cassio D. 2008. Which in vitro models could be best used to study hepatocyte polarity? *Biol. Cell* **100**:387–398.

DeLeve LD. 2013. Liver sinusoidal endothelial cells and liver regeneration. *J. Clin. Invest.* **123**:1861–6.

Dixon LJ, Barnes M, Tang H, Pritchard MT, Nagy LE. 2013. Kupffer cells in the liver. *Compr. Physiol.* **3**:785–797.

Du Y, Han R, Wen F, Ng San San S, Xia L, Wohland T, Leo HL, Yu H. 2008. Synthetic sandwich culture of 3D hepatocyte monolayer. *Biomaterials* **29**:290–301.

Dunn JC, Yarmush ML, Koebe HG, Tompkins RG. 1989. Hepatocyte function and extracellular matrix geometry: long-term culture in a sandwich configuration. *FASEB J.* **3**:174–177.

Edling Y, Sivertsson LK, Butura A, Ingelman-Sundberg M, Ek M. 2009. Increased sensitivity for troglitazone-induced cytotoxicity using a human in vitro co-culture model. *Toxicol. Vitr.* **23**:1387–1395.

Forbes SJ, Gupta S, Dhawan A. 2015. Cell therapy for liver disease: From liver transplantation to cell factory. *J. Hepatol.* **62**:S157–S169.

Frevert U, Engelmann S, Zougbédé S, Stange J, Ng B, Matuschewski K, Liebes L, Yee H. 2005. Intravital observation of plasmodium berghei sporozoite infection of the liver. *PLoS Biol.* **3**:1034–1046.

Giraudi PJ, Barbero VJ, Marin V, Chavez-tapia NC, Tiribelli C, Rosso N. 2015. The importance of the interaction between hepatocyte and hepatic stellate cells in fi brogenesis induced by fatty accumulation. *Exp. Mol. Pathol.* **98**:85–92.

Godoy P, Hewitt NJ, Albrecht U, Andersen ME, Ansari N, Bhattacharya S, Bode JG, Bolleyn J, Borner C, Böttger J, Braeuning A, Budinsky R a, Burkhardt B, Cameron NR, Camussi G, Cho C-S, Choi Y-J, Craig Rowlands J, Dahmen U, Damm G, Dirsch O, Donato MT, Dong J, Dooley S, Drasdo D, Eakins R, Ferreira KS, Fonsato V, Fraczek J, Gebhardt R, Gibson A, Glanemann M, Goldring CEP, Gómez-Lechón MJ, Groothuis GMM, Gustavsson L, Guyot C, Hallifax D, Hammad S, Hayward A, Häussinger D, Hellerbrand C, Hewitt P, Hoehme S, Holzhütter H-G, Houston JB, Hrach J, Ito K, Jaeschke H, Keitel V, Kelm JM, Kevin Park B, Kordes C, Kullak-Ublick G a, LeCluyse EL, Lu P, Luebke-Wheeler J, Lutz A, Maltman DJ, Matz-Soja M, McMullen P, Merfort I, Messner S, Meyer C, Mwinyi J, Naisbitt DJ, Nussler AK, Olinga P, Pampaloni F, Pi J, Pluta L, Przyborski S a, Ramachandran A, Rogiers V, Rowe C, Schelcher C, Schmich K, Schwarz M, Singh B, Stelzer EHK, Stieger B, Stöber R, Sugiyama Y, Tetta C, Thasler WE, Vanhaecke T, Vinken M, Weiss TS, Widera A, Woods CG, Xu JJ, Yarborough KM, Hengstler JG. 2013. Recent advances in 2D and 3D in vitro systems using primary hepatocytes, alternative hepatocyte

sources and non-parenchymal liver cells and their use in investigating mechanisms of hepatotoxicity, cell signaling and ADME. *Arch. Toxicol.* Vol. 87 1315-530 p.

Gonzalez SA, Keeffe EB. 2011. Chronic viral hepatitis: epidemiology, molecular biology, and antiviral therapy. *Front Biosci* **16**:225–250.

De Graaf IAM, Olinga P, de Jager MH, Merema MT, de Kanter R, van de Kerkhof EG, Groothuis GMM. 2010. Preparation and incubation of precision-cut liver and intestinal slices for application in drug metabolism and toxicity studies. *Nat. Protoc.* **5**:1540–1551.

Guengerich FP. 2008. Cytochrome P450 and chemical toxicology. *Chem. Res. Toxicol.*

Guguen-Guillouzo C, Guillouzo A. 2010. General review on in vitro hepatocyte models and their applications. *Methods Mol. Biol.*

Hariparsad N, Carr BA, Evers R, Chu X. 2008. Comparison of immortalized Fa2N-4 cells and human hepatocytes as in vitro models for cytochrome P450 induction. *Drug Metab. Dispos.* **36**:1046–55.

Hart SN, Li Y, Nakamoto K, Subileau E, Steen D, Zhong X. 2010. A comparison of whole genome gene expression profiles of HepaRG cells and HepG2 cells to primary human hepatocytes and human liver tissues. *Drug Metab. Dispos.* **38**:988–994.

Hay M, Thomas DW, Craighead JL, Economides C, Rosenthal J. 2014. Clinical development success rates for investigational drugs. *Nat. Biotechnol.* **32**:40–51.

Hewitt NJ, Lechón MJG, Houston JB, Hallifax D, Brown HS, Maurel P, Kenna JG, Gustavsson L, Lohmann C, Skonberg C, Guillouzo A, Tuschl G, Li AP, LeCluyse E, Groothuis GMM, Hengstler JG. 2007. Primary hepatocytes: current understanding of the regulation of metabolic enzymes and transporter proteins, and pharmaceutical practice for the use of hepatocytes in metabolism, enzyme induction, transporter, clearance, and hepatotoxicity studies. *Drug Metab. Rev.* **39**:159–234.

Hoekstra R, Nibourg G a a, Van Der Hoeven T V., Plomer G, Seppen J, Ackermans MT, Camus S, Kulik W, Van Gulik TM, Oude Elferink RP, Chamuleau R a FM. 2013. Phase 1 and phase 2 drug metabolism and bile acid production of HepaRG cells in a bioartificial liver in absence of dimethyl sulfoxide. *Drug Metab. Dispos.* **41**:562–567.

Hoffmaster KA, Turncliff RZ, LeCluyse EL, Kim RB, Meier PJ, Brouwer KLR. 2004. P-glycoprotein expression, localization, and function in sandwich-cultured primary rat and human hepatocytes: relevance to the hepatobiliary disposition of a model opioid peptide. *Pharm. Res.* **21**:1294–302.

Hofmann U, Maier K, Niebel A, Vacun G, Reuss M, Mauch K. 2008. Identification of metabolic fluxes in hepatic cells from transient 13C-labeling experiments: Part I. Experimental observations. *Biotechnol. Bioeng.* **100**:344–54.

Huang BQ, Masyuk T V, Muff MA, Tietz PS, Masyuk AI, Larusso NF. 2006. Isolation and characterization of cholangiocyte primary cilia. *Am. J. Physiol. Gastrointest. Liver Physiol.* **291**:G500–G509.

Inamori M, Mizumoto H, Kajiwara T. 2009. An approach for formation of vascularized liver tissue by endothelial cell-covered hepatocyte spheroid integration. *Tissue Eng. Part A* **15**:2029–2037.

Jain E, Damania A, Kumar A. 2013. Biomaterials for liver tissue engineering. *Hepatol. Int.* **8**:185–197.

Jitraruch S, Dhawan A, Hughes RD, Filippi C, Soong D, Philippeos C, Lehec SC, Heaton ND, Longhi MS, Mitry RR. 2014. Alginate Microencapsulated Hepatocytes Optimised for Transplantation in Acute Liver Failure. Ed. Valquiria Bueno. *PLoS One* **9**:e113609.

Jung J, Choi JH, Lee Y, Park J-W, Oh I-H, Hwang S-G, Kim K-S, Kim GJ. 2013. Human placenta-derived mesenchymal stem cells promote hepatic regeneration in CCl4 -injured rat liver model via increased autophagic mechanism. *Stem Cells* **31**:1584–96.

Jungermann K, Heilbronn R, Katz N, Sasse D. 1982. The glucose/glucose-6-phosphate cycle in the periportal and perivenous zone of rat liver. *Eur. J. Biochem.* **123**:429–436.

Jungermann K, Kietzmann T. 2000. Oxygen: modulator of metabolic zonation and disease of the liver. *Hepatology* **31**:255–260.

Kang YBA, Rawat S, Cirillo J, Bouchard M, Noh HM. 2013. Layered long-term co-culture of hepatocytes and endothelial cells on a transwell membrane: toward engineering the liver sinusoid. *Biofabrication* **5**:045008.

Khetani SR, Bhatia SN. 2008a. Microscale culture of human liver cells for drug development. *Nat. Biotechnol.* **26**:120–126.

Khetani SR, Bhatia SN. 2008b. Microscale culture of human liver cells for drug development. *Nat. Biotechnol.* **26**:120–126.

Khetani SR, Szulgit G, Del Rio J a, Barlow C, Bhatia SN. 2004. Exploring interactions between rat hepatocytes and nonparenchymal cells using gene expression profiling. *Hepatology* **40**:545–54.

Khuu DN, Scheers I, Ehnert S, Jazouli N, Nyabi O, Buc-Calderon P, Meulemans A, Nussler A, Sokal E, Najimi M. 2011. In vitro differentiated adult human liver progenitor cells display mature hepatic metabolic functions: a potential tool for in vitro pharmacotoxicological testing. *Cell Transplant.* **20**:287–302.

Kim M-D, Kim S-S, Cha H-Y, Jang S-H, Chang D-Y, Kim W, Suh-Kim H, Lee J-H. 2014. Therapeutic effect of hepatocyte growth factor-secreting mesenchymal stem cells in a rat model of liver fibrosis. *Exp. Mol. Med.* **46**:e110.

Kostadinova R, Boess F, Applegate D, Suter L, Weiser T, Singer T, Naughton B, Roth A. 2013. A long-term three dimensional liver co-culture system for improved prediction of clinically relevant drug-induced hepatotoxicity. *Toxicol. Appl. Pharmacol.* **268**:1–16.

LeCluyse EL, Witek RP, Andersen ME, Powers MJ. 2012. Organotypic liver culture models: Meeting current challenges in toxicity testing. *Crit. Rev. Toxicol.*

Lee KY, Mooney DJ. 2012. Alginate: Properties and biomedical applications. *Prog. Polym. Sci.* **37**:106–126.

Lee PJ, Hung PJ, Lee LP. 2007. An artificial liver sinusoid with a microfluidic endothelial-like barrier for primary hepatocyte culture. *Biotechnol. Bioeng.* **97**:1340–1346.

Lee S-A, No DY, Kang E, Ju J, Kim D-S, Lee S-H. 2013. Spheroid-based three-dimensional liver-on-a-chip to investigate hepatocyte-hepatic stellate cell interactions and flow effects. *Lab Chip* **13**:3529–37.

Leite SB, Teixeira AP, Miranda JP, Tostões RM, Clemente JJ, Sousa MF, Carrondo MJT, Alves PM. 2011. Merging bioreactor technology with 3D hepatocyte-fibroblast culturing approaches: Improved in vitro models for toxicological applications. *Toxicol. Vitr.* **25**:825–832.

Lutolf MP, Hubbell JA. 2005. Synthetic biomaterials as instructive extracellular microenvironments for morphogenesis in tissue engineering. *Nat. Biotechnol.* **23**:47–55.

El Manoubi L, Callikan S, Duee PH, Ferre P, Girard J. 1983. Development of gluconeogenesis in isolated hepatocytes from the rabbit. *Am. J. Physiol.* **244**:E24–30.

March S, Hui EE, Underhill GH, Khetani S, Bhatia SN. 2009. Microenvironmental regulation of the sinusoidal endothelial cell phenotype in vitro. *Hepatology* **50**:920–928.

Martinsen A, Skjåk-Braek G, Smidsrød O. 1989. Alginate as immobilization material: I. Correlation between chemical and physical properties of alginate gel beads. *Biotechnol. Bioeng.* **33**:79–89.

Masyuk AI, Masyuk T V., LaRusso NF. 2008. Cholangiocyte primary cilia in liver health and disease. *Dev. Dyn.*

Milosevic N, Schawalder H, Maier P. 1999. Kupffer cell-mediated differential down-regulation of cytochrome P450 metabolism in rat hepatocytes. *Eur. J. Pharmacol.* **368**:75–87.

Miranda JP, Leite SB, Muller-Vieira U, Rodrigues A, Carrondo MJ, Alves PM. 2009. Towards an extended functional hepatocyte in vitro culture. *Tissue Eng. Part C, Methods* **15**:157–167.

Miranda JP, Rodrigues A, Tostões RM, Leite S, Zimmerman H, Carrondo MJ, Alves PM. 2010. Extending hepatocyte functionality for drug-testing applications using high-viscosity alginate-encapsulated three-dimensional cultures in bioreactors. *Tissue Eng. Part C, Methods* **16**:1223–1232.

Murray JW, Thosani AJ, Wang P, Wolkoff AW. 2011. Heterogeneous accumulation of fluorescent bile acids in primary rat hepatocytes does not correlate with their homogenous expression of ntcp. *Am. J. Physiol. Gastrointest. Liver Physiol.* **301**:G60–8.

Pan XP, Li LJ. 2012. Advances in cell sources of hepatocytes for bioartificial liver. *Hepatobiliary Pancreat. Dis. Int.*

Puche JE, Saiman Y, Friedman SL. 2013. Hepatic stellate cells and liver fibrosis. *Compr. Physiol.* **3**:1473–1492.

Qiu L, Wang J, Wen X, Wang H, Wang Y, Lin Q, Du Z, Duan C, Wang C, Wang C. 2012. Transplantation of co-microencapsulated hepatocytes and HUVECs for treatment of fulminant hepatic failure. *Int. J. Artif. Organs* **35**:458–65.

Salerno S, Campana C, Morelli S, Drioli E, De Bartolo L. 2011. Human hepatocytes and endothelial cells in organotypic membrane systems. *Biomaterials* **32**:8848–59.

Santos E, Pedraz JL, Hernández RM, Orive G. 2013. Therapeutic cell encapsulation: Ten steps towards clinical translation. *J. Control. Release*.

Schwartz RE, Fleming HE, Khetani SR, Bhatia SN. 2014. Pluripotent stem cell-derived hepatocyte-like cells. *Biotechnol. Adv.*

Sgroi A, Mai G, Morel P, Baertschiger RM, Gonelle-Gispert C, Serre-Beinier V, Buhler LH. 2011. Transplantation of encapsulated hepatocytes during acute liver failure improves survival without stimulating native liver regeneration. *Cell Transplant.* **20**:1791–1803.

Spence JR, Mayhew CN, Rankin SA, Kuhar M, Vallance E, Tolle K, Hoskins EE, Kalinichenko V V, Wells I, Zorn AM, Shroyer NF, Wells JM. 2011. Directed differentiation of human pluripotent stem cells into intestinal tissue in vitro. *Nature* **470**:105–109.

Takebe T, Sekine K, Enomura M, Koike H, Kimura M, Ogaeri T, Zhang R-R, Ueno Y, Zheng Y-W, Koike N, Aoyama S, Adachi Y, Taniguchi H. 2013. Vascularized and functional human liver from an iPSC-derived organ bud transplant. *Nature* **499**:481–4.

Thomas RJ, Bhandari R, Barrett DA, Bennett AJ, Fry JR, Powe D, Thomson BJ, Shakesheff KM. 2005. The effect of three-dimensional co-culture of hepatocytes and hepatic stellate cells on key hepatocyte functions in vitro. *Cells. Tissues. Organs* **181**:67–79.

Tostões RM, Leite SB, Miranda JP, Sousa M, Wang DI, Carrondo MJ, Alves PM. 2011. Perfusion of 3D encapsulated hepatocytes--a synergistic effect enhancing long-term functionality in bioreactors. *Biotechnol. Bioeng.* **108**:41–49.

Tostões RM, Leite SB, Serra M, Jensen J, Bjorquist P, Carrondo MJ, Brito C, Alves PM. 2012. Human liver cell spheroids in extended perfusion bioreactor culture for repeated-dose drug testing. *Hepatology* **55**:1227–1236.

Treyer A, Müsch A. 2013. Hepatocyte polarity. *Compr. Physiol.* **3**:243–287.

Tukov FF, Maddox JF, Amacher DE, Bobrowski WF, Roth RA, Ganey PE. 2006. Modeling inflammation-drug interactions in vitro: A rat Kupffer cell-hepatocyte coculture system. *Toxicol. Vitr.* **20**:1488–1499.

Uygun BE, Soto-Gutierrez A, Yagi H, Izamis M-L, Guzzardi MA, Shulman C, Milwid J, Kobayashi N, Tilles A, Berthiaume F, Hertl M, Nahmias Y, Yarmush ML, Uygun K. 2010. Organ reengineering through development of a transplantable recellularized liver graft using decellularized liver matrix. *Nat. Med.* **16**:814–820.

Uygun BE, Yarmush ML. 2013. Engineered liver for transplantation. *Curr. Opin. Biotechnol.*

Le Vee M, Jigorel E, Glaise D, Gripon P, Guguen-Guillouzo C, Fardel O. 2006. Functional expression of sinusoidal and canalicular hepatic drug transporters in the differentiated human hepatoma HepaRG cell line. *Eur. J. Pharm. Sci.* **28**:109–117.

Westerink WMA, Schoonen WGEJ. 2007. Cytochrome P450 enzyme levels in HepG2 cells and cryopreserved primary human hepatocytes and their induction in HepG2 cells. *Toxicol. In Vitro* **21**:1581–1591.

Wolf KK, Brouwer KR, Pollack GM, Brouwer KLR. 2008. Effect of albumin on the biliary clearance of compounds in sandwich-cultured rat hepatocytes. *Drug Metab. Dispos.* **36**:2086–92.

Yang Y, Li J, Pan X, Zhou P, Yu X, Cao H, Wang Y, Li L. 2013. Co-culture with mesenchymal stem cells enhances metabolic functions of liver cells in bioartificial liver system. *Biotechnol. Bioeng.* **110**:958–68.

Zamek-Gliszczynski MJ, Xiong H, Patel NJ, Turncliff RZ, Pollack GM, Brouwer KLR. 2003. Pharmacokinetics of 5 (and 6)-carboxy-2',7'-dichlorofluorescein and its diacetate promoiety in the liver. *J. Pharmacol. Exp. Ther.* **304**:801–809.

Zhang S, Chen L, Liu T, Zhang B, Xiang D, Wang Z, Wang Y. 2012. Human umbilical cord matrix stem cells efficiently rescue acute liver failure through paracrine effects rather than hepatic differentiation. *Tissue Eng. Part A* **18**:1352–64.

CHAPTER 2

Optimization of the isolation of human hepatocytes from resected liver tissue towards 3D culture

TABLE OF CONTENTS

ABSTRACT

Human resected liver tissue is a potential source of mature hepatocytes, which retain most hepatic features and are representative of the population variability, being useful for *in vitro* culture. The culture of hepatocytes as three-dimensional spheroids (3D) has been proven to be an efficient strategy to sustain long term functions of hepatocytes. However, most of the protocols available have been developed for monolayer culture and may not be adjusted for the aggregation of hepatocytes. Moreover, the factors affecting the efficiency of isolation are controversial, being important the selection of the best candidates for isolation.

This chapter describes the optimization of the isolation of hepatocytes from resected liver tissue towards 3D culture of hepatocyte spheroids. 21 liver samples obtained from patients undergoing liver resection were processed according to a modified two-step collagenase perfusion. A descriptive analysis of the most critical variables for the quality of the isolation and hepatocytes obtained was performed. For perfusion optimization 4 variables were manipulated. The yield of hepatocytes after isolation, hepatocyte viability, adhesion and aggregation in stirred systems were assessed to evaluate the perfusion performance. An average yield of 4.4±1.4 x 10^6 hepatocytes *per* gram of tissue perfused and an average viability of 55.3±3.8% were obtained with the optimized protocol. Additionally, hepatocyte aggregation significantly improved, showing the optimized protocol is adequate for the 3D culture of hepatocytes in stirred conditions.

In conclusion, the established protocol is suitable for the isolation of hepatocytes from resected liver tissue and the obtained hepatocytes may be cultured as 3D cell spheroids, for application in biotechnology and tissue engineering fields.

1. Introduction

The liver is responsible for maintaining body homeostasis, biosynthetic metabolism and drug detoxification. Despite the significant contribution of animal studies to understand liver physiology and pathology, some cellular mechanisms differ significantly between species. Thus, *in vitro* models of human hepatocytes are critical for elucidating hepatocellular mechanisms and pathways, which may be applied in translational research and toxicology. Moreover, cell therapy using human hepatocytes is a potential solution to overcome the shortage of liver donors to treat patients with liver failure and human hepatocytes may also be used as biocomponents in extracorporeal liver support devices (Struecker et al., 2013). Thus, it is necessary to obtain high quality hepatocytes in enough quantities to be applied in the aforementioned areas.

Isolation of adult hepatocytes from the liver using the two-step collagenase perfusion method has been first described by Berry and Friend (Friend and Berry, 1969) and modified by Seglen (Seglen, 1976) using adult rats. This technique has later been adapted to the isolation of human hepatocytes from whole organs from cadaveric donors (Alexandrova et al., 2005; Anon, Baccarani et al., 2003) or resected liver tissue from patients undergoing surgical hepatectomy (Lecluyse and Alexandre, 2010; Vondran et al., 2008), being a valuable source for the *in vitro* culture of human hepatocytes.

The two-step perfusion method is based on the liver perfusion through the vasculature, by the use of catheters placed into the major vessels of the liver. The key aspect of the process is to ensure efficient tissue perfusion by the existence of a good vascular network, without leaky vessels and, preferentially, with a tissue sample encapsulated in the Glisson´s capsule. The first step of perfusion makes use of buffers to remove blood and pre-warm the tissue to ensure the optimal temperature for collagenase activity. Moreover, during this step, most protocols use solutions containing calcium-chelating reagents such as Ethylene Glycol Tetraacetic Acid (EGTA) to promote calcium depletion within the tissue. The calcium depletion will cause a structural alteration in the desmossomes, responsible for cell-cell adhesion, disrupting the cell-cell contacts within the tissue and, thereby, loosening the tissue. Afterwards, a second step of perfusion with collagenase is performed, to digest the extracellular matrix mostly composed of collagen, leading to complete tissue loosening and disruption (Godoy et al., 2013). Despite the number of protocols that has arisen in the recent years, the isolation of hepatocytes from resected liver tissue is still an inefficient process. Moreover, the effect of the perfusion protocols on the aggregation of hepatocytes, which results in three-dimensional (3D) structures with differentiated functions for long-term, has barely been addressed and improvements on the current protocols may contribute to improve the aggregation process.

There are several variables affecting the success of hepatocyte isolation, which may be subdivided into 3 subgroups: donor information and pre-operative factors, liver sample characteristics and collection and tissue processing and cell isolation (Table 2.1). Several studies have evaluated the factors that mostly affect the isolation procedure, with the aim of predicting the best candidates for hepatocyte isolation. Nevertheless, the data originated is somewhat controversial, with the donor age, liver pathologies such as fibrosis, steatosis and cirrhosis, chemotherapy and time of ischemia among the most significant variables affecting the isolation procedure (Kawahara et al., 2010; Lee et al., 2014; Lloyd et al., 2004; Vondran et al., 2008).

In this work, the protocol for the isolation of human hepatocytes from resected liver tissue was developed and optimized using a two-step collagenase-based isolation method. Liver samples from 21 patients undergoing hepatic resection were used. A descriptive analysis of the non-controlled variables and the controlled variables, which encompass optimization of the isolation process, were performed. Finally, the impact of these variables on the efficiency of isolation was assessed by evaluating the yield of the process, viability of hepatocytes and aggregation rate (Table 2.2).

Table 2.1 Variables potentially affecting efficiency of hepatocyte isolation from liver tissue and subsequent culture, including controlled and non-controlled variables assessed in this study.

	Variables	Categories/units
Non-controlled	**Donor information & perioperative factors**	
	Age	*years*
	Gender	Male; Female
	Surgical indication	CRC, HCC
	Chemotherapy	Yes, No
	Comorbidities	None; DM ; D; MS ; HT; CRP; CCP ; Other
	Clinical chemistry	
	AST	*U/L*
	ALT	*U/L*
	BilT	*mg/dL*
	Sample characteristics & collection	
	Weight of perfused liver	*g*
	Histopathology	Normal parenchyma; Steatosis (mild, moderate, severe); Cirrhosis
	Time of cold ischemia	*min*
Controlled	**Tissue processing and cell isolation**	
	Type of collagenase	(1) Collagenase P (2) collagenase type IV
	Time of digestion	min
	Buffers	(1) HEPES-EGTA + HEPES (2) HEPES only
	Purification	(1) 50*g*, 5 min (2) 180*g*, 2 min

M - Masculin; F - Feminin; CRC – Colorectal Carcinoma; HCC – Hepatocarcinoma; DM - Diabetes mellitus; D – Dysplidemia; MS - Metabolic syndrome; HT – Hypertension; CRP - Chronic respiratory pathology; CCP - Chronic cardiac pathlology ; AST – Aspartate Transaminase; ALT – Alanine Transaminase; BilT – Total bilirubin

Table 2.2 Outcome variables used to assess the efficiency of isolation in the study.

Outcome variables	Categories/Units
Isolation yield	Viable cell/g tissue
Viability	%
Adhesion rate (12h post-isolation)	No adhesion; sub-confluence; confluence
Aggregation rate (72h post-isolation)	No aggregation; Average aggregate diameter ≤ 50 μm; Average aggregate diameter ≥ 50 μm

2. Material and methods

2.1 Biological material source and collection

Liver samples were collected from Hospital Curry Cabral (HCC) and Hospitais Universitários de Coimbra (HUC) from 23 patients who underwent partial hepatectomy, due to secondary liver tumor or hepatocarcinoma. Sample collection was performed according to the ethical and institutional guidelines. Immediately after surgical resection, the liver tissue was analyzed by the surgeon, who selected the tissue to histopathological evaluation and discarded the remaining tissue. The discarded fraction, preferentially enclosing the Glisson´s capsule, was collected for isolation and maintained in cold HEPES buffer (10 mM HEPES 136 mM NaCl, 5 mM KCl, 0.5 % (w/v) Glucose, pH 7.6) for a period ranging from 30 min to 4h before beginning the isolation procedure.

2.2 Hepatocyte isolation

The liver collection and subsequent hepatocyte isolation was performed in sterile conditions (laminar flow hood) by a single individual (S.P.R.) to eliminate interindividual variability. The liver segments were flushed with HEPES buffer at 4ºC to remove excess blood and were examined for the presence of blood vessels. Depending on vessels' availability, size and interconnection, 2-3 vessels were chosen to proceed with the perfusion and, in cases where leaky vessels were present, they were clamped with a needle and thread. The buffers were pre-warmed to 42ºC in a water bath and the liver tissue was maintained at a temperature of approximately 37ºC throughout the entire procedure. The perfusion and purification processes were optimized, by manipulating the variables assigned as controlled variables in Table 1.1. The variables were manipulated in a combined manner, thus the combination of variables 1) is hereafter classified as method 1 and the combination of variables 2) is classified as method 2.

2.2.1 Perfusion – First step

The liver segment was either 1) perfused with HEPES buffer with 0.5 mM EGTA (HEPES-EGTA) for 10-15 min and then perfused with HEPES buffer for an additional period of 10 min or 2) perfused with HEPES buffer for 10-15 min only. This step was performed without recirculation.

2.2.2 Perfusion – Second step

The tissue was immediately perfused with HEPES buffer supplemented with 70 mM $CaCl_2$ (HEPES-$CaCl_2$) and either 1) 0.5 g/L of Collagenase P (Roche, Basel, Switzerland) or 2) 0.64 g/L Collagenase type IV (Worthington Biochemical corporation, NJ, USA). The solution was perfused with recircularization for 10-15 min, until the tissue started to dissociate.

2.2.3 Tissue disruption and hepatocyte purification

The digested liver segment was transferred to a new vessel and covered with HEPES buffer supplemented with 5 g/L of BSA to stop the collagenase digestion. The tissue was gently disrupted and filtered through a nylon mesh of 100 µm.

2.2.4 Hepatocyte purification

Hepatocyte suspension was purified by 3 sequential centrifugation steps according to 2 different procedures: 1) 50 *g* for 5 min or 2) 180 *g* for 2 min, both at 4ºC. After each centrifugation step, the cell pellet was gently ressuspended by successive pipetting up and down 5 times.

2.3 Hepatocyte culture

Freshly isolated hepatocytes (FIH) were cultured in Williams' E medium (Sigma-Aldrich, St. Lois, MO) supplemented with 1% (v/v) GlutaMAX™, 1% (v/v) penicillin/streptavidin, 10% (v/v) FBS (all from Gibco/Invitrogen, Grand Island, NY) and the Hepatocyte Culture Medium (HCM) SingleQuots kit (Lonza, Switzerland).

2.3.1 2D culture

FIH were seeded onto 24 wells collagen-coated culture plates (BD, Bedford, UK) at cell concentrations ranging from 2 to 2.75 × 10^5 cell/cm^2 and cultured in 37°C in a humidified atmosphere with 5% CO_2. The culture medium was changed 8-12 h after cell seeding.

2.3.2 3D culture

FIH were inoculated using an inoculum concentration of 5x10^5 total cell/mL in spinner vessels equipped with paddle (Wheaton) or trapezoid impellers (Corning) and stirred at 50 rpm.

2.4 Efficiency of isolation

Four outcome variables were used to assess the efficiency of isolation (Table 2):

2.4.1 Cell viability

The number of viable and non-viable cells was estimated by the Trypan blue exclusion method. Cells were counted in a haemacytometer chamber (Marienfeld- Superior, Lauda-konigshofen).

2.4.2 Isolation yield

The yield of isolation was estimated based on the total viable cells obtained at the end of isolation, which were quantified by the Trypan blue exclusion method, per gram of liver tissue perfused.

2.4.3 Hepatocyte adhesion

The adhesion was analyzed by microscopic visualization and determined based on the area of cell-covered surface 12h after seeding. 3 categories were established, based on the percentage of total surface covered: 0 to 20%- no adhesion; 20 to 70 % - sub-confluence; 70 to 100% - confluence.

2.4.4 Hepatocyte aggregation

Aggregate size was determined by measuring Ferret's diameter using the open source ImageJ software version 1.47m. The aggregation was classified according to the aggregate size at 72h: no aggregation (clusters of 2-3 cells); aggregates with average diameters ≤ 50 µm; aggregates with average diameters ≥ 50 µm.

2.5 Data analysis and statistics

Standard descriptive analysis were used to describe the data. Data are expressed as the mean ± standard error of the mean (SEM). Mean comparisons were performed using an unpaired Student´s t test. Correlation between independent and categorical dependent variables were performed using

the Chi-squared test. Correlations between independent and continuous dependent variables were performed by linear regression (univariate) or multiple regression analysis (multivariate). A 95% confidence interval was considered to be significant and statistical significance was defined based on *p*-value (***p<0.001; **p<0.01; *p<0.05). Analysis were performed using GraphPad Prism (version 5.01) or SPSS Statistics (version 17.0)

3. Results

3.1 Characterization of the donor population

From the 23 liver samples collected, 21 were processed for hepatocyte isolation. Two liver samples were discarded due to the low weight (below 5 g) and fibrotic tissue. The population of liver donors had an average age of 66.2 years old, with a minimal age of 50 and a maximum of 78. From the total population, 16 donors were male and 5 were female. Regarding the indication for surgery, 91% of the resected livers were originated from patients with metastasis in the liver originated from Colorectal Carcinoma (CRC) and 9% from patients with Hepatocellular carcinoma (HCC). 17 donors had undergone previous chemotherapy, with an average of 8.6 cycles (Table 2.3).

Table 2.3 Donor information and perioperative factors.

Category	Data
Age	66.2 ± 2.1
Gender	M (16); F (5)
Indication	CRC (19); HCC (2)
Chemotherapy	Yes (17); No (4)
Comorbidities	None (4); DM (2); D (1) MS (1); HT (3); CRP (3); CCP (3); Other (3)
Clinical chemistry	
ALT	547 ± 105
AST	694 ± 119
BilT	1.13 ± 0.11

M - Masculin; F - Feminin; CRC – Colorectal Carcinoma; HCC – Hepatocarcinoma; DM - Diabetes mellitus; D – Dysplidemia; MS - Metabolic syndrome; HT – Hypertension; CRP - Chronic respiratory pathology; CCP - Chronic cardiac pathlology ; AST – Aspartate Transaminase; ALT – Alanine Transaminase; BilT – Total bilirubin

Regarding the sample characteristics, the average weight of the samples collected was 32.6 g (Figure 2.1 A). The histopathological evaluation of the tissue indicated the existence of pathologies including mild cirrhosis (5%), and mild to severe steatosis, representing a total of 48% (mild – 33%, moderate – 9%, severe – 5%) (Figure 2.1 B). Cold ischemia time, which corresponds to the time the liver segment was maintained at 4ºC during collection and transport, was on average 148 ± 21 min (Figure 2.1 C). The warm ischemia time was not herein considered due to insufficient data.

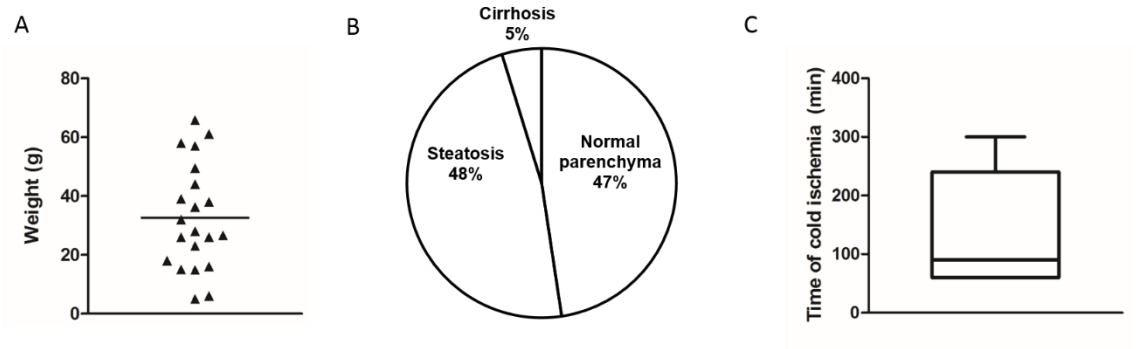

Figure 2.1 Sample characteristics and collection information. A) Weight distribution of the liver samples. B) Histophatological evaluation of the non-tumoral parenchyma. C) Cold ischemia time (time maintained at 4ºC).

3.2 Perfusion process optimization

Process optimization implied the manipulation of variables in the first and second perfusion steps and in the purification procedure, according to method 1 or 2. The removal of HEPES-EGTA perfusion in the first step and alteration of the type of collagenase in the second step of perfusion affected the total perfusion time, which can also account for the efficiency of isolation. Among the total liver samples perfused, 7 samples were perfused using method 1 and 14 samples were processed according to method 2. The total time of the perfusion process was significantly reduced from 46.7±4.9 to 24.5±0.9 min (Figure 2.2), with an average reduction of collagenase digestion time of approximately 30%.

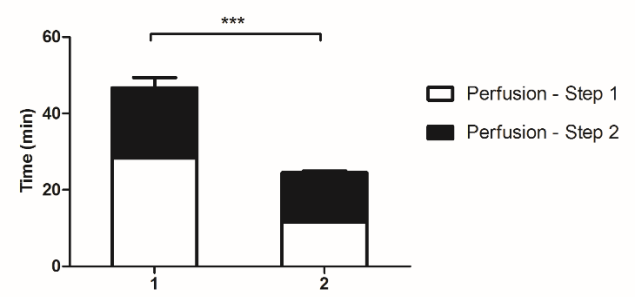

Figure 2.2 Comparison of perfusion process time between methods 1 and 2. Perfusion – step 1 and 2 average perfusion times are indicated by white and black areas, respectively. Asterisks indicate significant differences between protocols (*** p≤0.001).

Hepatocyte yield, viability, adhesion in 2D collagen-coated plates and aggregation in stirred culture were the outcome variables used to evaluate the success of the isolation procedure. Although the viability was comparable between both protocols, the isolation yield was significantly higher using method 2, increasing from an average of 1.2±0.4 to 4.4±1.4 x 10^6 viable cells *per* gram of tissue perfused (Figure 2.3 A, B), which represents a fold increase of 3.7. The number of sub-confluent and confluent cultures in 2D collagen-coated plates also improved with perfusion method 2 (Figure 2.3 C), resulting in 5 confluent cultures (Figure 2.4 A).

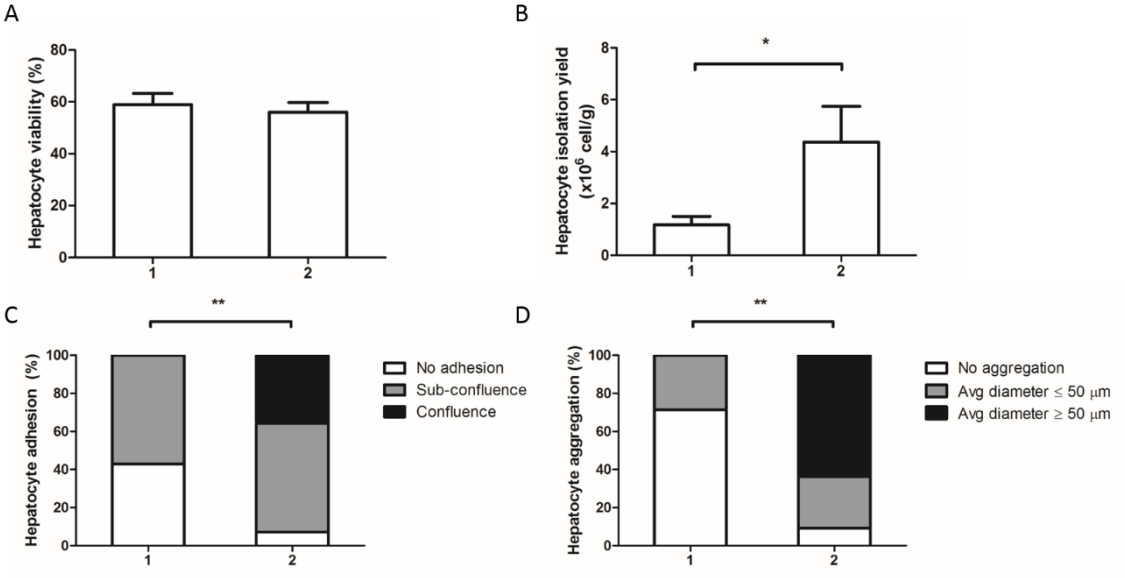

Figure 2.3 Effect of perfusion methods on isolation outcome variables. A) Hepatocyte viability. B) Hepatocyte yield. C) Hepatocyte adhesion to collagen-coated plates (2D). D) Hepatocyte aggregation in stirred culture (3D). Asterisks indicate significant differences between protocols (* p≤0.05; ** p≤0.01).

Aggregation of FIH in stirred culture significantly improved using perfusion method 2, with 91% of aggregation (Figure 2.3 D). The aggregation was only evaluated in 11 cultures, since three liver perfusions yielded an insufficient cell number for 3D culture. The aggregation profile varied among different isolation processes, typically forming duplets and triplets in the first 24h and compact spheroids after 72h (Figure 2.4 B).

Although the average yield improved using method 2, its variation between samples was high. The correlation between the variables described in Table 1.1 and viability and yield was performed using univariate and multivariate analysis, but no significant correlations (p>0.05) were determined (data not shown).

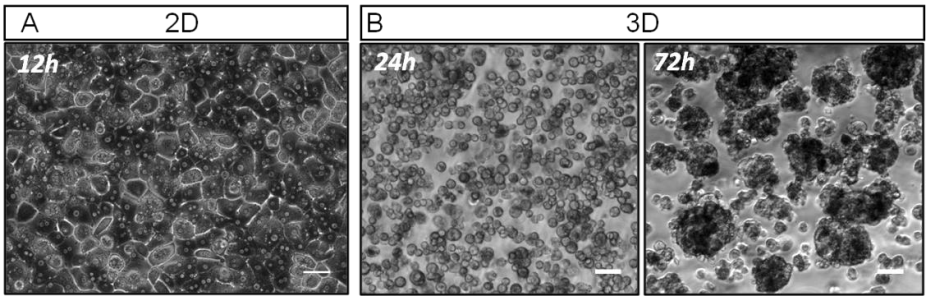

Figure 2.4 2D and 3D culture of isolated hepatocytes. A) 2D cultures 12h after seeding. B) Aggregates after 24 and 72h of inoculation.

4. Discussion

The protocol of hepatocyte isolation from resected liver tissue was successfully implemented and further optimized at iBET and primary cultures of hepatocytes were inoculated in stirred vessels and cultured in 3D. The isolation protocol was optimized, being achieved an average yield of 4.4±1.4 x 10^6 hepatocytes per gram of tissue, an average viability of 55.3±3.8% and a significant improvement in hepatocyte adhesion and aggregation in stirred culture.

Protocol optimization involved 3 major changes: removal of the HEPES-EGTA perfusion step, change of the type of enzyme used (from collagenase P to IV) and centrifugation speed and duration. EGTA is a calcium-chelating agent used to disrupt cell-cell adhesions during perfusion to facilitate the isolation process. The depletion of Ca^{2+} and inherent structural change in cell-cell adhesion molecules caused by EGTA presence might decrease the aggregative potential of hepatocytes. Thus, it was hypothesized that its removal could improve the aggregation process. A previous study with rat hepatocytes has shown that EGTA removal in the first perfusate combined with calcium removal in the second perfusate did not influence isolation yield neither viability but had a strong impact on the efficiency of aggregation (Okubo et al., 2002). Moreover, the removal of the HEPES-EGTA led to a reduction of perfusion time. Since the resected liver tissue is maintained in warm conditions (37ºC) during perfusion, the reduction of the procedure time may improve cell viability due to minimization of ischemia and enhance cell integrity, which is affected by enzymatic activity.

Regarding the digestion step, the collagenase P is a mixture of at least 12 different enzymes, of which collagenases form the biggest group of active enzymes. Collagenase type IV is purified, well characterized and, in contrast to crude preparations, it contains less lot-variable contaminating proteases, esterases and other enzymes. Moreover, it has less tryptic activity compared to other collagenase types, being commonly used for applications where receptor integrity is required. All the aforementioned characteristics account for a potential collagen digestion with reduced effects on cell integrity. Finally, the reduction of centrifugation time combined with higher acceleration, might have contributed to a more selective centrifugation process, in which cell debris and other isolation contaminants were removed. Although this aspect may not have had impact on yield and viability, it may have affected the adhesive and aggregative potential of the hepatocytes. To depict the impact of each controlled variable in the isolation performance, further studies with individual manipulation of variables would be necessary. However, it may be concluded that, altogether, the protocol optimization resulted in an improvement of the yield, viability, adhesive properties for 3D culture.

The yield and viability obtained with the optimized protocol are comparable with the data existent in the literature, in which the average yields range from 4 to 13 x 10^6 hepatocytes per gram of liver tissue and viabilities from 40 to 89% (Alexandre et al., 2002; Bhogal et al., 2011; Hewes et al., 2006; Kawahara et al., 2010; Lee et al., 2014; Lloyd et al., 2004; Vondran et al., 2008). Nevertheless, a substantial variability in the yields attained using perfusion method 2 was observed. The univariate and multivariate analysis performed did not indicate significant correlations between the variables studied and the yields attained. This might be related with the statistical power of analysis due to the sample number (n=14). The few studies that could establish significant correlations between donor or sample characteristics with the outcome of the isolation have used larger samples (Alexandre et

al., 2002; Kawahara et al., 2010; Lee et al., 2014). Though, variables such as the donor age have been have been consistently associated with poor isolation outcomes, including viability, yield (Lee et al., 2014; Lloyd et al., 2004; Vondran et al., 2008) and unsuccessful engraftment in mice (Kawahara et al., 2010). Similarly, liver sample weight, the presence of liver fat, high AAT and Bilirrubin levels and time of ischemia have also accounted for low yields in isolation (Alexandre et al., 2002; Lee et al., 2014; Lloyd et al., 2004). Although studies indicate that previous chemotherapy treatment has no impact in isolation yield (Alexandre et al., 2002; Hewes et al., 2006), recent results have shown that the treatment may be associated with higher efficient isolations due to the reduction of ECM in the liver prior to the isolation (Lee et al., 2014). Overall, considering the samples might have been suboptimal for isolation, the results obtained with the isolation procedure are acceptable. Finally, this study has shown that isolation of hepatocytes from resected liver tissue was successfully implemented and that the two step perfusion protocol was optimized by modifying the 1st and 2nd steps of perfusion and purification. The protocol modification led to a higher isolation yield and an increase of the adhesive and aggregative potential of the hepatocytes isolated. Thus, this protocol is suitable for the 3D culture of human hepatocytes isolated from resected liver tissue.

Acknowledgments

I gratefully acknowledge to Dr. H. Alexandrino and Prof. J. Tralhão from Hospitais Universitários de Coimbra and Dr. S. Silva and Dr. P. Marcelino from Hospital Curry Cabral for the supply of biological material and collaboration in the primary human hepatocyte project; to Rita Costa for the support and collaboration in the isolation procedure; to Ruoya Li and Christophe Chesné from Biopredic for sharing protocols and knowledge on the isolation procedure.

5. Bibliography

Alexandre E, Cahn M, Abadie-Viollon C, Meyer N, Heyd B, Mantion G, Cinqualbre J, David P, Jaeck D, Richert L. 2002. Influence of pre-, intra- and post-operative parameters of donor liver on the outcome of isolated human hepatocytes. *Cell Tissue Bank.* **3**:223–33.

Alexandrova K, Griesel C, Barthold M, Heuft H-G, Ott M, Winkler M, Schrem H, Manns MP, Bredehorn T, Net M, Vidal MMI, Kafert-Kasting S, Arseniev L. 2005. Large-scale isolation of human hepatocytes for therapeutic application. *Cell Transplant.* **14**:845–853.

Baccarani U, Sanna A, Cariani A, Sainz-Barriga M, Adani GL, Zambito AM, Piccolo G, Risaliti A, Nanni-Costa A, Ridolfi L, Scalamogna M, Bresadola F, Donini A. 2003. Isolation of human hepatocytes from livers rejected for liver transplantation on a national basis: results of a 2-year experience. *Liver Transpl.* **9**:506–12.

Bhogal RH, Hodson J, Bartlett DC, Weston CJ, Curbishley SM, Haughton E, Williams KT, Reynolds GM, Newsome PN, Adams DH, Afford SC. 2011. Isolation of primary human hepatocytes from normal and diseased liver tissue: a one hundred liver experience. *PLoS One* **6**:e18222.

Friend DS, Berry MN. 1969. ISOLATED RAT LIVER PARENCHYMAL CELLS A Biochemical and Fine Structural Study. *J. Cell Biol.* **43**.

Godoy P, Hewitt NJ, Albrecht U, Andersen ME, Ansari N, Bhattacharya S, Bode JG, Bolleyn J, Borner C, Böttger J, Braeuning A, Budinsky R a, Burkhardt B, Cameron NR, Camussi G, Cho C-S, Choi Y-J, Craig Rowlands J, Dahmen U, Damm G, Dirsch O, Donato MT, Dong J, Dooley S, Drasdo D, Eakins R, Ferreira KS, Fonsato V, Fraczek J, Gebhardt R, Gibson A, Glanemann M, Goldring CEP, Gómez-Lechón MJ, Groothuis GMM, Gustavsson L, Guyot C, Hallifax D, Hammad S, Hayward A,

Häussinger D, Hellerbrand C, Hewitt P, Hoehme S, Holzhütter H-G, Houston JB, Hrach J, Ito K, Jaeschke H, Keitel V, Kelm JM, Kevin Park B, Kordes C, Kullak-Ublick G a, LeCluyse EL, Lu P, Luebke-Wheeler J, Lutz A, Maltman DJ, Matz-Soja M, McMullen P, Merfort I, Messner S, Meyer C, Mwinyi J, Naisbitt DJ, Nussler AK, Olinga P, Pampaloni F, Pi J, Pluta L, Przyborski S a, Ramachandran A, Rogiers V, Rowe C, Schelcher C, Schmich K, Schwarz M, Singh B, Stelzer EHK, Stieger B, Stöber R, Sugiyama Y, Tetta C, Thasler WE, Vanhaecke T, Vinken M, Weiss TS, Widera A, Woods CG, Xu JJ, Yarborough KM, Hengstler JG. 2013. Recent advances in 2D and 3D in vitro systems using primary hepatocytes, alternative hepatocyte sources and non-parenchymal liver cells and their use in investigating mechanisms of hepatotoxicity, cell signaling and ADME. *Arch. Toxicol.* Vol. 87 1315-530 p.

Hewes JC, Riddy D, Morris RW, Woodrooffe AJ, Davidson BR, Fuller B. 2006. A prospective study of isolated human hepatocyte function following liver resection for colorectal liver metastases: the effects of prior exposure to chemotherapy. *J. Hepatol.* **45**:263–70.

Kawahara T, Toso C, Douglas DN, Nourbakhsh M, Lewis JT, Tyrrell DL, Lund G a, Churchill T a, Kneteman NM. 2010. Factors affecting hepatocyte isolation, engraftment, and replication in an in vivo model. *Liver Transpl.* **16**:974–82.

Lecluyse EL, Alexandre E. 2010. Hepatocytes. Ed. Patrick Maurel. Totowa, NJ: Humana Press. Vol. 640. Methods in Molecular Biology.

Lee SML, Schelcher C, Laubender RP, Fröse N, Thasler RMK, Schiergens TS, Mansmann U, Thasler WE. 2014. An algorithm that predicts the viability and the yield of human hepatocytes isolated from remnant liver pieces obtained from liver resections. *PLoS One* **9**:e107567.

Lloyd TDR, Orr S, Patel R, Crees G, Chavda S, Vadyar H, Berry DP, Sherlock D, Dennison a R. 2004. Effect of patient, operative and isolation factors on subsequent yield and viability of human hepatocytes for research use. *Cell Tissue Bank.* **5**:81–7.

Okubo H, Matsushita M, Kamachi H, Kawai T, Takahashi M, Fujimoto T, Nishikawa K, Todo S. 2002. A Novel Method for Faster Formation of Rat Liver Cell Spheroids. *Artif. Organs* **26**:497–505.

Seglen PO. 1976. Chapter 4 Preparation of Isolated Rat Liver Cells. *Methods Cell Biol.* **13**:29–83.

Struecker B, Raschzok N, Sauer IM. 2013. Liver support strategies: cutting-edge technologies. *Nat. Rev. Gastroenterol. Hepatol.* **11**:166–176.

Vondran FWR, Katenz E, Schwartlander R, Morgul MH, Raschzok N, Gong X, Cheng X, Kehr D, Sauer IM. 2008. Isolation of primary human hepatocytes after partial hepatectomy: criteria for identification of the most promising liver specimen. *Artif. Organs* **32**:205–13.

CHAPTER 3

3D co-culture of human hepatocytes and mesenchymal stem cells in bioreactors

This chapter was adapted from:

Rebelo SP, Costa R, Silva M, Marcelino P, Brito C, Alves PM. 2014. 3D co-culture of human hepatocytes and mesenchymal stem cells: improved functionality in long-term bioreactor cultures. Submitted to J Tissue Eng Regen Med

TABLE OF CONTENTS

ABSTRACT

The development of human cell models that can efficiently restore hepatic functionality and cope with the reproducibility and scalability required for preclinical development poses a significant effort in tissue engineering and biotechnology. Primary cultures of human hepatocytes (HH), the preferred model for *in vitro* toxicity testing, dedifferentiate and have short-term viability in two-dimensional cultures (2D). In this work, hepatocytes isolated from human liver tissue were co-cultured with human bone marrow mesenchymal stem cells (BM-MSC) as spheroids in automated computer-controlled stirred tank bioreactors with perfusion operation mode. A dual step inoculation strategy was used, resulting in an inner core of parenchymal liver tissue with an outer layer of stromal cells. Hepatocyte polarization and morphology as well as the mesenchymal phenotype of BM-MSC were maintained throughout the culture period and the crosstalk between the two cell types was depicted. The viability, compact morphology and phenotypic stability of hepatocytes were enhanced in co-cultures in comparison to mono-cultures. Gene expression of phase I and II enzymes was higher and CYP3A4 and CYP1A2 activity was inducible until the second week of culture, being applicable for repeated-dose toxicity testing. Moreover, the excretory activity was maintained in co-cultures and the biosynthetic hepatocellular functions (albumin and urea secretion) were not affected by the presence of BM-MSC. Overall, this strategy might be extended to other hepatic cell sources and the characterization performed brings knowledge on the interplay between both cell types, which may be relevant for therapeutic applications.

1. Introduction

The development of human cellular models that effectively recapitulate hepatic metabolism and the toxicological profile of drugs may be used for pre-clinical research, contributing to support efficient drug development processes and prevent drug induced liver injury (DILI) events. Pre-clinical studies in animal models fail to fully predict drug toxicity in humans due to inter-species variability in detoxification mechanisms. Hepatic immortalized cell lines and hepatocyte-like cells derived from pluripotent stem cells (PSC) are available but display low activity levels of the cytochrome P450 (CYP450) enzymes, requiring the development of tissue engineering strategies such as better differentiation and/or culture protocols (LeCluyse et al., 2012).

Primary cultures of human hepatocytes (HH) are still the preferred cellular model to undertake toxicological assessment, as they retain drug biotransformation activity and are representative of the metabolic variability among populations. Nevertheless, the rapid dedifferentiation of hepatocytes in adherent culture conditions results in loss of hepatocytic-specific functions and short-term viability, impeding its use for long-term toxicity assessment (Hewitt et al., 2007). Since the mechanisms underlying acute and chronic toxicity may differ substantially (Slikker Jr. et al., 2004), it is crucial to address the prolonged exposure to drugs in human cell models.

Several *in vitro* studies have reported the role of the stroma in the maintenance of differentiated hepatocytic phenotype by co-culturing hepatocytes with non-parenchymal liver cells such as liver sinusoidal endothelial cells (LSECs), stellate, kupffer and other non-hepatic cellular types (Khetani and Bhatia, 2008; Kostadinova et al., 2013). Mesenchymal stem cells (MSC) are multipotent stromal cells, presenting an inherent capacity to self-renew and differentiate into osteoblasts, adipocytes, and chondroblasts. Particularly, bone marrow-derived mesenchymal stem cells (BM-MSC) have immunomodulatory properties, making them suitable for cell therapy applications (Ghannam et al., 2010). The therapeutic potential of MSC has been evaluated in rats with acute liver failure (ALF) (Jung et al., 2013; Salomone et al., 2013), liver fibrosis (Kim et al., 2014; Nasir et al., 2013) or to induce regeneration after partial hepatectomy (Kaibori et al., 2012), showing the important role of MSC in supporting liver function *in vivo*. Moreover, few *in vitro* studies have reported the role of MSC on supporting proliferation, viability and improving functions of rat (Isoda et al., 2004; van Poll et al., 2008), porcine (Gu et al., 2009) and, recently, human hepatocytes in 2D (Fitzpatrick et al., 2015). Moreover, the co-culture of MSC with the hepatic cell line HepG2 has been applied to develop a bioartifical liver (BAL) (Yang et al., 2013) and the injection of BM-MSC in patients with alcoholic cirrhosis led to the improvement of hepatic fibrosis in a phase III clinical trial (Jang et al., 2014). Nevertheless, the underlying mechanisms of HH co-cultured with BM-MSC and the effects on human hepatic functionality remain largely unknown.

Liver engineering strategies that recreate the liver microenvironment and tissue architecture may overcome some of the limitations of *in vitro* culture of human hepatocytes. Primary cultures in the collagen sandwich model keep a stable phenotype up to two weeks due to the effects of the ECM and, primarily, to the quasi three-dimensional (3D) architecture acquired and mechanical tension exerted by the collagen overlay (Dunn et al., 1992). In cell spheroids, the 3D architecture is enhanced due to the maximization of cell-cell contacts, which allow the assembly of polarity proteins

and transporters, supporting some of the apical and basolateral polarity features of hepatocytes. The cell spheroid system has been broadly described for HH primary cultures, hepatic cell lines and PSC-derived hepatocytes (Godoy et al., 2013; Miranda et al., 2009).

Cell aggregation may be promoted by hydrodynamic forces in stirred systems, in which the enhanced mass transfer prevents the formation of necrotic centers and minimizes gradients. In computer controlled automated stirred tank bioreactors, the control of culture parameters such as dissolved oxygen (DO), pH, temperature and the gradual exchange of culture medium achieved by perfusion operation mode, minimizes microenvironment shifts (Tostões et al., 2011). In addition, perfusion bioreactors simulate the *in vivo* processes of drug biotransformation in which the concentration of the drug constantly changes, being an attractive tool to mimic chronic toxicity. Previous studies from our group have demonstrated the effects of automated bioreactor culture and perfusion on the maintenance of hepatic features in rat (Tostões et al., 2011) and human (Tostões et al., 2012) cultures, with stable liver-specific functions and *de novo* synthesis of CYP450 mRNA after repeated induction with prototypical inducers (Tostões et al., 2012).

This study describes a novel culture strategy based on the establishment of a 3D co-culture with human hepatocytes and mesenchymal stem cells in an automated stirred tank bioreactor environment. This is, to our knowledge, the first report of co-culture of primary cultures of human hepatocytes and BM-MSC in 3D and presents an extensive characterization of the hepatocytic and mesenchymal phenotypes throughout the culture period, allowing better comprehension of the interplay between the two cell types. Moreover, the co-culture was exposed to repeated dosage of Acetaminophen (APAP) to evaluate the applicability of HH-MSC spheroids as cell models for *in vitro* toxicological studies.

2. Materials and methods

2.1 Cell culture

2.1.1 Human hepatocyte isolation and culture

Human liver samples were obtained from patients undergoing liver resection due to secondary liver tumor (Table 1). Sample collection was performed according to the ethical and institutional guidelines, upon approval from the local ethical committee of Centro Hospitalar de Lisboa Central, EPE. Immediately after surgical resection, the liver tissue was analyzed by the surgeon, who selected the tissue to histopathological evaluation and discarded the remaining tissue. The discarded fraction was processed for isolation, according to the two-step collagenase method previously described by (Seglen, 1976) with slight modifications. Briefly, the liver piece was perfused with perfusion Buffer (PB: 0.01 M HEPES 0.136M NaCl, 0.005M KCl, 0.5 % (w/v) Glucose, pH 7.6) and, afterwards, with a solution of collagenase type IV (Worthington Biochemical corporation, NJ, USA) in PB. The liver was dissociated in PB with 5 g/L of BSA and filtrated through a nylon mesh of 100 µm. The suspension was purified by sequential centrifugation steps (2 min, 180 *g*, 4ºC) and the viability was assessed by the Trypan blue exclusion method. Freshly isolated hepatocytes were cultured in Williams' E (WE) medium (Sigma-Aldrich, St. Lois, MO) supplemented with 10% (v/v) FBS, 1% (v/v) GlutaMAX™, 1% (v/v) penicillin/streptavidin, (all from

Gibco/Invitrogen, Grand Island, NY) and Hepatocyte Culture Medium (HCM) SingleQuots kit (Lonza, Switzerland). As control for hepatocyte adhesion, cells were seeded onto 24-wells collagen-coated culture plates (BD, Bedford, UK) at a density of 0.4×10^6 cell/well and cultured in 37°C in a humidified atmosphere of 5% CO2.

T**able 3.1** Donor information.

Donor	Sex	Age
1	M	66
2	M	53
3	M	71

2.1.2 Human Bone Marrow Mesenchymal Stem cells culture

Bone marrow-derived human mesenchymal stem cells (hMSC cat. no MSC-0017; STEM CELL Technologies™, Grenoble, France) were cultured in MesenCult-XF medium (STEM CELL Technologies™) supplemented with 2mM L-Glutamine (Life Technologies, Carlsbon, USA), and propagated in tissue culture flasks, previously coated with MesenCult-SF Attachment Substrate (STEM CELL Technologies™), according to the manufacturer's instructions. For bioreactor cultures, hMSC in passages 3 to 5 were used. As a control, hMSC were seeded onto 24-wells plates in WE medium (Sigma-Aldrich, St. Lois, MO) supplemented as described above.

2.1.3 Three-dimensional culture

A dual-step 3D co-culture strategy was used, with an initial step of aggregation of HH in stirred conditions, using an inoculum of $5x10^5$ cell/ml and a stirring rate of 50-80 rpm. After 3 days of aggregation, the HH spheroid culture was diluted to a concentration of $1x10^5$ cell/mL and a single cell suspension of BM-MSC was inoculated at a concentration of $0.5x10^5$ cell/mL to attain a ratio of approximately 2:1 (HH to MSC), as it has previously been described as optimal ratio for this type of co-culture (Barakat et al., 2012; Yang et al., 2013). Monocultures from the same donor were cultured in parallel and used as control. Mono and co-cultures were maintained in 200 ml DASGIP bioreactors with a trapezoid-shaped paddle agitator (DASGIP Technology, Julich, Germany). The stirring rate during inoculation of MSC was 80 rpm, being adjusted up to 110 rpm throughout the culture. Perfusion was initiated 2 days after MSC inoculation and was kept at dilution rate of 0.2 day^{-1}.Bioreactor cultures were controlled at 37ºC, DO at 30% air saturation and pH at 7.4. WE culture medium supplemented as described above was used for aggregation and, when perfusion was initiated, the FBS was gradually removed to keep serum-free conditions.

2.2. Culture Characterization

2.2.1 Cell viability

Samples were collected periodically from the 3D cultures and used for cell viability monitorization by a fluorescent cell membrane integrity assay. Spheroids were incubated with the substrate Fluorescein Diacetate (FDA) (Sigma-Aldrich) at 10 µg/ml for detection of viable cells and the DNA dye TO-PRO®3 (Life Technologies) at 1 µM for visualization of dead cells. Spheroids were visualized by fluorescence microscopy (DMRB6000, Leica).

2.2.2 LDH activity

Cellular viability was assessed by measuring lactate dehydrogenase (LDH) activity from the culture supernatant. LDH activity was determined spectrophotometrically (at 340nm) following the conversion of pyruvate into lactate, by NADH oxidation to NAD^+. The rate of LDH release (LDH) was calculated for each time interval and normalized to the total cell number (estimated through nuclei counting), using the following equation:

$LDH = \Delta LDH/(\Delta t \times \Delta Xv)$, where ΔLDH is the change in LDH activity over the time period Δt, and ΔXv is the average of the total cell number during the same time period.

2.2.3 Nuclei counting

Culture samples were collected daily for nuclei counting (in duplicates). After supernatant removal, lysis solution (1% Triton in 0.1 M of Citric Acid) was added and incubated at 37ºC for 24h. The samples were diluted in 0.1% Crystal Violet solution (Merck Millipore, Darmstadt, Germany) and counted in a haemacytometer chamber (Marienfeld- Superior, Lauda-konigshofen, Germany).

2.2.4 Spheroid diameter

Aggregate size was determined by measuring Ferret's diameter using the open source ImageJ software version 1.47m.

2.3 Phenotypic characterization

2.3.1 Immunofluorescence microscopy

Spheroids were fixed in 4% (w/v) paraformaldehyde with 4% (w/v) sucrose in PBS for 20 min. For detection of intracellular epitopes in whole mount immunofluorescence, spheroids were permeabilized with 1% (v/v) Triton X-100 (Sigma-Aldrich) and blocked with 0.2% (w/v) fish-skin gelatine solution in PBS for 2h. After 2h of incubation with primary antibodies (ABs) and 1h with secondary ABs, spheroids were mounted with Prolong containing DAPI (Life Technologies). For cryosections, spheroids were fixed as described above and frozen in O.C.T.™ Tissue Tek (Sakura Finetek Europe, NL) at -80ºC. The frozen samples were sectioned in 10 µm thick slices onto glass coverslips in a cryomicrotome (Cryostat I, Leica, Wetslar, Germany). Cryosections were processed for immunofluorescence as described above, with a reduction of permeabilization time to 30 min. The primary ABs used for hepatic characterization were: human serum albumin, HNF4α, collagen type I, CYP3A4, (all from Abcam, Cambridge, U.K.) and FITC conjugated anti-Cytokeratin 18 (Sigma-Aldrich-). Alexa 488 conjugated Phalloidin was used for F-actin visualization (Life Technologies) and vimentin AB (Sigma-Aldrich-) for mesenchymal characterization. Samples were visualized using point scanning (SP5, Leica, Wetslar, Germany) and 2-photon Prairie Ultima (Bruker, MA, USA).

2.3.2 Scanning electron microscopy (SEM)

HH spheroids were collected from mono and co-cultures at day 8 and washed with Sorensen's Buffer (0.1 M NaH_2PO_4, 0.1 M Na_2HPO_4, pH 7.4). Samples were fixed in 4% Formaldehyde + 2.5% Glutaraldehyde Solution (both from Sigma-Aldrich, St. Lois, MO) for 1h at RT, followed by overnight incubation at 4°C. After washing with Sorensen's Buffer, spheroids were dehydrated in a sequential gradient from 30 to 99% ethanol (v/v) in water and stored at 4ºC. Before visualization, samples were dryed in the critical point dryer EMS3100, coated with a thin layer of gold and visualized in a JEOL JSM-5200LV scanning electron microscope.

2.3.3 Cytokine analysis

Culture supernatant was collected from the HH and HH-MSC bioreactors at days 5, 13 and 15 of culture and stored at -80ºC. WE culture medium and medium collected from BM-MSC monocultures in 2D were used as control for cytokine analysis. The samples were concentrated using 3KDa Amicon columns (Merck, NJ, USA) and detected using the human cytokine array panel A (R&D Systems, MN, USA) according to manufacturer's instructions.

2.3.4 Collagen quantification

Cell pellets were collected from mono and co-cultures at day 13 of culture and stored at -80ºC. The total collagen was quantified using the Sircol™ Collagen Assay, according to manufacturer´s instructions.

2.3.5 Intracellular glycogen content

Periodic Acid-Schiff (PAS) kit (Sigma Aldrich) was used accordingly to manufacturer's instructions. Briefly, cryosections obtained as described above, were incubated with the Periodic Acid solution for 5 min, followed by incubation with Schiff's reagent for 15 min also, both at RT.

2.3.6 Gene expression analysis

Samples for RNA analysis were collected from mono and co-cultures at days 3, 5, 8 and 13 and stored at -80ºC after fast freezing in liquid nitrogen. Total RNA was extracted using High Pure RNA Isolation kit and reverse transcription was performed using the Transcriptor High Fidelity cDNA Synthesis Kit (both from Roche, Basel, Switzerland), according to manufacturer´s instructions. Real-time PCR was performed in LightCycler 480 using SYBR green I Master kit (Roche). GAPDH was used as endogenous control and the primer sequences used are described in the supplementary information (Table 3.2).

Table 3.2. List of the genes analyzed for qRT-PCR and respective forward and reverse sequences.

Symbol	Forward Primer (5'- 3')	Reverse primer (5'- 3')
CYP1A2	TGGAGACCTTCCGACACTCCT	CGTTGTGTCCCTTGTTGTGC
CYP3A4	AAGTCGCCTCGAAGATACACA	AAGGAGAGAACACTGCTCGTG
CYP2C9	CGGATTTGTGTGGGAGAAGC	AGGCCATCTGCTCTTCTTCAG
HNF4α	AGAGCAGGAATGGGAAGGAT	GCAGTGGCTTCAACATGAGA
UGT1A1	CAGCAGAGGGGACATGAAAT	ATGGCACAGGGTACGTCTTC
ALB	ACACAAGCCCAAGGCAACAA	TATCGTCAGCCTTGCAGCAC
GAPDH	TCGACAGTCAGCCGCATCT	CCGTTGACTCCGACCTTCA

2.4 Functional characterization

2.4.1 Albumin secretion

Culture samples were collected throughout the culture period and stored at -20ºC. Albumin concentration was determined using an enzyme-linked immunosorbent assay (ELISA), the Exocell Albuwell albumin test kit (Exocell Inc., Philadelphia, PA). The assay was performed according to the manufacturer's instructions.

2.4.2 Urea synthesis

Culture samples were collected throughout the culture period and stored at -20ºC. The urea synthesis rate was determined using a quantitative colorimetric urea kit (QuantiChrom™ Urea Assay Kit, DIUR-500, ref DIUR-500; BioAssay Systems), according to the manufacturer's instructions.

2.4.3 CYP450 activity

For determination of CYP450 activity, cultures at day 2 and 10 of co-culture were collected from the BRs and transferred to ultra-low adherence multiwell plates, being induced for 48h with prototypical inducers – 10 μM of Rifampicin (Rif) for isoform 3A4 and 25 μM of β-Naphthoflavone (BNF) for isoform 1A2. Medium containing 0.1% DMSO was used as vehicle control. After induction, P450 activity was assessed by a luciferase based system – P450-glo™ (Promega, Madison, WI) and metabolite analysis by HPLC. The luciferase-based system was performed according to the supplier's instructions and luminescence was determined in a microplate reader (Modulus™, Turner Biosystems, Sunnyvale, CA). For HPLC analysis, cultures were incubated for 2h with 50 μM Midazolam for assessment of CYP3A4 activity and with Phenacetin 200 μM for 5h for assessment of CYP1A2 activity. Supernatants were stored at -20ºC and further analysed by HPLC for the presence of metabolites (OH-Midazolam and APAP, respectively).

2.4.4 Efflux transporter activity

A fluorescence-based assay was used to address bile canaliculli functionality in Human hepatocytes spheroids, through MRP2 activity. At the 5th day of culture spheroids were collected,

washed with PBS and incubated for 10 min with 2 µg/ml of 5-(and-6)-carboxy-20,70-dichlorofluorescein diacetate, CDFDA (Invitrogen, Carlsbad, CA), in culture medium. The aggregates were washed three times with PBS and imaged by confocal spinning-disk microscopy (Andor Technology PLC, Belfast, Northern Ireland)). MRP2 specificity was demonstrated by co-incubation of CDFDA with 500 µM of Indomethacin (MRP2 inhibitor).

2.4.5 Repeated dose toxicity testing

After 10 days of co-culture, the bioreactor inlet was supplemented with APAP (Sigma, St. Louis, MO) dissolved in DMSO (0.2% v/v), at a final concentration of 15 mM and the continuous influx of fresh medium containing APAP was maintained for 5 days. Supernatants and cell pellets were collected daily and stored at -80ºC and 4ºC for further analysis.

2.5 Data analysis and statistics

All presented results were obtained from independent cultures from three donors (n=3). Data are expressed as the mean ± standard error (SE). Data were analysed using GraphPad Prism (version 5.01) by an analysis of variance (ANOVA), followed by Tukey's post-hoc multiple comparison test and for collagen quantification an unpaired t-student test. A 95% confidence interval was considered to be significant and statistical significance was defined based on *p*-value (***$p<0.001$; **$p<0.01$; *$p<0.05$).

3. Results

3.1 Aggregation profile, compact morphology and increased viability of HH-MSC spheroids

A dual step inoculation strategy was used for the co-culture of HH-MSC, with a first step of HH inoculation and aggregation, and a second step of MSC inoculation and adhesion to HH spheroids (Figure 3.1). This strategy aimed to allow the assembly of cell-cell contacts between parenchymal liver cells and, after micro-tissue formation, add an outer layer of non-parenchymal cells. MSC were inoculated when the average spheroid diameter was 113.3±5.9 µm for the three different donors. The average spheroid diameter was kept constant throughout the culture period for mono- and co-cultures, increasing up to 123.6±6.8 µm in mono-cultures and 135.8±6.4 µm in co-cultures after two weeks (Figure 3.2 A). The compact morphology of HH-MSC spheroids was evident through microscopic visualization (Figure 3.2 A). Thus, detailed morphological characterization was performed through scanning electron microscopy (SEM), confirming that HH-MSC spheroids had a smoother surface in comparison to HH spheroids, which texture rougher and looser (Figure 3.2 C). Microscopic monitorization using fluorescent dyes also indicated that HH-MSC spheroids maintained higher cellular integrity and viability after 2 weeks of culture (Figure 3.2 A), being maintained up to 3 weeks. The activity of lactate dehydrogenase (LDH) leaked to the supernatant was determined to quantify cellular membrane integrity. Despite variations between cultures from different donors, LDH activity was higher in mono-culture supernatants (Figure 3.2 C), corroborating enhanced viability in co-cultures.

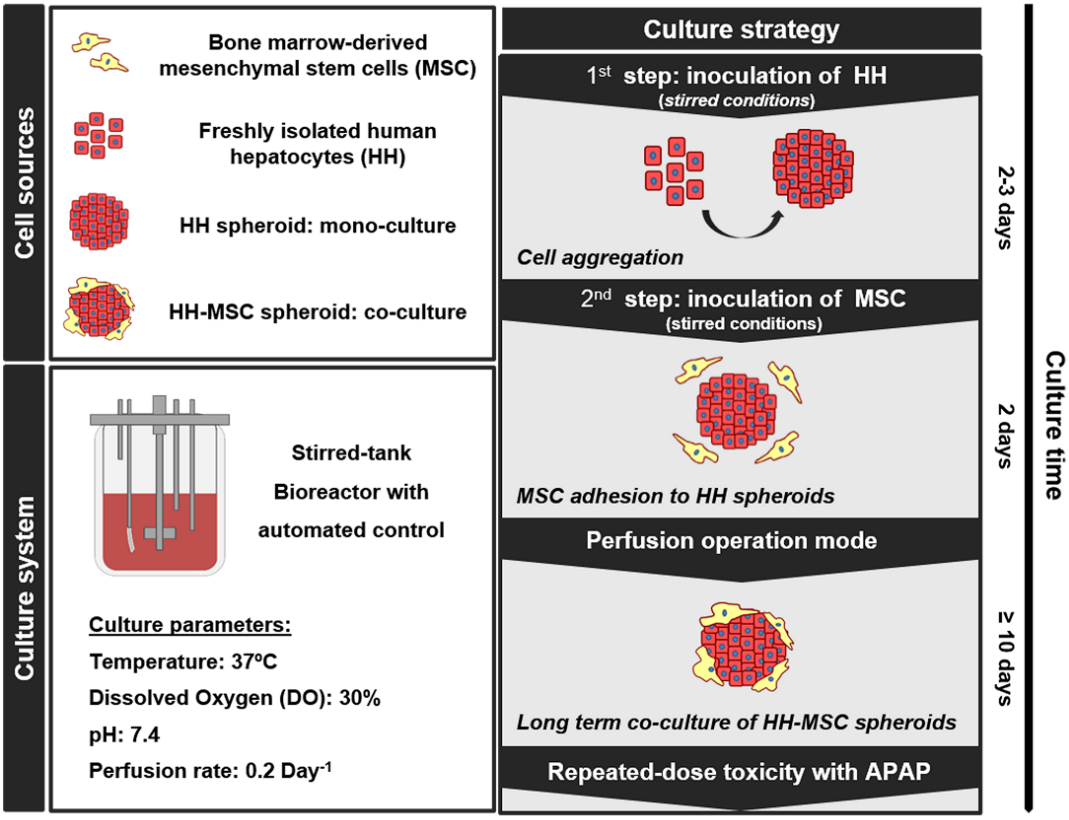

Figure 3.1 Schematic representation of the experimental design, including cell sources, culture system and strategy for the 3D co-culture of HH-MSC in perfusion stirred-tank bioreactors. The representation is not to scale.

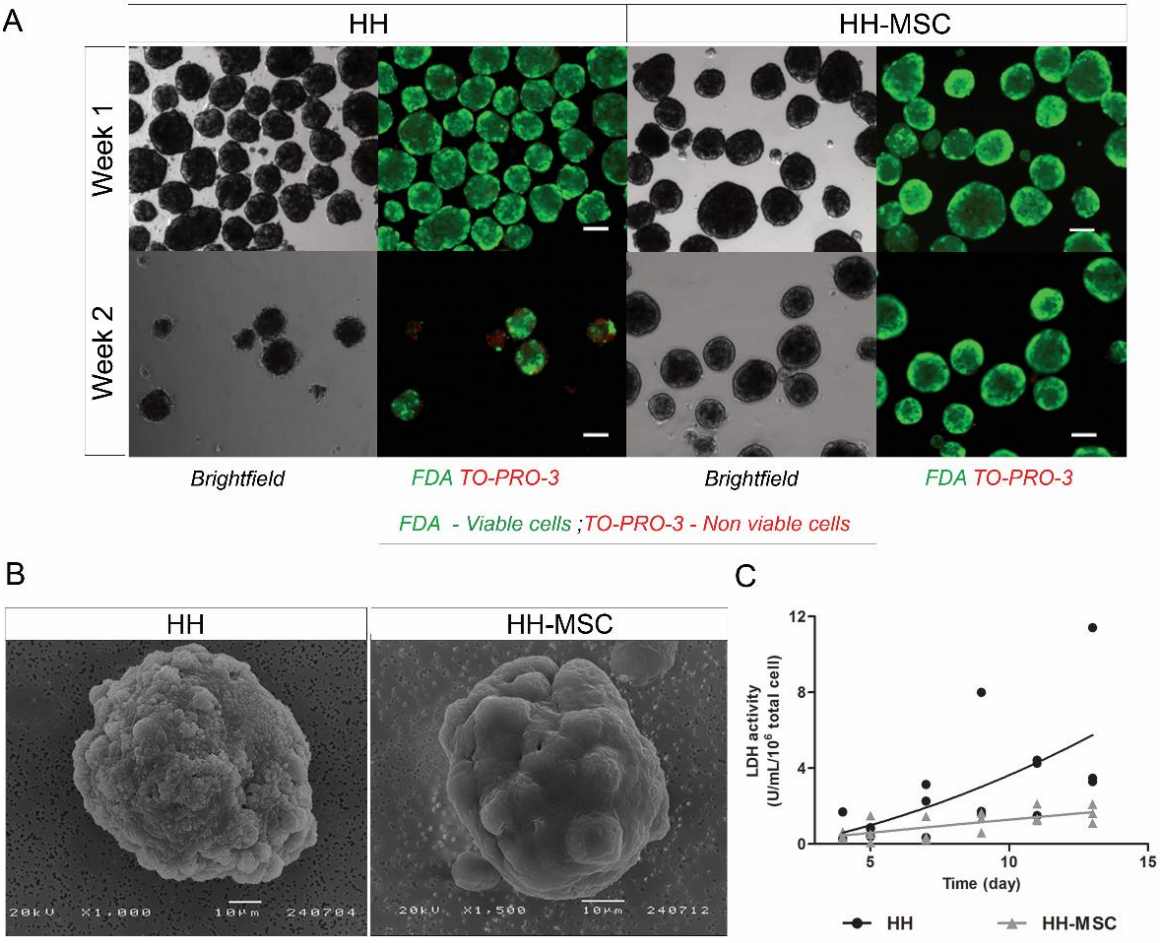

Figure 3.2 Morphology and viability of mono- and co-cultures in the bioreactor. A) Brightfield and fluorescence images of spheroids at week 1 (2 days after MSC inoculation) and week 2 of culture. Viability assessed by staining with fluorescein diacetate (live, green) and TO-PRO-3 (dead, red). Scale bars represent 100 µm. B) SEM characterization of HH and HH-MSC spheroids at day 8 of culture. C) LDH activity determined for the different donors. Lines represent the polynomial fit to the average LDH activity of the 3 donors.

3.2 Mesenchymal and hepatocytic phenotypes are maintained in HH-MSC spheroids

The distribution of MSC on spheroids was assessed by immunofluorescence detection of vimentin, an intermediary filament present in cells of mesenchymal origin. The hepatocyte-specific transcription factor HNF4α and the intermediate filament cytokeratin 18, were combined with vimentin to distinguish hepatocytic and mesenchymal populations. MSC were distributed on the spheroid surface, as shown in Figure 3.3 A-C and cells in the inner spheroid region were positive for HNF4α and ck18 (Figure 3.2 A, B). Moreover, phalloidin labeling showed highly polarized epithelial cells with actin enrichment in regions of cell-cell contacts and compact cellular arrangement after 2 weeks of culture (Figure 3.3 C). In HH spheroids, vimentin was not detected (Figure 3.7 A in appendix) and in 2D monocultures of MSC maintained in WE medium as control, vimentin was present and mesenchymal cell morphology was kept (Figure 3.8 in appendix). Cell proliferation using the nuclear marker Ki67 was not detected in HH-MSC spheroids (Figure 3.7 B in appendix), consistently with nuclei counting which did not increase throughout the culture (data not shown). HNF4α expression in co-cultures was constant up to day 13 (Figure 3.3 F). In mono-cultures, however, a significant decrease was observed.

The presence of COL 1 on HH-MSC spheroids was investigated, being mostly detected in the intercellular space between mesenchymal cells (vimentin positive) and the inner cells of the spheroid (Figure 3.3 D). Total collagen quantification confirmed that HH-MSC have higher collagen than HH spheroids (Figure 3.3 F).

An array of cytokines which included cytokines, chemokines and acute phase proteins was used to identify the soluble factors secreted by HH and MSC. The cytokines detected in MSC, HH and HH-MSC supernatants in the second week of culture included complement 5 (C5/C5a), GROα, sICAM-1, IL-1Ra, IL-6, IL-8, MCP-1, MIF and Serpin E1 (Figure 3.3 G). IL-6 was only detected in MSC and HH-MSC and IL-1Ra was restricted to HH and HH-MSC culture supernatants. A semi quantitative analysis was performed in the first and second week of culture, however, no differences were observed in the relative levels of mono and co-cultures (data not shown).

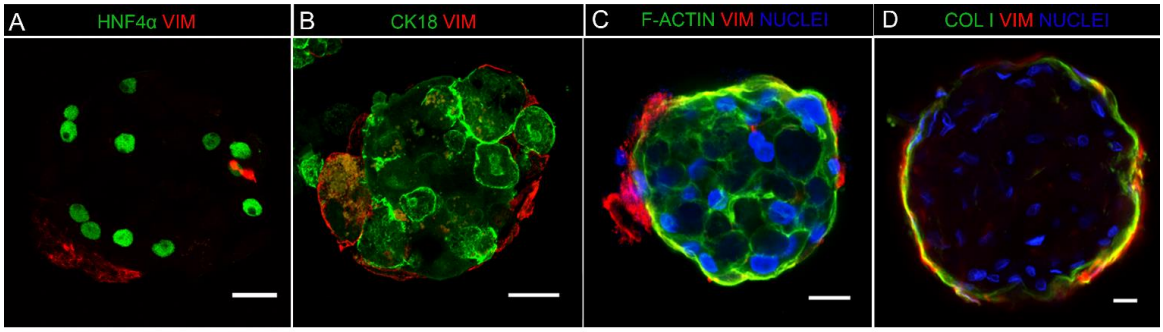

G

	C5/C5a	GROα	sICAM-1	IL-1Ra	IL-6	IL-8	MCP-1	MIF	Serpin E1
MSC	+	+	+	ND	+	+	+	+	+
HH	+	+	+	+	ND	+	+	+	+
HH-MSC	+	+	+	+	+	+	+	+	+

ND – Not detected

Figure 3.3 Characterization of hepatocytic and mesenchymal populations of spheroid co-cultures. Immunofluorescence detection of A) vimentin (red) and HNF4α (green) of cryosections at day 5; B) vimentin (red) and cytokeratin 18 (green) of cryosections at day 8; C) vimentin (red), F-actin (Phalloidin, green) and nuclei (DAPI, blue) of confocal sections at day 13. Scale bars represent 20 μm. D) Immunofluorescence detection of vimentin (red), collagen type I (green) and nuclei (DAPI, blue) of confocal sections at day 19 of culture. Scale bar represents 20 μm.E) qRT-PCR analysis of HNF4α gene expression. Fold changes in gene expression normalized to mono and co-cultures at day 3 of culture, GAPDH was used as reference gene. Data are mean ± SE of 3 cultures from different donors, * indicate significant differences between mono and co-cultures, ϕ indicate significant differences from day 3 of monoculture (***,ϕϕϕ p<0.001; **, ϕϕ p<0.01). F) Total collagen quantification of mono and co-cultures at the 13th day of culture normalized to the total collagen of co-cultures. Data are mean ± SE of 3 cultures from different donors, asterisks indicate significant difference (**P < 0.01) G) Cytokines detected in supernatants of MSC, HH and HH-MSC cultures in the 2nd week of culture.

3.3 MSC do not affect HH biosynthetic metabolism

To evaluate the hepatic biosynthetic metabolism, the expression levels of the blood protein albumin were assessed. The gene expression in co-cultures was higher than mono-cultures, with an increase up to 7-fold in gene expression at day 8 of culture, whereas for mono-cultures the expression decreased after day 5 (Figure 3.4 A). Interestingly, secreted albumin levels did not correlate with mRNA levels. Despite the variation between different donors, no significant difference was detected in the secretion levels of mono- and co-cultures. Nevertheless, the albumin levels were kept constant throughout the culture period (Figure 3.4 B) and the protein was detected by immunofluorescence on HH-MSC spheroids by the 2nd week of culture (Figure 3.4 D). Urea secretion was neither affected by the presence of MSC cells, being the major differences detected between different donors (Figure 3.4 C). Regarding glucose metabolism, the presence of glycogen in hepatic cells was detected by the Periodic Acid Schiff (PAS) staining (Figure 3.4 E).

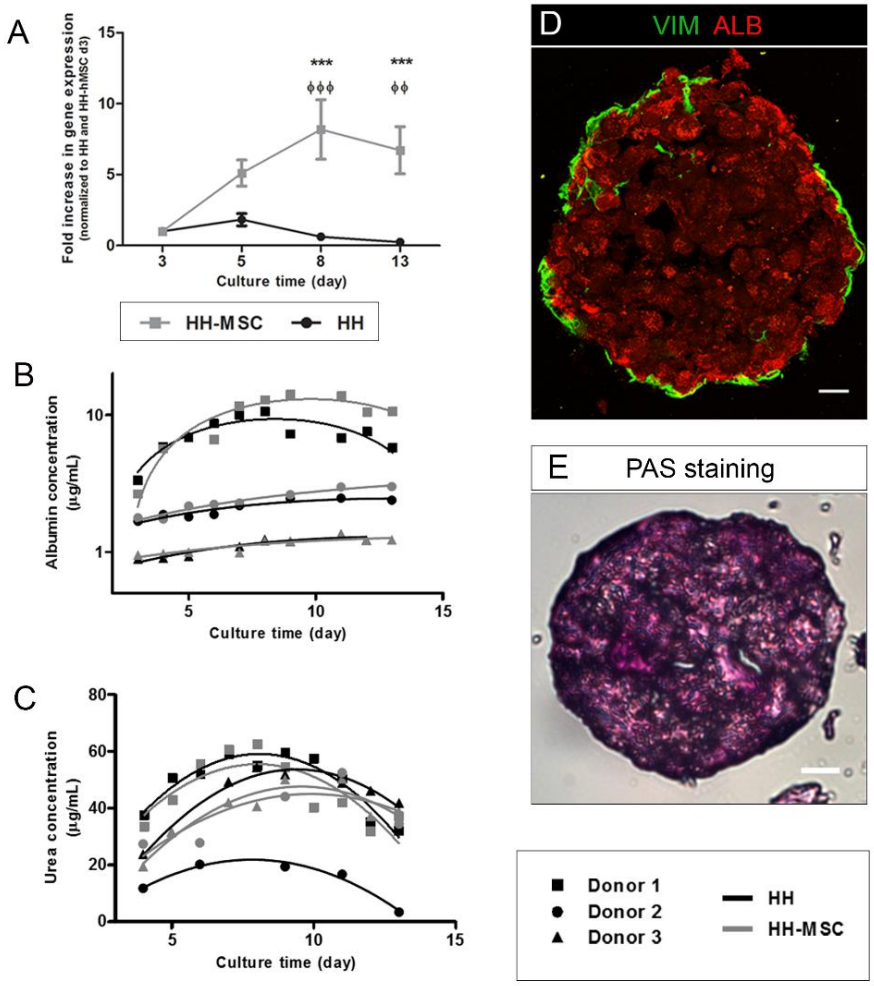

Figure 3.4 Biosynthetic metabolism. A) qRT-PCR analysis of albumin gene expression. Fold changes in gene expression normalized to mono and co-cultures at day 3 of culture, GAPDH was used as reference gene. Data are mean ± SE of 3 cultures from different donors, asterisks indicate significant differences between mono and co-cultures, ϕ indicate significant differences from day 3 of co-culture (***,ϕϕϕ $p<0.001$; ϕϕ $p<0.01$). B) Albumin and C) Urea concentration in bioreactor cultures represented for the three donors. D) Immunofluorescence detection of Alb (red), vimentin (green) in cyrosections of HH-MSC spheroids at day 13. E) Glycogen storage detected by Periodic Acid Schiff (PAS) staining of HH-MSC spheroids at day 8. Scale bars represent 20 µm.

3.4 HH-MSC spheroids retain xenobiotic metabolism

A higher increase in gene expression for all isoforms was observed on co-cultures after 2 weeks of culture, despite the different trends among the isoforms 3A4, 2C9 and 1A2 along the culture period. The expression of CYP3A4 increased on both cultures, with a significantly higher increase was on co-cultures (255.4±80.9 vs. 38.4±12.1; Figure 3.6 A). In contrast, the expression of 1A2 and 2C9 isoforms only increased in co-cultures being maintained (22.7±7.2 vs.2.4±0.5) or decreased (6.8±2.8 vs. 0.53±0.16) in mono-cultures, respectively (Figure 3.5 A) The phase II enzyme UGT1A1, involved in the glucoronidation of bilirubin and conjugation reactions of other substances, exhibited a stable expression for both mono- and co-cultures (7.9±1.7 vs. 2.0±0.9) (Figure 3.5 A).

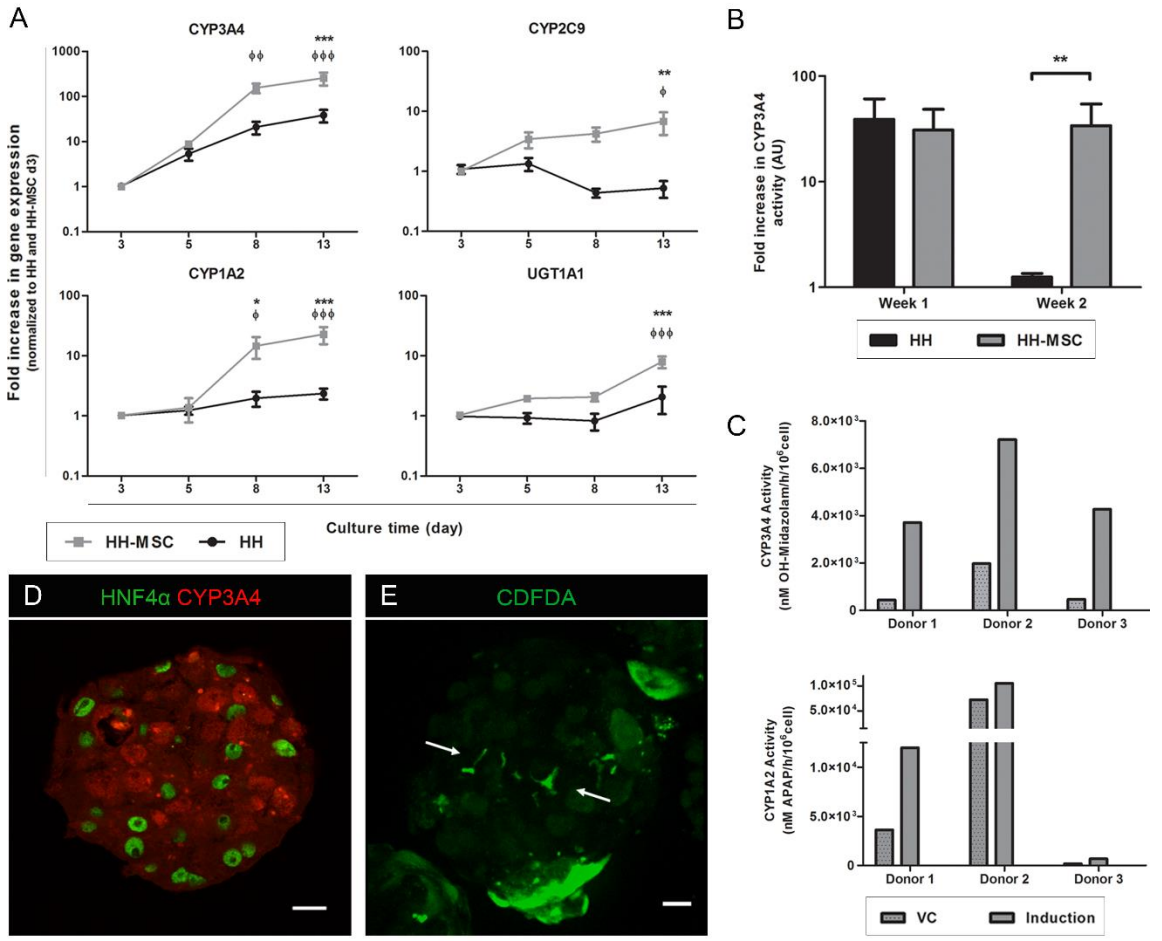

Figure 3.5 Xenobiotic metabolism**.** A) qRT-PCR analysis of CYP3A4, 1A2 and 2C9 and UGT1A1 gene expression. Fold changes normalized to mono and co-cultures at day 3 of culture, GAPDH was used as reference gene. * indicate significant differences between mono and co-cultures, ϕ indicate significant differences from day 3 of co-culture (***,ϕϕϕ p<0.001; **,ϕϕ p<0.01, *,ϕ p<0.05) B) Fold increase in CYP3A4 activity determined by a luciferase-based method in mono and co-cultures after induction in the 1st and 2nd week of culture. Asterisks indicate significant difference (**P < 0.01) C) CYP3A4 and CYP1A2 activity assessed by HPLC analysis of Midazolan and Phenacetin metabolism in the 2nd week of HH-MSC co-culture for different donors. D) Immunofluorescence detection of CYP3A4 and HNF4α in cryosections of HH-MSC at day 5 of culture. E) Excretory activity of HH-MSC spheroids visualized by efflux of CDFDA. Arrows indicate canalicular-like regions. Scale bars represent 20 µm.

To assess the activity of CYP3A4 and its stability over time, spheroids of mono and co-cultures were collected in the first and second week of culture and induced with the prototypical inducer Rifampicin in multiwell plates. The average fold increase after induction in mono- and co-cultures was comparable in the 1st week (approximately 40 and 30 respectively) but, in the second week, CYP3A4 inducibility was only maintained in co-cultures (approximately 30) (Figure 3.5 B). Since the stability of P450 enzymes activity was higher in co-cultures, the rate of metabolism of 3A4 and 1A2 substrates of HH-MSC spheroids was further analyzed by incubation with Midazolam and Phenacetin, respectively (Figure 3.5 C). The different rates of metabolism of Phenacetin reflected inter-donor variability (Gunes and Dahl, 2008) and the activity of CYP1A2 after induction increased from 1.4- to 3.8-fold for the different donors. Midazolam metabolism by CYP3A4 also reflected inter-donor variability but was less variable between different donors. Consistently, the presence of CYP3A4 and HNF4α was detected in co-cultured spheroids (Figure 3.5 D).

To evaluate the efflux activity of co-cultures, spheroids were incubated with CDFDA, which is metabolized by the phase II esterases into CDF and excreted by the transporter MRP2 (Zamek-Gliszczynski et al., 2003). CDF fluorescence was detected in intercellular regions inside the spheroid and was accumulated inside the cells at the surface of the spheroid (Figure 3.5 E), most likely MSC which lack MRP2 and excretory activity. Co-incubation with the MRP2 inhibitor indomethacin resulted in intracellular accumulation of CDF, blocking excretion and indicating MRP2-dependent excretion (Figure 3.9 in appendix).

3.5 Repeated dose toxicity in HH-MSC spheroids

As a proof of concept, HH-MSC spheroids were continuously perfused with 15 mM of APAP in a repeated dose regimen under perfusion. The LDH activity released to the supernatant demonstrated a high increase in cell death shortly after APAP supplementation (Figure 3.6 A), which culminated 72h after treatment. At this time, low viability was detected by live/dead assays (Figure 3.6 B) and a reduction of aggregate concentration was observed (data not shown). Gene expression after 48h of treatment indicated a decrease of phase I genes, in contrast to the phase II gene UGT1A1 (Figure 3.6 C). The levels of acute phase proteins were analysed but did not change after APAP treatment (data not shown).

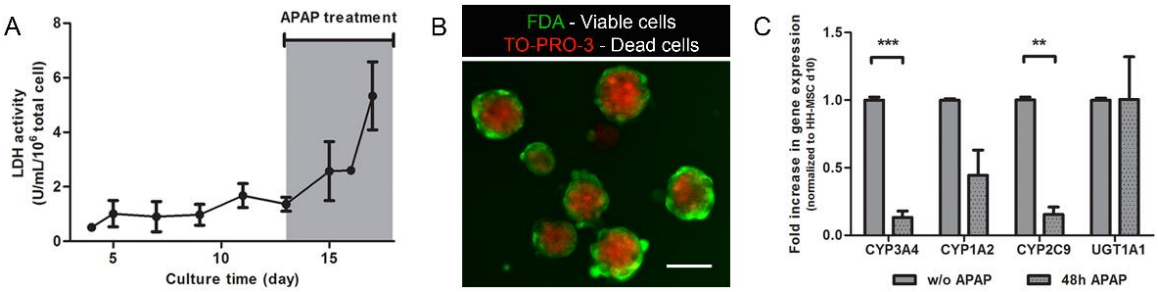

Figure 3.6 Repeated dose toxicity in bioreactors of co-cultures**.** A) Average LDH activity for 2 donors before and after treatment with APAP. B) Viability assessed by staining with fluorescein diacetate (live, green) and TO-PRO-3 (dead, red) 72h after APAP treatment. Scale bar represents100 µm. C) qRT-PCR analysis of phase I and II genes expression before and 48h after APAP treatment. Fold changes in gene expression of CYP3A4, 1A2 and 2C9 and UGT1A1 normalized to day 0 of APAP treatment, GAPDH was used as reference gene. Data are mean ± SE of cultures from 2 donors. * indicate significant differences before and after treatment (*** $p<0.001$; ** $p<0.01$).

4. Discussion

In this work, a novel 3D co-culture strategy was implemented for the long term maintenance of hepatic spheroids in bioreactors and, following a detailed characterization, the HH-MSC spheroids were validated for prediction of hepatotoxicity. The dual step inoculation of human hepatocytes and BM-MSC resulted in the formation of an inner core of parenchymal liver tissue with an overlay of stromal cells. The distribution of mesenchymal and hepatocytic populations was maintained throughout the culture time without dedifferentiation of hepatocytic cells, which presented the hepatic markers HNF4α, ck18 and polarized actin organization (Figure 3.3 A-C). Despite their migratory potential, the mesenchymal cells were restricted to the outer region of spheroids, without penetration of the compact hepatic core structure. Importantly, the spatial segregation of both cellular types within the spheroid allowed the assembly and maintenance of hepatocyte polarity, with bile canalicular-like structures and functional transporters, recapitulating a central feature of hepatic tissues.

Despite the ability of BM-MSC to differentiate into hepatic cells (Lee et al., 2004), the presence of the mesenchymal marker vimentin in the HH-MSC spheroids 10 to 16 days after co-culture and the HNF4α mRNA levels (Figure 3.3 E) showed that the proportion of hepatocyte to mesenchymal cells did not change significantly during the co-culture, indicating negligible differentiation of MSC towards hepatocyte-like cells. This suggests that BM-MSC in co-culture with HH function mostly as supportive stromal cells, resembling fibroblasts, and that the increased hepatic functionally cannot be attributed to the differentiation of BM-MSC into hepatocyte-like cells.

In comparison with mono-cultures of hepatocyte spheroids, the co-cultures of HH-MSC maintained high viability, cellular integrity and stable hepatic phenotype for longer periods. The beneficial effects of MSC on hepatic survival and functionality observed are consistent with several reports of *in vivo* and *in vitro* studies (Gómez-Aristizábal et al 2009). Among the multiple factors that may account for this effect, the secretion of soluble factors (growth factors and cytokines) by BM-MSC plays a major role, being the paracrine effects alone responsible for numerous hepatocellular responses (van Poll et al 2008; Zhang et al 2012). The analysis of cytokines secreted by MSC, HH and HH-MSC did not show substantial differences in the secretion of inflammatory proteins (Figure 3.3 G), which may be due to the absence of immune competent cells and lack of inflammatory stimuli. IL-6, a multifactorial pro-inflammatory cytokine, was present uniquely in co-cultures, being the major difference observed in the supernatants secretome analyzed. The role of IL-6 has been previously studied through the use of conditioned medium, cytokine supplementation and anti-IL6 antibodies, showing that it directly promotes albumin and urea secretion and influences drug metabolism (De Bartolo et al., 2006; Isoda et al., 2004). Moreover, IL-6 has dual effects on regeneration, since it directly induces quiescence in hepatocytes, but the proliferation is promoted in the presence of liver non-parenchymal cells (Sun et al., 2005). This dual role of IL-6 is consistent with the quiescent state of HH-MSC spheroids, as demonstrated by the absence the nuclear protein Ki67. Although not analyzed in this work, additional growth factors such as HGF, EGF and SCF typically secreted by BM-MSC have been shown to influence hepatic phenotype (Gómez-Aristizábal et al., 2009).

Despite the important role of paracrine signaling, direct co-cultures of HH-MSC may be additionally regulated by contact mediators and influenced by the presence of ECM. The membrane-associated liver-regulating protein (LRP), which is expressed by all liver cell types (hepatocytes, HSC, LSEC, Kupffer cells) and also by BM-MSC (Corlu et al., 1994), has been shown to mediate the support of hepatic morphology (Corlu et al., 1997) and also the polarized state (Mizuguchi et al., 2002). Moreover, the secretion of ECM components, namely collagen type I (COL I), by MSC has been previously reported (Harvey et al., 2013). Morphological differences observed by optical and scanning electron microscopy indicated that HH-MSC were more compact than HH spheroids (Figure 3.2 A, B), which may be attributed to the deposition of ECM in the periphery of the spheroids. Consistently, higher collagen levels were detected in co-cultures and collagen type I was detected in the intercellular space between MSC and HH, overlaying the hepatic cells (Figure 3.3 D,F), as occurs in the collagen sandwich model (Dunn et al., 1992). The collagen overlay may create a protective shield, providing mechanical protection to the hepatic cells. The role of the ECM secreted by BM-MSC in hepatic functionality has been depicted by Gu. et al (2009) using porcine hepatocytes. The characterization of the secreted ECM showed that, in addition to collagen type I, collagens type III and IV, laminin and fibronectin were also present. Moreover, by impairing ECM secretion, the hepatic metabolism was significantly reduced, highlighting the role of ECM in the maintenance of hepatic metabolism. Thus, the ECM may have a dual role in supporting hepatocyte viability and functionality – one related with cell signaling, provided by anchorage of cellular receptors to ECM molecules and mechanotransduction and another one related with mechanical support and protection which is particularly relevant in stirred systems, preventing shear stress-induced damage. Altogether, these results suggest that the cytoprotective and functionally-inducing effects of BM-MSC on hepatocytes are most likely due to synergistic effects which include cytokine secretion, direct cell-cell contacts and ECM secretion.

The secreted albumin levels were comparable between mono and co-cultures, despite the higher mRNA levels in co-cultures (Figure 3.4 A, B). Although several studies show the improvement of albumin secretion by MSC, it has been reported that in contact co-cultures, the levels of both albumin and urea are lower than in cultures with conditioned media (Gu et al., 2009). This observation highlights the role of soluble factors on biosynthetic metabolism and may clarify the result obtained in spheroid co-culture. In addition to the albumin and urea production, glycogen storage was also detected in co-culture spheroids (Figure 3.4 E), showing biosynthetic metabolism is sustained in HH-MSC co-cultures.

The drug metabolism of mono and co-cultures, assessed by mRNA expression of phase I and II enzymes and fold increase in activity after induction of CYP3A4 in the 1st and 2nd week of culture (Figure 3.5 A,B), indicated that the detoxification mechanisms were more stable in co-cultures, in agreement with the previously discussed effects of MSC in sustaining hepatic phenotype/functionality. Moreover, the metabolization rates of Midazolan and Phenacetin, substrates of CYP3A4 and CYP1A2, respectively indicated that the activity of these isoforms was maintained up to the second week of culture and that the inter donor variability was represented in the co-cultures (Figure 3.5 C). Importantly, the activity assays were performed outside the BR,

minimizing drug-induced variations in the phenotype of the spheroid culture and validating the BR as a feeder system to perform analyses in multiplexed formats. Moreover, phase III functionality, dependent of the polarization status and localization of transporters at the apical regions of the hepatocytes, was demonstrated by assessment of MRP2 activity. CDFDA excretion showed that bile canalicular-like structures assembled in the inner region of HH-MSC spheroids sustain excretory functionality (Figure 3.5 E).

To address the applicability of HH-MSC spheroids in toxicity studies, the co-cultures were continuously exposed to a constant concentration of APAP, which overdose or idiosyncratic chronic use may lead to liver failure (Yuan and Kaplowitz, 2013). APAP is metabolized by phase I enzymes CYP1A2 and CYP2E1 into the highly toxic product N-acetyl-p-benzoquinone (NAPQI), which excessive presence causes mitochondrial impairment and results in oxidative stress and necrotic cell death (Bruschi, 2005). Concentrations ranging from 10 to 20 mM have been previously described to affect hepatocellular activities and induce low toxicity in 2D cultures (Ullrich et al., 2009). At a concentration of 15 mM, cell death was detected 24h upon APAP exposure, phase I and II genes were downregulated after 48h and massive depletion of viable spheroids occurred after 72h (Figure 3.6 A-C). This indicated that the co-cultures are metabolically competent to transform APAP, displaying functional phase I enzymes. A recent report focusing on APAP-induced hepatotoxicity in primary cultures of HH demonstrated increased sensitivity in 3D cultures, mostly due to the presence of functional APAP-specific transporters such as MRP1 (Schyschka et al., 2013) . Since in 3D the sensitivity to APAP correlates better with *in vivo* data (0.5 to 1 mM of APAP induce necrosis) (Bruschi, 2005), lower dosages may be used in further studies to mimic chronic toxicity. Although this study demonstrated that co-cultures are sensitive to APAP exposure, the underlying mechanisms and the extent to which the presence of MSC affects APAP-induced hepatotoxicity would require further investigation.

In conclusion, HH and BM-MSC co-cultured as spheroids in bioreactors sustain liver-specific functions for long periods, being suitable to depict the toxicological profile of drugs. Importantly, the newly developed model was extensively characterized, showing that the mesenchymal and hepatic phenotypes are maintained throughout the time and drug metabolism was enhanced in co-cultures in comparison to mono-cultures. The strategy herein developed represents a novel approach for improving the culture of hepatocytes, being applicable for other hepatic sources, and relevant to understand the interplay between BM-MSC and HH for possible therapeutic applications.

Acknowledgements

I gratefully acknowledge Dra. S. Silva, Dr. P. Marcelino, Dr. H. Alexandrino and Prof. Dr. J. Tralhão for the supply of biological material and collaboration in the implementation of isolation of human hepatocytes; Marcos Sousa and João Clemente for support in the bioreactors and perfusion operations; Telmo Nunes for SEM characterization and Marta Estrada for support on cytokine arrays. This work was supported by PhD fellowship to S.R., SFRH / BD / 70264 / 2010 and by PTDC/EBB-BIO/112786/2009, funded by Fundação para a Ciência e Tecnologia.

5. Appendix

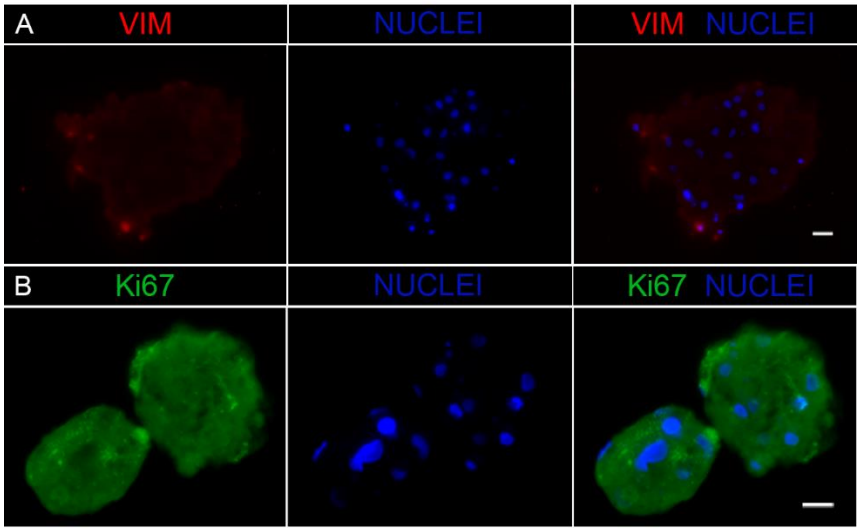

Figure 3.7 Immunofluorescence detection of A) Ki67 (green), nuclei (DAPI, blue) in cyrosections of HH-MSC spheroids at day 8 and B) Vimentin (red) and), nuclei (DAPI, blue) in cyrosections of HH spheroids at day 6. Scale bars represent 20 µm.

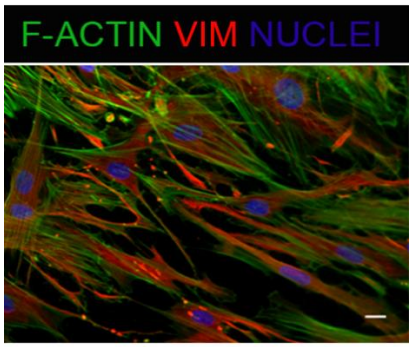

Figure 3.8 Immunofluorescence detection of F-actin (phalloidin, green), vimentin (red) and nuclei (DAPI, blue) in monocultures of BM-MSC after 6 days of 2D culture in WE medium. Scale bars represent 10 µm.

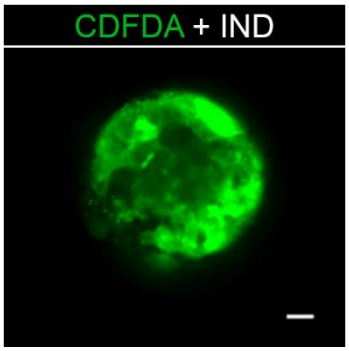

Figure 3.9 Accumulation of CDF in the presence of the MRP2 inhibitor Indomethacin in co-cultured spheroids. Scale bar represents 20 µm.

6. References

Barakat O, Abbasi S, Rodriguez G, Rios J, Wood RP, Ozaki C, Holley LS, Gauthier PK. 2012. Use of decellularized porcine liver for engineering humanized liver organ. *J. Surg. Res.* **173**.

De Bartolo L, Salerno S, Morelli S, Giorno L, Rende M, Memoli B, Procino A, Andreucci VE, Bader A, Drioli E. 2006. Long-term maintenance of human hepatocytes in oxygen-permeable membrane bioreactor. *Biomaterials* **27**:4794–803.

Bruschi S. 2005. Methods and Approaches to Study Metabolism and Toxicity of Acetaminophen. In: Las, L, editor. *Drug Metab. Transp. SE - 8*. Humana Press. Methods in Pharmacology and Toxicology, pp. 197–232.

Corlu A, Ilyin G, Cariou S, Lamy I, Loyer P. 1997. The coculture : A system for studying the regulation of liver di ¡ erentiation / proliferation activity and its control:235–242.

Corlu A, Ilyin GP, Gérard N, Kneip B, Rissel M, Jégou B, Guguen-Guillouzo C. 1994. Tissue distribution of liver regulating protein. Evidence for a cell recognition signal common to liver, pancreas, gonads, and hemopoietic tissues. *Am. J. Pathol.* **145**:715–727.

Dunn JCY, Tompkins RG, Yarmush ML. 1992. Hepatocytes in collagen sandwich: Evidence for transcriptional and translational regulation. *J. Cell Biol.* **116**:1043–1053.

Fitzpatrick E, Wu Y, Dhadda P, Hughes RD, Mitry RR, Qin H, Lehec SC, Heaton ND, Dhawan A. 2015. Coculture with mesenchymal stem cells results in improved viability and function of human hepatocytes. *Cell Transplant.* **24**:73–83.

Fouraschen SMG, Pan Q, de Ruiter PE, Farid WRR, Kazemier G, Kwekkeboom J, Ijzermans JNM, Metselaar HJ, Tilanus HW, de Jonge J, van der Laan LJW. 2012. Secreted factors of human liver-derived mesenchymal stem cells promote liver regeneration early after partial hepatectomy. *Stem Cells Dev.* **21**:2410–9.

Ghannam S, Bouffi C, Djouad F, Jorgensen C, Noël D. 2010. Immunosuppression by mesenchymal stem cells: mechanisms and clinical applications. *Stem Cell Res. Ther.* **1**:2.

Godoy P, Hewitt NJ, Albrecht U, Andersen ME, Ansari N, Bhattacharya S, Bode JG, Bolleyn J, Borner C, Böttger J, Braeuning A, Budinsky R a, Burkhardt B, Cameron NR, Camussi G, Cho C-S, Choi Y-J, Craig Rowlands J, Dahmen U, Damm G, Dirsch O, Donato MT, Dong J, Dooley S, Drasdo D, Eakins R, Ferreira KS, Fonsato V, Fraczek J, Gebhardt R, Gibson A, Glanemann M, Goldring CEP, Gómez-Lechón MJ, Groothuis GMM, Gustavsson L, Guyot C, Hallifax D, Hammad S, Hayward A, Häussinger D, Hellerbrand C, Hewitt P, Hoehme S, Holzhütter H-G, Houston JB, Hrach J, Ito K, Jaeschke H, Keitel V, Kelm JM, Kevin Park B, Kordes C, Kullak-Ublick G a, LeCluyse EL, Lu P, Luebke-Wheeler J, Lutz A, Maltman DJ, Matz-Soja M, McMullen P, Merfort I, Messner S, Meyer C, Mwinyi J, Naisbitt DJ, Nussler AK, Olinga P, Pampaloni F, Pi J, Pluta L, Przyborski S a, Ramachandran A, Rogiers V, Rowe C, Schelcher C, Schmich K, Schwarz M, Singh B, Stelzer EHK, Stieger B, Stöber R, Sugiyama Y, Tetta C, Thasler WE, Vanhaecke T, Vinken M, Weiss TS, Widera A, Woods CG, Xu JJ, Yarborough KM, Hengstler JG. 2013. Recent advances in 2D and 3D in vitro systems using primary hepatocytes, alternative hepatocyte sources and non-parenchymal liver cells and their use in investigating mechanisms of hepatotoxicity, cell signaling and ADME. *Arch. Toxicol.* Vol. 87 1315-530 p.

Gómez-Aristizábal A, Keating A, Davies JE. 2009. Mesenchymal stromal cells as supportive cells for hepatocytes. *Mol. Ther.* **17**:1504–8.

Gu J, Shi X, Zhang Y, Ding Y. 2009. Heterotypic interactions in the preservation of morphology and functionality of porcine hepatocytes by bone marrow mesenchymal stem cells in vitro. *J. Cell. Physiol.* **219**:100–8.

Gunes A, Dahl M-L. 2008. Variation in CYP1A2 activity and its clinical implications: influence of environmental factors and genetic polymorphisms. *Pharmacogenomics* **9**:625–637.

Harvey A, Yen T-Y, Aizman I, Tate C, Case C. 2013. Proteomic analysis of the extracellular matrix produced by mesenchymal stromal cells: implications for cell therapy mechanism. *PLoS One* **8**:e79283.

Hewitt NJ, Lechón MJG, Houston JB, Hallifax D, Brown HS, Maurel P, Kenna JG, Gustavsson L, Lohmann C, Skonberg C, Guillouzo A, Tuschl G, Li AP, LeCluyse E, Groothuis GMM, Hengstler JG.

2007. Primary hepatocytes: current understanding of the regulation of metabolic enzymes and transporter proteins, and pharmaceutical practice for the use of hepatocytes in metabolism, enzyme induction, transporter, clearance, and hepatotoxicity studies. *Drug Metab. Rev.* **39**:159–234.

Isoda K, Kojima M, Takeda M, Higashiyama S, Kawase M, Yagi K. 2004. Maintenance of hepatocyte functions by coculture with bone marrow stromal cells. *J. Biosci. Bioeng.* **97**:343–6.

Jang YO, Kim YJ, Baik SK, Kim MY, Eom YW, Cho MY, Park HJ, Park SY, Kim BR, Kim JW, Soo Kim H, Kwon SO, Choi EH, Kim YM. 2014. Histological improvement following administration of autologous bone marrow-derived mesenchymal stem cells for alcoholic cirrhosis: a pilot study. *Liver Int.* **34**:33–41.

Jung J, Choi JH, Lee Y, Park J-W, Oh I-H, Hwang S-G, Kim K-S, Kim GJ. 2013. Human placenta-derived mesenchymal stem cells promote hepatic regeneration in CCl4 -injured rat liver model via increased autophagic mechanism. *Stem Cells* **31**:1584–96.

Kaibori M, Adachi Y, Shimo T, Ishizaki M, Matsui K, Tanaka Y, Ohishi M, Araki Y, Okumura T, Nishizawa M, Kwon a H. 2012. Stimulation of liver regeneration after hepatectomy in mice by injection of bone marrow mesenchymal stem cells via the portal vein. *Transplant. Proc.* **44**:1107–9.

Khetani SR, Bhatia SN. 2008. Microscale culture of human liver cells for drug development. *Nat. Biotechnol.* **26**:120–126.

Kim M-D, Kim S-S, Cha H-Y, Jang S-H, Chang D-Y, Kim W, Suh-Kim H, Lee J-H. 2014. Therapeutic effect of hepatocyte growth factor-secreting mesenchymal stem cells in a rat model of liver fibrosis. *Exp. Mol. Med.* **46**:e110.

Kostadinova R, Boess F, Applegate D, Suter L, Weiser T, Singer T, Naughton B, Roth A. 2013. A long-term three dimensional liver co-culture system for improved prediction of clinically relevant drug-induced hepatotoxicity. *Toxicol. Appl. Pharmacol.* **268**:1–16.

LeCluyse EL, Witek RP, Andersen ME, Powers MJ. 2012. Organotypic liver culture models: Meeting current challenges in toxicity testing. *Crit. Rev. Toxicol.*

Lee K-D, Kuo TK-C, Whang-Peng J, Chung Y-F, Lin C-T, Chou S-H, Chen J-R, Chen Y-P, Lee OK-S. 2004. In vitro hepatic differentiation of human mesenchymal stem cells. *Hepatology* **40**:1275–1284.

Miranda JP, Leite SB, Muller-Vieira U, Rodrigues A, Carrondo MJ, Alves PM. 2009. Towards an extended functional hepatocyte in vitro culture. *Tissue Eng. Part C, Methods* **15**:157–167.

Mizuguchi T, Palm K, Hui T, Aoki T, Mochizuki Y, Mitaka T, Demetriou A, Rozga J. 2002. Effects of bone marrow stromal cells on the structural and functional polarity of primary rat hepatocytes. *Vitr. Cell. Dev. Biol. - Anim.* **38**:62–65.

Nasir GA, Mohsin S, Khan M, Shams S, Ali G, Khan SN, Riazuddin S. 2013. Mesenchymal stem cells and Interleukin-6 attenuate liver fibrosis in mice. *J. Transl. Med.* **11**:78.

Van Poll D, Parekkadan B, Cho CH, Berthiaume F, Nahmias Y, Tilles AW, Yarmush ML. 2008. Mesenchymal stem cell-derived molecules directly modulate hepatocellular death and regeneration in vitro and in vivo. *Hepatology* **47**:1634–43.

Rebelo SP, Costa R, Estrada M, Shevchenko V, Brito C, Alves PM. 2014. HepaRG microencapsulated spheroids in DMSO-free culture: novel culturing approaches for enhanced xenobiotic and biosynthetic metabolism. *Arch Toxicol*.

Salomone F, Barbagallo I, Puzzo L, Piazza C, Li Volti G. 2013. Efficacy of adipose tissue-mesenchymal stem cell transplantation in rats with acetaminophen liver injury. *Stem Cell Res.* **11**:1037–44.

Schyschka L, Sánchez JJM, Wang Z, Burkhardt B, Müller-Vieira U, Zeilinger K, Bachmann A, Nadalin S, Damm G, Nussler AK. 2013. Hepatic 3D cultures but not 2D cultures preserve specific transporter activity for acetaminophen-induced hepatotoxicity. *Arch. Toxicol.* **87**:1581–1593.

Seglen PO. 1976. Chapter 4 Preparation of Isolated Rat Liver Cells. *Methods Cell Biol.* **13**:29–83.

Slikker Jr. W, Andersen ME, Bogdanffy MS, Bus JS, Cohen SD, Conolly RB, David RM, Doerrer NG, Dorman DC, Gaylor DW, Hattis D, Rogers JM, Woodrow Setzer R, Swenberg JA, Wallace K.

2004. Dose-dependent transitions in mechanisms of toxicity. *Toxicol. Appl. Pharmacol.* **201**:203–225.

Sun R, Jaruga B, Kulkarni S, Sun H, Gao B. 2005. IL-6 modulates hepatocyte proliferation via induction of HGF/p21 cip1: Regulation by SOCS3. *Biochem. Biophys. Res. Commun.* **338**:1943–1949.

Tostões RM, Leite SB, Miranda JP, Sousa M, Wang DI, Carrondo MJ, Alves PM. 2011. Perfusion of 3D encapsulated hepatocytes--a synergistic effect enhancing long-term functionality in bioreactors. *Biotechnol. Bioeng.* **108**:41–49.

Tostões RM, Leite SB, Serra M, Jensen J, Bjorquist P, Carrondo MJ, Brito C, Alves PM. 2012. Human liver cell spheroids in extended perfusion bioreactor culture for repeated-dose drug testing. *Hepatology* **55**:1227–1236.

Ullrich A, Stolz DB, Ellis EC, Strom SC, Michalopoulos GK, Hengstler JG, Runge D. 2009. Long term cultures of primary human hepatocytes as an alternative to drug testing in animals. *ALTEX Altern. zu Tierexperimenten* **26**:295–302.

Xie Y, McGill MR, Dorko K, Kumer SC, Schmitt TM, Forster J, Jaeschke H. 2014. Mechanisms of acetaminophen-induced cell death in primary human hepatocytes. *Toxicol. Appl. Pharmacol.* **279**:266–74.

Yang Y, Li J, Pan X, Zhou P, Yu X, Cao H, Wang Y, Li L. 2013. Co-culture with mesenchymal stem cells enhances metabolic functions of liver cells in bioartificial liver system. *Biotechnol. Bioeng.* **110**:958–68.

Yuan L, Kaplowitz N. 2013. Mechanisms of drug-induced liver injury. *Clin. Liver Dis.*

Zamek-Gliszczynski MJ, Xiong H, Patel NJ, Turncliff RZ, Pollack GM, Brouwer KLR. 2003. Pharmacokinetics of 5 (and 6)-carboxy-2',7'-dichlorofluorescein and its diacetate promoiety in the liver. *J. Pharmacol. Exp. Ther.* **304**:801–809.

Zhang S, Chen L, Liu T, Zhang B, Xiang D, Wang Z, Wang Y. 2012. Human umbilical cord matrix stem cells efficiently rescue acute liver failure through paracrine effects rather than hepatic differentiation. *Tissue Eng. Part A* **18**:1352–64.

CHAPTER 4

HepaRG microencapsulated spheroids in DMSO-free culture

This chapter was adapted from:

Rebelo SP, Costa R, Estrada M, Shevchenko V, Brito C, Alves PM. 2014. HepaRG microencapsulated spheroids in DMSO-free culture: novel culturing approaches for enhanced xenobiotic and biosynthetic metabolism. *Arch Toxicol*.

TABLE OF CONTENTS

ABSTRACT

The need for models that recapitulate liver physiology is perceived for drug development, study of liver disease and bioartificial liver support. The bipotent cell line HepaRG constitutes an efficient surrogate of liver function, yet its differentiated status relies on high concentrations of DMSO, which may compromise the study of drug metabolism and limit the applicability of this hepatic model.

Herein, we present a three-dimensional (3D) strategy for the differentiation of HepaRG based on alginate microencapsulation of cell spheroids and culture in DMSO-free conditions. A ratio of 2.9:1 hepatocyte-like to biliary-like cells was obtained in the 3D culture, with an improvement of 35.9% in the hepatocyte differentiation when compared with 2D cultures. The expression of the hepatic identity genes HNF4α and PXR in 3D cultures was comparable to 2D differentiated cultures, while the expression of homeostatic-associated genes ALB and CPS1 was higher in 3D. Moreover, the spheroids presented a polarized organization, exhibiting an interconnected bile canalicular network and excretory functionality, assessed by specific activity of MRP2. Importantly, despite variability in basal gene expression levels, the activity of the phase I enzymes CYP3A4 and CYP1A2 upon induction was comparable to differentiated 2D cultures and albumin production and ammonia detoxification were enhanced in 3D. The presented model is suitable for toxicological applications, as it allows high throughput analysis of multiple compounds in a DMSO-free setting. Due to the high xenobiotic metabolism and maintenance of biosynthetic functions, the applicability of this model might be broadened to understand liver physiology and for bioartificial liver applications.

1. Introduction

Mimicking *in vivo* liver complexity has been a major challenge in biotechnology, drug development and regenerative medicine fields. Though the pressure to move away from animal models for toxicology purposes and to develop strategies for Bioartifical Liver (BAL) systems is high, the development of efficient models and culture systems is still in progress. Primary human hepatocyte cultures are hampered by the limited availability of biological material and phenotypic instability, while the protocols for differentiation from pluripotent stem cells (PSC) still yield hepatocyte-like cells with immature phenotype (Godoy et al. 2013). Among hepatic cell lines, the bipotent line HepaRG stands out due to its unique hepatic features, including high cytochrome P450 activity, as well as phase II and phase III functionality (Parent et al. 2004; Le Vee et al. 2013).

HepaRG is a highly proliferative progenitor cell line with differentiation potential towards biliary-like cells (BLC) and hepatocyte-like cells (HLC) which organize into clusters. Differentiation is initiated when cells attain the confluent state and supplementation of culture medium with 2% (v/v) Dimethyl Sulfoxide (DMSO) for subsequent 14 days enhances the detoxification machinery function and polarization state (Cerec et al. 2007). DMSO´s pleiotropic effects on cell behavior include transcriptional regulation of gene expression, promotion of cell cycle arrest and anti-apoptotic activity (Santos et al. 2003). In hepatic cells, DMSO acts as an inducer of phase I, II and III enzyme activity but represses homeostasis-related hepatic features, such as albumin production, glycogen storage and ammonia detoxification in the form of urea (Pal et al. 2012; Hoekstra et al. 2011). *In vivo*, a functional zonation occurs in the liver in which the hepatocytes display specialized functions related to ammonia detoxification, glucose/energy and xenobiotic metabolism according to the proximity to the central vein and hepatic artery in the liver lobule. Pericentral (PC) associated functions include high xenobiotic metabolism, glycolysis and glutamine synthesis while in periportal (PP) hepatocytes, gluconeogenesis and urea production are predominant (Jungermann 1995).

Culture strategies that promote increased cell-cell, cell-matrix contacts and spatial constriction such as collagen sandwich or spheroid culture, have been demonstrated to enhance and prolong hepatic-specific functions both for primary cultures (Tostoes et al. 2012), hepatic cell lines (Elkayam et al. 2006) and PSC-derived cells (Takayama et al. 2013). The three-dimensional (3D) architecture of spheroids provides maximization of cell-cell interactions resembling the *in vivo* structural arrangement of the hepatic lobule, which results on correct assembly of polarity proteins and transporters (LeCluyse et al. 2012). Moreover, within the 3D structure of the spheroids, there is formation of a nutrient and oxygen gradient which may mimic the functional zonation existent in the liver - (towards PC or PP phenotype). Stirred systems ensure the necessary diffusion of soluble factors and oxygen to prevent formation of necrotic centers, yet the hydrodynamic shear stress applied may compromise viability and alter morphology and gene expression. Microencapsulation of cell spheroids with biomaterials, such as alginate, confers protection to shear stress, while creating an extracellular environment that enables diffusion of nutrients and soluble factors through the hydrogel structure and prevents the constant washout of extracellular matrix and soluble factors. Indeed, alginate microencapsulation has been previously applied for culture of primary rat liver spheroids, resulting in a synergistic effect with perfusion for increased hepatic functionality (Tostões

et al. 2011). Given to its tunable mechanical properties and unique characteristics of biocompatibility, biosafety and permeability, it has also been used for *in vivo* engraftment of Langerhans islets (Sun et al. 1984) or hepatocytes (Cai et al. 1988).

3D-based culture systems using the HepaRG cell line have been applied and validated for toxicological applications, in stirred (Leite et al. 2012) and static conditions (Gunness et al. 2013; Mueller et al. 2013). In these studies, using the established DMSO-dependent protocol, the 3D architecture *per se* contributed to improve complex P450 activities and to attain a toxicological profile that better correlates with *in vivo* or primary human hepatocyte culture data. In addition to the toxicological applications, HepaRG has been suggested as a suitable cell source for BAL in the absence of DMSO (Hoekstra et al. 2011; Higuchi et al. 2013), especially due to its proliferative ability and high hepatic metabolism. When cultured in a dynamic 3D support, the AMC bioreactor, metabolic parameters such as ammonia detoxification were enhanced, extending up to 50% the survival of rats with acute liver failure (ALF) (Nibourg et al. 2012). This culture configuration led to an improvement of phase 1 and 2 drug metabolism and bile production (Hoekstra et al. 2013), yet it is barely applicable for toxicological purposes. Recent work presented data on the development of humanized mice with HepaRG cells, constituting an *in vivo* model for liver physiology (Higuchi et al. 2013).

Herein, we present a 3D culture-based strategy for the differentiation of HepaRG, yielding a hepatic model capable of displaying the full set of hepatic features that recapitulate xenobiotic metabolic activity and homeostatic roles. Importantly, the newly developed model was cultured in DMSO-free conditions and exhibited a highly polarized structure. An increase in albumin production and in the ammonia elimination was observed as well as high drug metabolizing activity and phase III functionality. Altogether, the presented model represents a powerful tool for toxicological applications and to better understand liver physiology. Ultimately the strategy presented may be potentially applied for other systems for differentiation towards HLC.

2. Material and methods

2.1 2D culture

2.1.1 Cell expansion

HepaRG cells were routinely propagated in static conditions, as previously described (Gripon et al. 2002). Briefly, culture medium Williams E (Sigma-Aldrich) was supplemented with 1% (v/v) Glutamax, 1% (v/v) pen/strep, 10% (v/v) FBS (all from Gibco/Invitrogen, Grand Island, NY), 5 µg/ml bovine insulin and 50 µM hydrocortisone hemissuccinate (both from Sigma-Aldrich, St. Lois, MO). Cells were passaged every two weeks up until passage 19, with medium replenishment twice per week. The cultures were maintained in a humidified environment at 37ºC, 5% CO_2.

2.1.2 Cell differentiation

As previously described, cells were maintained for 2 weeks in DMSO-free medium to attain the committed but imamature hepatic stage (2D d14). Induction of differentiation was performed by supplementing the previously described medium with 2% (v/v) of DMSO for an additional period of 2 weeks (2D d28).

2.2 3D culture

2.2.1 Aggregation

Aggregation was performed in stirred conditions using spinner vessels with ball impeller (Wheaton, Millville, NJ). After expansion for one week in 2D monolayers, spinner vessels were inoculated with approximately $7x10^5$ cell/mL and an agitation ranging from 35 to 45 rpm for 3 days. Aggregate size was determined by measuring Ferret's diameter using the open source ImageJ software version 1.47m (http://rsbweb.nih.gov/ij/).

2.2.2 Alginate microencapsulation

Spheroids were encapsulated with 1.1% (w/v) of Ultra Pure Ca^{2+} MVG alginate (UP MVG NovaMatrix, Pronova Biomedical, Oslo, Norway) prepared in NaCl 0.9% (w/v) solution. After aggregation, cell spheroids were briefly centrifuged at low speed and an alginate-cell mixture was prepared at a concentration of $6x10^6$ cell/mL of alginate. Microencapsulation was performed in an electrostatically driven microencapsulation unit, VarV1 (Nisco, Zurich, Switzerland) to generate beads with a diameter ranging from 500-600 µm. Alginate cross-linkage was attained with a solution of 100 mM $CaCl_2$/10 mM HEPES (pH 7.4) and dissociation of alginate beads was performed by incubating the beads for 5 min in a solution of Sodium citrate 50 mM and Sodium Chloride 104 mM.

2.2.3 Cell differentiation

Encapsulated HepaRG spheroids (3D) were maintained in spinner vessels with ball impeller with a stirring rate of 60 rpm for 14 days, at which point most characterization was performed, and maintained up to 4 weeks in culture. The culture medium was DMSO-free and 50% of the culture medium was exchanged twice per week. Cell concentration and viability were monitored throughout the culture period.

2.2.4 Monitoring of cell viability and concentration

Samples were collected periodically from the 3D cultures and used for monitorization of cell viability by a fluorescent cell membrane integrity assay and by the Trypan blue exclusion method. For the

fluorescent assay, capsules were incubated with the substrate Fluorescein Diacetate (FDA) (Sigma-Aldrich, St. Lois, MO) at 10 µg/mL for detection of viable cells and the DNA dye TO-PRO®3 (Invitrogen, Carlsbad, CA) at 1 µM for visualization of dead cells. Encapsulated spheroids were visualized by fluorescence microscopy (DMRB6000, Leica). For the Trypan blue exclusion method, alginate beads were dissociated as described above and cells were trypsinized with 0.05% Trypsin (Gibco, Grand Island, NY) for 5 min at 37ºC. Cell concentration and viability were determined by mixing the cell suspension with 0.1% Trypan blue dye and counting in a Fuchs-Rosenthal haemacytometer chamber (colorless cells – viable; blue cells – non viable).

2.3 Immunofluorescence characterization

2.3.1 Whole mount microscopy

At day 14 of differentiation, HepaRG spheroids were fixed in 4% (w/v) paraformaldehyde (PFA) with 4% (w/v) sucrose in PBS for 20 min. For detection of intracellular epitopes, spheroids were permeabilized with 1% (v/v) Triton X-100 (Sigma-Aldrich, St. Lois, MO) and blocked with 0.2% (w/v) fish-skin gelatine (FSG) solution in PBS for 2 hours before incubation with primary antibodies. An incubation of 2 hours was performed in a solution containing 0.1% (v/v) Triton X-100 and 0.125% (w/v) FSG and spheroids were washed before incubation with secondary antibodies in the same solution for 1 hour. Finally, spheroids were mounted with Prolong containing DAPI (Invitrogen, Carlsbad, CA) and visualized using point scanning (SP5, Leica, Wetslar, Germany) and spinning disk microscopy (Andor Revolution xD, Andor Technology PLC, Belfast, Northern Ireland). The antibodies used for hepatic characterization included human serum albumin, HNF4α, collagen type I, CYP3A4, Ki67, (all from Abcam, Cambridge, U.K.), HNF3β (Santa Cruz Biotechnology, Dallas, TX) and ZO-1 (Invitrogen, Carlsbad, CA) and phalloidin for F-actin visualization (Invitrogen, Carlsbad, CA).

2.3.2 Cryosections and monolayer microscopy

Encapsulated HepaRG spheroids and monolayer cultures were fixed as described above. The spheroids were incubated in a solution of 30% (w/v) of sucrose o/n and frozen in O.C.T. Tissue Tek (Sakura, Alphen aan den Rijn, Netherlands) at -80ºC. The frozen samples were sectioned in 10-µm thick slices onto glass coversticks in a cryomicrotome (Cryostat I, Leica, Wetslar, Germany). Cryosections and monolayers were processed for immunofluorescence as described above, with exception for the permeabilization step which was reduced to 10 min.

2.4 Gene expression profiling

Samples for RNA analysis were collected from 3D cultures at day 14 of differentiation and from 2D cultures at day 14 and 28 and stored at -80ºC after fast freezing in liquid nitrogen. Total RNA was extracted using High Pure RNA Isolation kit and reverse transcription was performed using the Transcriptor High Fidelity cDNA Synthesis Kit (both from Roche, Basel, Switzerland), according to manufacturer´s instructions. Real-time PCR was performed in LightCycler 480 using SYBR green I Master kit (Roche, Basel, Switzerland). RPL22 was used as endogenous control and the primer sequences used are described in Table 4.1.

Table 4.1 List of the genes analyzed for qRT-PCR and respective forward and reverse sequences

Symbol	Forward Primer (5'-3')	Reverse primer (5'-3')
CYP1A2	TGGAGACCTTCCGACACTCCT	CGTTGTGTCCCTTGTTGTGC
CYP3A4	AAGTCGCCTCGAAGATACACA	AAGGAGAGAACACTGCTCGTG
CYP2C9	CGGATTTGTGTGGGAGAAGC	AGGCCATCTGCTCTTCTTCAG
HNF4α	AGAGCAGGAATGGGAAGGAT	GCAGTGGCTTCAACATGAGA
PXR/ NR112	CCAGGACATACACCCCTTTG	CTACCTGTGATGCCGAACAA
GS/ GLUL	CGTAGCTATCCGGACAGAGC	CCCAACCCCTACCTTCTCTC
CPS1	ATTCCTTGGTGTGGCTGAAC	ATGGAAGAGAGGCTGGGATT
ALB	ACACAAGCCCAAGGCAACAA	TATCGTCAGCCTTGCAGCAC
RPL22	CACGAAGGAGGAGTGACTGG	TGTGGCACACCACTGACATT

2.5 Functional characterization

2.5.1 Albumin secretion

Albumin concentration was determined using an enzyme-linked immunosorbent assay (ELISA), the Exocell Albuwell albumin test kit (Exocell Inc., Philadelphia, PA) The assay was performed according to the manufacturer's instructions.

2.5.2 Ammonia detoxification

Cultures at day 14 (2D and 3D) and day 28 (2D) were incubated with 5 mM NH_4Cl for 24 hours. After incubation, the supernatants were analysed by GC-MS for the presence of glutamine and urea. Briefly, [$^{13}C^{15}N$]-urea and [^{13}C]-Gln (both from CIL, Tewksbury, MA), used as internal controls at 25 nmol, were added to 10 µl of culture supernatant before derivatization, which was performed as previously described (Hofmann et al. 2008).

2.5.3 CYPP450 activity

For determination of CYP450 activity, cultures either at day 14 (2D and 3D) and day 28 (2D) were induced for 72h with prototypical inducers – 10 µM of Rifampicin (Rif) for isoform 3A4 and 25 µM of β-Naphthoflavone (BNF) for isoform 1A2. Medium containing 0.1% DMSO was used as vehicle control, since the prototypical inducers were dissolved in DMSO and used at a concentration of 0.1% in the culture medium. After induction, P450 activity was assessed by a luciferase based system – P450-glo™ (Promega, Madison, WI) and metabolite analysis by HPLC. The luciferase-based system was performed according to the supplier's instructions and luminescence was determined in a microplate reader (Modulus™, Turner Biosystems, Sunnyvale, CA). For HPLC analysis, cultures were incubated for 2h with 50 µM Midazolam for assessment of CYP3A4 activity

and with Phenacetin 200 µM for 5h for assessment of CYP1A2 activity. Supernatants were stored at -20ºC and further analyzed by HPLC for the presence of metabolites.

2.5.4 Efflux transporter activity

A fluorescence-based assay was used to address bile canaliculli functionality in HepaRG spheroids, through MRP2 activity. After 14 days of differentiation, encapsulated spheroids were collected from 3D cultures, washed with PBS and incubated for 10 min with 2 µg/mL of 5-(and-6)-carboxy-20,70-dichlorofluorescein diacetate, CDFDA (Invitrogen, Carlsbad, CA), in culture medium. The beads were washed three times with PBS and imaged by confocal spinning-disk microscopy (Andor Technology PLC, Belfast, Northern Ireland)). MRP2 specificity was demonstrated by co-incubation of CDFDA with 500 µM of Indomethacin (MRP2 inhibitor).

2.6 Data analysis and statistics

All presented results were obtained from at least three independent cultures ($n \geq 3$). Error bars denote the standard error of the mean. All results were subjected to an analysis of variance (ANOVA), with a 95% confidence level considered to be significant. P values are presented for statistically significant results ($P < 0.05$).

3. Results

3.1 3D culture

HepaRG cells at the proliferative stage were inoculated as single cells in spinner vessels and allowed to aggregate for 3 days. By that time, spheroids which presented an average diameter of 57.2 ± 4.9 µm (mean value ± SEM), were encapsulated in 1.1% (w/v) alginate and further cultured until the 14th day of differentiation for parallel comparison with the 2D protocol, in which DMSO is supplemented at this point (Figure 4.1 a). Culture viability was above 89%, showing that neither encapsulation nor stirred culture conditions negatively affected cell viability (Figure b, c). Moreover, cell concentration was kept stable throughout the 14 days of culture (Figure 4.1 c), suggesting growth arrest of the encapsulated spheroids, as confirmed by the absence of the nuclear protein Ki67 in immunofluorescence characterization (data not shown).

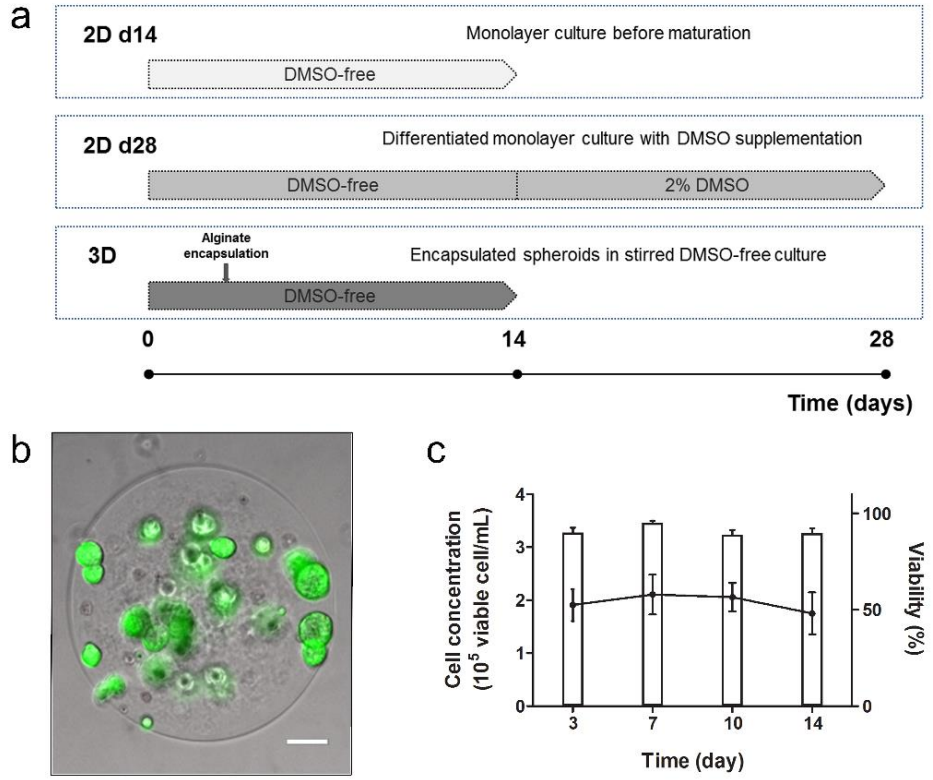

Figure 4.1 Characterization of encapsulated 3D HepaRG culture (a) Schematic representation of the conditions studied: 2D d14, 2D d28 and 3D (b) Viability assessed by staining with fluorescein diacetate (live, green) and TO-PRO®3 (dead, red) scale bar: 100 µm. (c) Cell density profile (line) and viability (bars) of 3D condition throughout 14 days of culture. Error bars represent ±SEM from 5 independent cultures.

3.2 Expression profile

A set of hepatic-specific genes including hepatic identity, homeostatic and xenobiotic metabolism, was analyzed and compared between 3D, 2D d14 and 2D d28 cultures. Globally, the expression of hepatic-specific genes was significantly upregulated in 3D versus the 2D d14 cultures for all genes analyzed, with exception for *glutamine synthethase (GS; GLUL)*, in which the expression levels were comparable. Concerning 3D and 2D d28 cultures, the expression levels were similar for the hepatic identity genes *hepatocyte nuclear factor 4 alpha* (*HNF4A)* and *pregnane X receptor* (*PXR;*

NR1I2) (Figure 4.2 a), whilst distinct profiles were observed in the expression levels of homeostatic and xenobiotic-related genes. Among homeostatic genes, the expression of the blood protein *albumin (ALB)* was maintained and genes involved in the ammonia elimination pathways, including *GS* and the urea cycle gene *carbamoyl phosphate synthetase I* (*CPS1*) displayed, respectively, equivalent and 11.7-fold increased expression levels in 3D cultures in comparison to 2D d28 (Figure 4.2 b). Regarding xenobiotic metabolism genes, only *cytochrome P450 1A2* (*CYP1A2*) expression was comparable between 3D and 2D d28 cultures, whereas the expression levels of *P450* isoforms *3A4 (CYP3A4)* and *2C9 (CYP2C9)* were 6 to 7 fold upregulated in the latter (Figure 4.2 c).

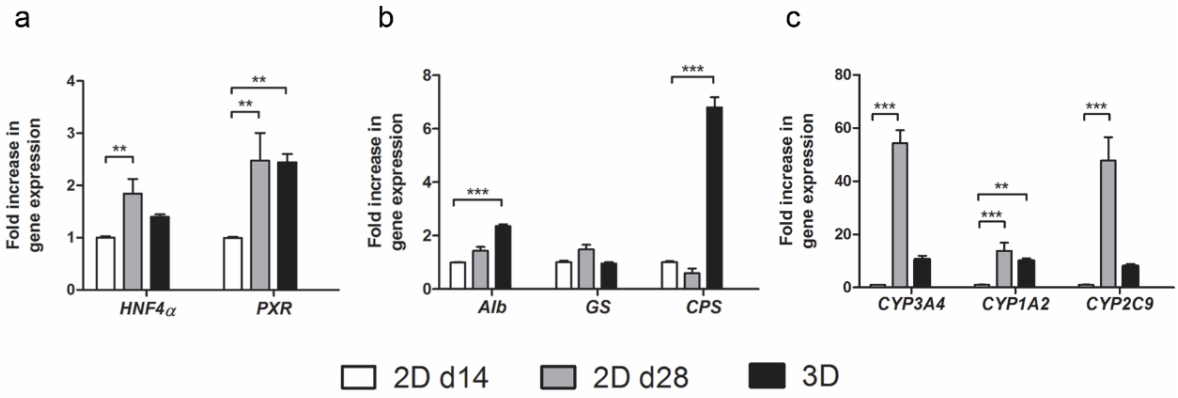

Figure 4.1 Gene expression profile of HepaRG cultures. (a) Expression of hepatic identity genes - *HNF4A* and *PXR* (b) homeostasis-related genes – *ALB*, *GS* and *CPS1* (c) xenobiotic metabolism-associated genes - *CYP3A4*, *CYP1A2* and *CYP2C9*. Gene expression was normalized to the 2D d14 cultures and *RPL22* was used as reference gene. Data are mean ± SEM of three independent cultures. Asterisks indicate significant difference (**P < 0.01; ***P < 0.001).

3.3 Phenotypic characterization

To assess the subcellular localization of hepatic specific proteins and structural organization of the cytoskeleton, samples were prepared in whole mount and visualized by confocal microscopy. Localization of F-actin at the intercellular regions indicated a highly polarized cellular organization. Moreover, actin enrichment at cellular junctional sites resembled biliary-like structures and was detected throughout the spheroid, revealing interconnectivity between the bile canalicular structures (Figure 4.3 a). The co-localization of the tight junction protein Zonula Occludens 1 (ZO-1) with actin enriched sites, confirmed that these constitute the apical regions of the cell, surrounding the bile canaliculli (Figure 4.3 c). Albumin was present in hepatic cells (Figure 4.3 a) and most cells in the spheroid expressed the hepatocyte specific protein HNF4α, suggesting a higher proportion of HLC than BLC in these cultures. Thus, the proportion of HLC/BLC cells was evaluated through co-localization of HNF4α with DAPI nuclear staining and compared with 2D d28 condition (Figure 4.3 b and 4 a). In spheroid cultures, 74.5 ± 3.7% of the nuclei were HNF4α-positive compared to 38.6 ± 1% in 2D d28 cultures (Figure 4.4 b), demonstrating higher yield of HLC to BLC obtained in the 3D differentiation strategy.

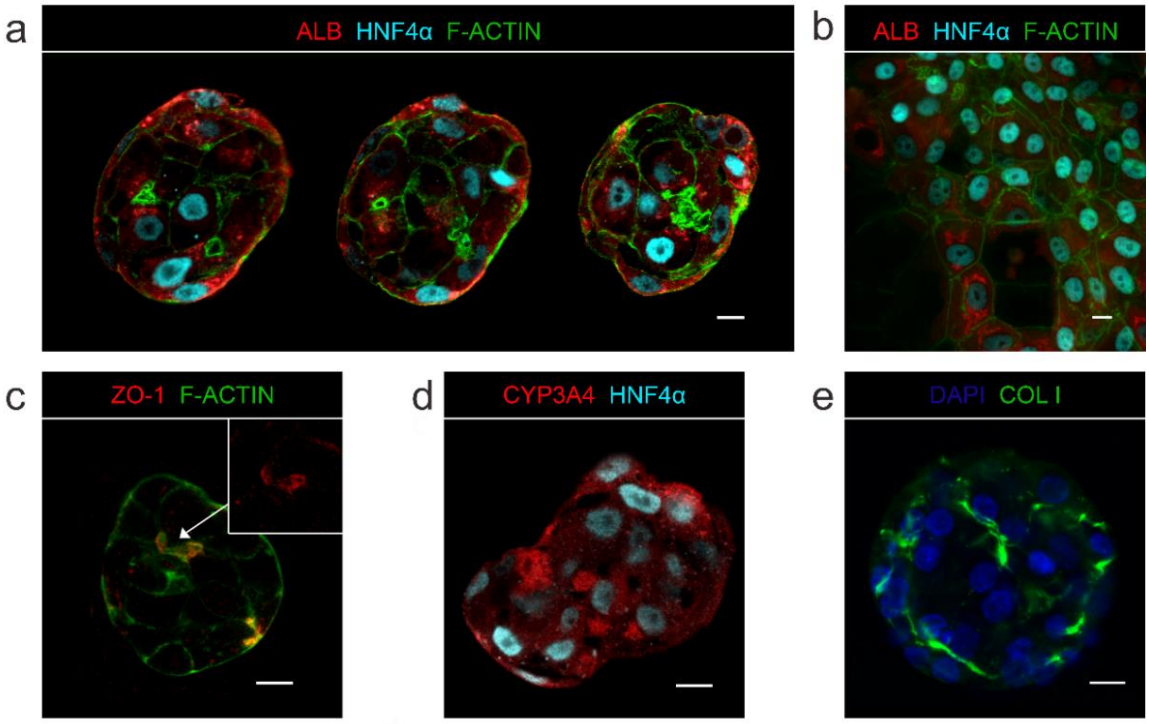

Figure 4.2 Phenotypic characterization of hepatic spheroids by immunolocalization of hepatic-specific markers. (A) Detection of the hepatic proteins HNF4α (cyan), albumin (red) and F–actin (green) in 3D cultures. Images are sequential confocal z-sections of 5 µm of the spheroid. (b) Detection of the hepatic proteins HNF4α (cyan), albumin (red) and F–actin (green) in 2D d28 cultures. (c) Co-localization of F-actin (green) and the apical marker ZO-1 (red). Arrow indicates ZO-1 localization (red) in a section of the spheroid. (d) Detection of HNF4α (cyan) and P450 isoform 3A4 (red) in a single confocal section. (e) Detection of collagen type I (COL I) and nuclei by with DAPI staining (blue). Scale bars represent 10 µm.

CYP3A4 protein was detected throughout the spheroid, even though its presence was not ubiquitous in HLC (Figure 4.3 d), similarly to what is observed in clusters of HLC in 2D d28 cultures (Hoekstra et al. 2011). In addition to hepatic specific proteins, fibers of collagen type I, the major extracellular matrix component found in the liver, was accumulated intercellularly and surrounding the spheroid (Figure 4.3 e). To assess whether undifferentiated cells were present in the spheroid, they were analyzed for the presence of the hepatic progenitor marker HNF3β which was detected in undifferentiated cultures but not observed in any of the spheroids analyzed (data not shown).

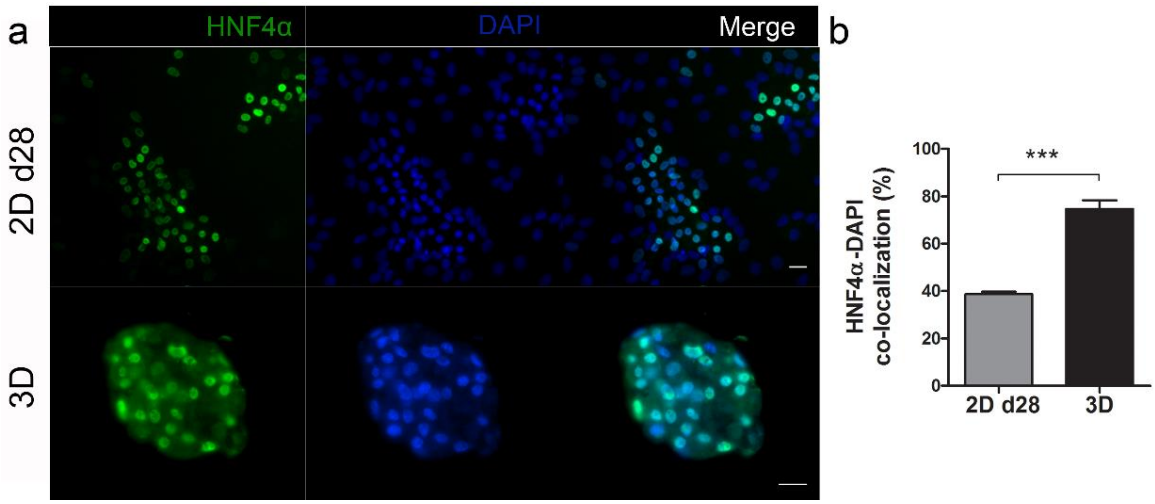

Figure 4.4 Co-localization of the hepatocyte-specific marker HNF4α with DAPI nuclear staining in cryosections of 2D d28 and 3D cultures. (a) Detection of HNF4α (green), DAPI nuclear staining (blue) and co-localization of HNF4α (green) and DAPI nuclear staining (blue). (b) Percentage of nuclei (identified by DAPI) labeled for HNF4α in 2D d28 and 3D cultures. Scale bars represent 10 µm.

3.4 Efflux transporter activity

As described above, immunofluorescence characterization of hepatic spheroids presented bile canalicular structures. To evaluate the functionality of these structures, spheroids were incubated with CDFDA, which is metabolized by phase II esterases into CDF and excreted by the phase III transporter MRP2 (Zamek-Gliszczynski et al. 2003). CDF fluorescence was detected in several cellular junctional regions and visualized along z-sections of the spheroid (Figure 4.5 a, b), demonstrating functional interconnectivity of canalicular-like structures and assembly of these structures towards the external milleau. Co-incubation with the MRP2 inhibitor indomethacin (Lengyel et al. 2008) resulted in intracellular accumulation of CDF (data not shown), blocking excretion and indicating specific MRP2-dependent excretion.

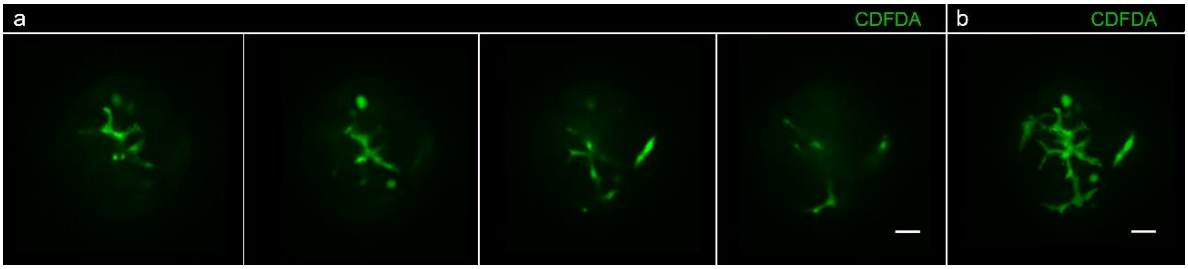

Figure 4.5 Excretory activity of HepaRG spheroids visualized by efflux of CDFDA. (a) Images are sequential confocal z-sections of 5 µm of the spheroid. (b) 3D projection of confocal sections of the whole spheroid. Scale bars represent 10 µm.

3.5 Xenobiotic metabolism

For assessment of xenobiotic metabolism, the activity of the 3A4 isoform of the P450 complex after induction with the prototypical inducer rifampicin was compared in 3D with 2D d14 and 2D d28 cultures. While all the conditions tested showed response to induction, HepaRG 3D cultures

displayed higher induction profiles (up to 8.3 fold increase) and activity levels comparable to the 2D d28 condition, in which CYP3A4 activity is typically high (Figure 4.6 a, b) (Su and Waxman 2004). CYP1A2 activity showed comparable activities in 3D and 2D d28 cultures upon induction with β-Naphthoflavone (Figure 4.6 c).

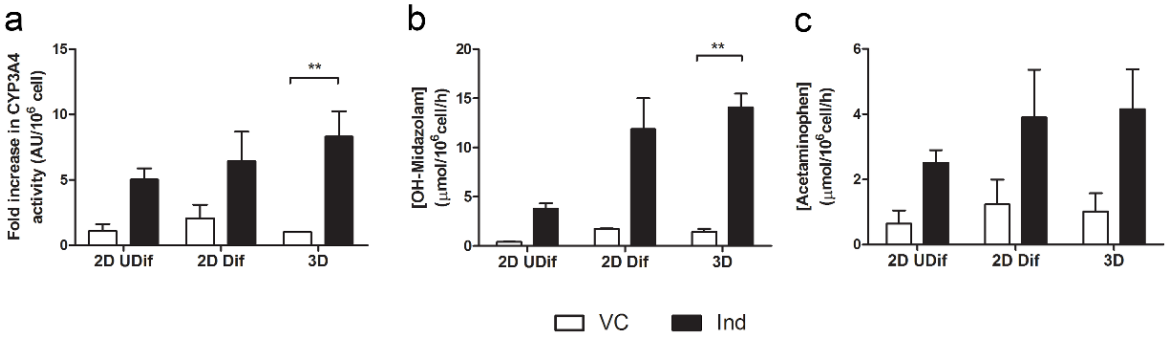

Figure 4.6 Xenobiotic drug metabolism. (a) CYP3A4 activity determined by a luciferase-based method, indicated by fold increase in activity after induction (normalized to vehicle control of 3D) . (b) CYP3A4 activity assessed by HPLC analysis of Midazolam metabolite. (c) CYP1A2 activity assessed by HPLC analysis of Phenacetin metabolite. White bars represent vehicle controls (VC) and black bars denote analysis of activity after induction for 72h with prototypical inducers (Ind). Data are mean ± SEM of four (a) or three (b, c) independent cultures. Asterisks indicate significant difference (*P < 0.05;**P < 0.01).

3.6 Homeostatic metabolism

Hepatic spheroids were further analyzed for the hepatic functions related with body homeostasis, including synthesis of blood proteins and ammonia elimination, which are determinant for BAL applications. Encapsulated 3D cultures showed significantly higher secretion rate of albumin, with 2.4 fold increase in albumin synthesis rate when compared to 2D d14 and 2D d28 cultures, respectively (Figure 4.7 a). To depict the ammonia elimination potential of the cultures, glutamine and urea concentration were determined after supplementation with ammonium chloride (NH_4Cl). An increase in urea levels was observed in 3D cultures (Figure 4.7 b) when compared with the 2D d28 cultures. Moreover, glutamine synthesis was maintained in all conditions (Figure 4.7 c). This might suggest direction towards ureagenesis in the ammonia elimination metabolic pathways.

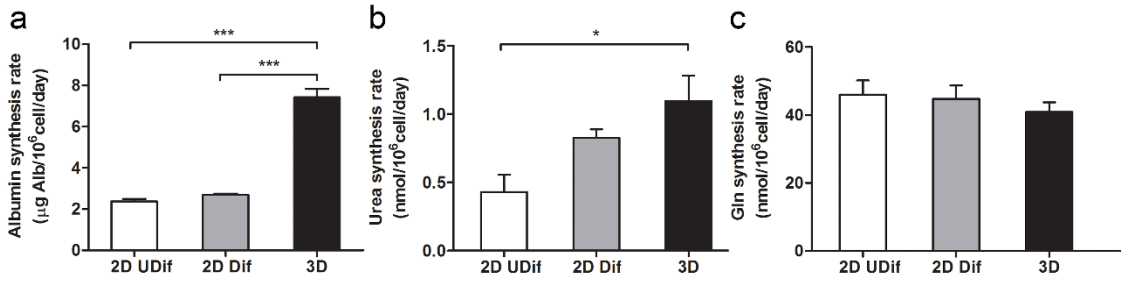

Figure 4.7 Homeostatic metabolism. (a) Albumin synthesis rate determined at day 14 for 2D d14 and 3D cultures and day 28 for 2D d28. (b) Urea and (c) glutamine synthesis rate determined after incubation with 5 mM of NH_4Cl for 24h. Data are mean ± SEM of three (a) or four (b, c) independent cultures. Asterisks indicate significant difference (*P < 0.05;**P < 0.01).

4. Discussion

The current study presents a 3D strategy for the differentiation of the hepatic cell line HepaRG, resulting in a hepatic model with enhanced functionality towards xenobiotic metabolism and homeostatic associated roles. This approach couples aggregation of HepaRG in spinner vessels with alginate encapsulation and culture in stirred DMSO-free conditions. Expression profiling of key hepatic genes revealed that the 3D cell model presented high expression levels of the hepatocyte-specific transcription factors HNF4α and PXR. This may be due either to an upregulation of these transcription factors in HLC caused by the 3D configuration or to the higher proportion of HLC/BLC resultant from the 3D differentiation. In 2D differentiated cultures (2D d28), the high HNF4α and PXR expression levels are directly related to DMSO supplementation, as DMSO acts as an inducer of these transcription factors (Su and Waxman 2004). In 3D, co-localization of HNF4α with DAPI nuclear staining demonstrated a higher proportion of HLC, which might account for the higher expression of hepatic specific genes.

HepaRG cell line exhibits the unique feature of transdifferentiation through a hepatic bipotent progenitor (Cerec et al. 2007). In 2D, the disruption of cell-cell contacts and active proliferation at low density seeding, leads to the appearance of the bipotent progenitor phenotype (Cerec et al. 2007). In the 3D strategy applied, cells were detached at confluence, when most cells were committed to biliary or hepatic fate. It is unclear to what extent the cells inoculated in spinner vessels retained the committed phenotype, since inoculation as single cells led to lack of cell-cell signaling for a short period of time, but without triggering proliferation. Nevertheless, the higher yield of hepatocytes in 3D demonstrates that a high proportion of cells could be directed to hepatocyte-like fate, indicating that the 3D differentiation strategy has the ability to determine cell fate of the undifferentiated progenitor cells.

The contribution of the 3D configuration for the preservation of cell functionality in primary cultures has been widely described (Du et al. 2008; Tostoes et al. 2012). This can be primarily attributed to the maintenance of the polygonal shape, as occurs in hepatocytes *in vivo*. Mechanical forces applied by cell-cell contacts in epithelia modulate the function of cell adhesion proteins such as E-cadherin, resulting in the coordination of cellular processes such as polarity, growth, and differentiation (Bhatt et al. 2013). In addition, the mechanical forces applied by the external microenvironment can also direct differentiation from stem cells (Engler et al. 2006) and maintain functionality in hepatic systems (You et al. 2013). In the 3D culture established, the tension promoted by the cell-cell contacts in the spheroid, coupled with encapsulation in a porous alginate scaffold, caused growth arrest (Fig. 4.1) and highly polarized organization (Figure 4.3).

Although the role of alginate encapsulation on differentiation cannot be fully depicted, the porous and flexible matrix of the scaffold facilitates diffusion of nutrients and gas exchange, provides protection from shear stress and prevents the washout of soluble factors and extracellular matrix components. These characteristics might account for the directed differentiation towards HLCs, as previously described for mesenchymal stem cells (Lin et al. 2010) or hepatoblasts (Cheng et al. 2008). Additionally, fibers of collagen I were detected in 3D cultures, not only in the intercellular regions of the spheroid but also accumulated in the alginate capsule, surrounding the spheroid

(Figure 4.3 e). Collagen type I is the major ECM component present in the liver and has been described to favor differentiation of hepatic stem cells (McClelland et al. 2008) and to enhance functionality of HepG2 cells in alginate-collagen beads (Capone et al. 2013). Thus, alginate encapsulation provides an approach that combines the advantages of a stirred system with the prevalence of the microenvironment, which is key for differentiation. Moreover, alginate-based hydrogels have been previously applied for toxicological applications and tested with several drug compounds, without drug binding to the scaffold (Lan and Starly 2011; Koizumi et al. 2007), making it a suitable system for pre-clinical development applications.

Apart from the mechanical forces provided in the 3D cell-cell contacts, the paracrine signaling must be considered as critical factor for differentiation, particularly since the commitment of HepaRG cells to HLC and BLC fates may not be equal during aggregation, as discussed above. Taken together, there seems to be a synergistic effect between the paracrine signaling and mechanical forces promoted by cell-cell contacts and the microenvironment provided by alginate for the cell fate of bipotent HepaRG cells.

The structural characterization provided insight on the functionality of the spheroids. F-actin enrichment on the junctional sites of the cells revealed the existence of interconnected biliary-like structures along the entire spheroid (Figure 4.3 a). Excretory functionality and specific activity of MRP2 was demonstrated by excretion of CDF to the external milieu (Figure 4.5). Previous studies showed that although the expression of MRP2 is comparable between differentiated, confluent HepaRG and primary human hepatocytes, the presence of the MRP2 protein in canalicular structures is only detected after treatment with DMSO (Le Vee et al. 2006; Schulze et al. 2012). Moreover, it has been proposed that differentiated HepaRG cells in 2D systems do not fully recapitulate the polarization status of primary human hepatocytes, due to the absence of canalicular phenotype of some HLC (Schulze et al. 2012). The results obtained suggest that 3D culture established represents a strategy to overcome this limitation, enabling the correct assembly of biliary structures, thus resulting in an interconnected network of canalicular structures within the spheroid. Moreover, proper assembly of polarity structures and function of membrane-associated transporters represent an advantageous feature for toxicological studies, as it is a limitation of the existent 2D systems.

Maintenance of polarity is also linked with high activity of drug metabolizing enzymes of the P450 complex (Godoy et al. 2013). Analysis of xenobiotic metabolism, by P450 complex expression and activity, evidenced that despite the marked difference of P450 isoforms expression levels in 3D cultures when compared with 2D d28, the activities of CYP3A4 and CYP1A2 were similar between both systems upon induction with prototypical inducers. The high expression levels of isoforms 3A4 and 2C9 observed in 2D d28 cultures are a consequence of the induction by DMSO present in the culture medium (Su and Waxman 2004). DMSO acts as an anti-apoptotic agent and modulates multiple cellular functions that may interact with the drug elimination mechanisms, making a DMSO-free culture desirable for toxicological studies. Previous reports showed that CYP3A4 expression levels of HepaRG cells in the presence of DMSO were higher than observed in cultured human hepatocytes (HH), while CYP2C9 expression was described to be equivalent and CYP1A2

markedly reduced (Antherieu et al. 2010; Hart et al. 2010). Regardless, differentiated HepaRG displayed activity levels of CYP3A4 comparable to HH after induction (Gerets et. al, 2012). Thus, 3D cultures of HepaRG might constitute an alternative to HH for assessing metabolism of xenobiotics.

Interestingly, immunolocalization of the CYP3A4 protein revealed differences in the intensity of CYP3A4 signal among HLC, in contrary to 2D d28 cultures which displayed a more homogenous CYP3A4 distribution and intensity. The heterogeneity of HepaRG-derived HLC in the absence of DMSO has been previously described, particularly regarding the cluster-neighboring cells of HLC whose phenotype is suppressed by DMSO (Hoekstra et al. 2011). In encapsulated spheroids, there seems to be a coexistence of two phenotypes - one in which CYP3A4 presence is higher, what could be correlated with a more pericentral-like phenotype and another with lower levels of CYP3A4, associated with periportal type of functions. Further characterization would be necessary to validate this hypothesis, by detecting the presence of specific proteins– CPS1 and G6PC for periportal phenotype and GS and CYP isoforms for pericentral phenotype (Torre et al. 2010).

The coexistence of a periportal and pericentral phenotype is consistent with the results obtained regarding albumin production and ammonia detoxification metabolism. Particularly, concerning ammonia elimination, an increase in the production of urea was observed in 3D. The absence of DMSO, as well as the high proportion of HLC is likely to contribute to the enhancement of ammonia detoxification metabolism. Ureagenesis, a crucial metabolic mechanism for ammonia detoxification, is often a limiting step in hepatic cell lines (Mavri-Damelin et al. 2008). Interestingly, the expression of CPS1, the initial enzyme of the urea cycle, was highly upregulated in 3D. Despite the significant increase in urea levels detected in 3D, it did not correspond to the high mRNA levels of CPS1. This might be explained by a bottleneck on the production of urea, by limitation on its allosteric activator N-acetylglutamate, as suggested by (Hoekstra et al. 2011). According to that report, pre-conditioning with an analogue of N-acetylglutamate increased the ureagenesis of HepaRG cultures. This strategy may be applied for the spheroid culture, enhancing its potential to be applied for BAL.

To our knowledge, this study presents a novel culture system for the differentiation of HepaRG in DMSO-free conditions, by culture in 3D configuration and alginate encapsulation. The hepatic model developed covers the most crucial hepatic functions – highly polarized phenotype with interconnected network of bile cannaliculi, inducible CYP3A4 and CYP1A2 activity, and phase III functionality. These features, particularly the advantage of being a DMSO-free model, contribute to a more physiological hepatic system and make it a valuable tool for toxicological applications. Additionally, encapsulated spheroids may be multiplexed for toxicological studies, comprising the possibility of high throughput with phenotypic characterization upon drug stimuli and may be coupled with high content screening platforms for identification of toxic compounds, as previously described for other 3D systems (Celli et al. 2014; Wenzel et al. 2014). On the other side, homeostatic features such as albumin production and ammonia elimination broaden the applicability of the model towards BAL support. Altogether, the strategy described represents a valuable tool for hepatic differentiation, may be adapted for other systems such as hepatic progenitors or pluripotent stem cells and delivers a relevant model to understand liver physiology.

Acknowledgments

I gratefully acknowledge Tiago Duarte for discussion and support in GC–MS technique and Daniel Simão for support in microscopy. This work was supported by PhD fellowship SFRH/BD/70264/2010 and by PTDC/EBB-BIO/112786/2009, funded by Fundação para a Ciência e Tecnologia.

5. References

Antherieu S, Chesne C, Li R, Camus S, Lahoz A, Picazo L, Turpeinen M, Tolonen A, Uusitalo J, Guguen-Guillouzo C, Guillouzo A (2010) Stable expression, activity, and inducibility of cytochromes P450 in differentiated HepaRG cells. Drug Metab Dispos 38 (3):516-525.

Bhatt T, Rizvi A, Batta SP, Kataria S, Jamora C (2013) Signaling and Mechanical Roles of E-cadherin. Cell Commun Adhes.

Cai ZH, Shi ZQ, O'Shea GM, Sun AM (1988) Microencapsulated hepatocytes for bioartificial liver support. Artif Organs 12 (5):388-393

Capone SH, Dufresne M, Rechel M, Fleury MJ, Salsac AV, Paullier P, Daujat-Chavanieu M, Legallais C (2013) Impact of alginate composition: from bead mechanical properties to encapsulated HepG2/C3A cell activities for in vivo implantation. PLoS One 8 (4):e62032.

Celli JP, Rizvi I, Blanden AR, Massodi I, Glidden MD, Pogue BW, Hasan T (2014) An imaging-based platform for high-content, quantitative evaluation of therapeutic response in 3D tumour models. Sci Rep 4:3751

Cerec V, Glaise D, Garnier D, Morosan S, Turlin B, Drenou B, Gripon P, Kremsdorf D, Guguen-Guillouzo C, Corlu A (2007) Transdifferentiation of hepatocyte-like cells from the human hepatoma HepaRG cell line through bipotent progenitor. Hepatology 45 (4):957-967. doi:10.1002/hep.21536

Cheng N, Wauthier E, Reid LM (2008) Mature human hepatocytes from ex vivo differentiation of alginate-encapsulated hepatoblasts. Tissue Eng Part A 14 (1):1-7.

Du Y, Han R, Wen F, Ng San San S, Xia L, Wohland T, Leo HL, Yu H (2008) Synthetic sandwich culture of 3D hepatocyte monolayer. Biomaterials 29 (3):290-301.

Elkayam T, Amitay-Shaprut S, Dvir-Ginzberg M, Harel T, Cohen S (2006) Enhancing the drug metabolism activities of C3A--a human hepatocyte cell line--by tissue engineering within alginate scaffolds. Tissue Eng 12 (5):1357-1368.

Engler AJ, Sen S, Sweeney HL, Discher DE (2006) Matrix elasticity directs stem cell lineage specification. Cell 126 (4):677-689.

Godoy P, Hewitt NJ, Albrecht U, Andersen ME, Ansari N, Bhattacharya S, Bode JG, Bolleyn J, Borner C, Bottger J, Braeuning A, Budinsky RA, Burkhardt B, Cameron NR, Camussi G, Cho CS, Choi YJ, Craig Rowlands J, Dahmen U, Damm G, Dirsch O, Donato MT, Dong J, Dooley S, Drasdo D, Eakins R, Ferreira KS, Fonsato V, Fraczek J, Gebhardt R, Gibson A, Glanemann M, Goldring CE, Gomez-Lechon MJ, Groothuis GM, Gustavsson L, Guyot C, Hallifax D, Hammad S, Hayward A, Haussinger D, Hellerbrand C, Hewitt P, Hoehme S, Holzhutter HG, Houston JB, Hrach J, Ito K, Jaeschke H, Keitel V, Kelm JM, Kevin Park B, Kordes C, Kullak-Ublick GA, Lecluyse EL, Lu P, Luebke-Wheeler J, Lutz A, Maltman DJ, Matz-Soja M, McMullen P, Merfort I, Messner S, Meyer C, Mwinyi J, Naisbitt DJ, Nussler AK, Olinga P, Pampaloni F, Pi J, Pluta L, Przyborski SA, Ramachandran A, Rogiers V, Rowe C, Schelcher C, Schmich K, Schwarz M, Singh B, Stelzer EH, Stieger B, Stober R, Sugiyama Y, Tetta C, Thasler WE, Vanhaecke T, Vinken M, Weiss TS, Widera A, Woods CG, Xu JJ, Yarborough KM, Hengstler JG (2013) Recent advances in 2D and 3D in vitro systems using primary hepatocytes, alternative hepatocyte sources and non-parenchymal liver cells and their use in investigating mechanisms of hepatotoxicity, cell signaling and ADME. Arch Toxicol 87 (8):1315-1530.

Gripon P, Rumin S, Urban S, Le Seyec J, Glaise D, Cannie I, Guyomard C, Lucas J, Trepo C, Guguen-Guillouzo C (2002) Infection of a human hepatoma cell line by hepatitis B virus. Proc Natl Acad Sci U S A 99 (24):15655-15660. doi:10.1073/pnas.232137699

232137699 [pii]
Gunness P, Mueller D, Shevchenko V, Heinzle E, Ingelman-Sundberg M, Noor F (2013) 3D organotypic cultures of human HepaRG cells: a tool for in vitro toxicity studies. Toxicol Sci 133 (1):67-78.

Hart SN, Li Y, Nakamoto K, Subileau EA, Steen D, Zhong XB (2010) A comparison of whole genome gene expression profiles of HepaRG cells and HepG2 cells to primary human hepatocytes and human liver tissues. Drug Metab Dispos 38 (6):988-994.

Higuchi Y, Kawai K, Yamazaki H, Nakamura M, Bree F, Guguen-Guillouzo C, Suemizu H (2013) The human hepatic cell line HepaRG as a possible cell source for the generation of humanized liver TK-NOG mice. Xenobiotica.

Hoekstra R, Nibourg GA, van der Hoeven TV, Ackermans MT, Hakvoort TB, van Gulik TM, Lamers WH, Elferink RP, Chamuleau RA (2011) The HepaRG cell line is suitable for bioartificial liver application. Int J Biochem Cell Biol 43 (10):1483-1489.

Hoekstra R, Nibourg GA, van der Hoeven TV, Plomer G, Seppen J, Ackermans MT, Camus S, Kulik W, van Gulik TM, Elferink RP, Chamuleau RA (2013) Phase 1 and phase 2 drug metabolism and bile acid production of HepaRG cells in a bioartificial liver in absence of dimethyl sulfoxide. Drug Metab Dispos 41 (3):562-567.

Hofmann U, Maier K, Niebel A, Vacun G, Reuss M, Mauch K (2008) Identification of metabolic fluxes in hepatic cells from transient 13C-labeling experiments: Part I. Experimental observations. Biotechnology and bioengineering 100 (2):344-354

Jungermann K (1995) Zonation of metabolism and gene expression in liver. Histochem Cell Biol 103 (2):81-91

Koizumi T, Aoki T, Kobayashi Y, Yasuda D, Izumida Y, Jin Z, Nishino N, Shimizu Y, Kato H, Murai N, Niiya T, Enami Y, Mitamura K, Yamamoto T, Kusano M (2007) Long-term maintenance of the drug transport activity in cryopreservation of microencapsulated rat hepatocytes. Cell Transplant 16 (1):67-73

Lan S-F, Starly B (2011) Alginate based 3D hydrogels as an in vitro co-culture model platform for the toxicity screening of new chemical entities. Toxicology and applied pharmacology 256 (1):62-72

Le Vee M, Jigorel E, Glaise D, Gripon P, Guguen-Guillouzo C, Fardel O (2006) Functional expression of sinusoidal and canalicular hepatic drug transporters in the differentiated human hepatoma HepaRG cell line. Eur J Pharm Sci 28 (1-2):109-117.

Le Vee M, Noel G, Jouan E, Stieger B, Fardel O (2013) Polarized expression of drug transporters in differentiated human hepatoma HepaRG cells. Toxicol In Vitro 27 (6):1979-1986.

LeCluyse EL, Witek RP, Andersen ME, Powers MJ (2012) Organotypic liver culture models: meeting current challenges in toxicity testing. Crit Rev Toxicol 42 (6):501-548.

Leite SB, Wilk-Zasadna I, Zaldivar JM, Airola E, Reis-Fernandes MA, Mennecozzi M, Guguen-Guillouzo C, Chesne C, Guillou C, Alves PM, Coecke S (2012) Three-dimensional HepaRG model as an attractive tool for toxicity testing. Toxicol Sci 130 (1):106-116.

Lengyel G, Veres Z, Tugyi R, Vereczkey L, Molnar T, Glavinas H, Krajcsi P, Jemnitz K (2008) Modulation of sinusoidal and canalicular elimination of bilirubin-glucuronides by rifampicin and other cholestatic drugs in a sandwich culture of rat hepatocytes. Hepatol Res 38 (3):300-309.

Lin N, Lin J, Bo L, Weidong P, Chen S, Xu R (2010) Differentiation of bone marrow-derived mesenchymal stem cells into hepatocyte-like cells in an alginate scaffold. Cell Prolif 43 (5):427-434.

Mavri-Damelin D, Damelin LH, Eaton S, Rees M, Selden C, Hodgson HJ (2008) Cells for bioartificial liver devices: the human hepatoma-derived cell line C3A produces urea but does not detoxify ammonia. Biotechnol Bioeng 99 (3):644-651.

McClelland R, Wauthier E, Uronis J, Reid L (2008) Gradients in the liver's extracellular matrix chemistry from periportal to pericentral zones: influence on human hepatic progenitors. Tissue Eng Part A 14 (1):59-70.

Mueller D, Kramer L, Hoffmann E, Klein S, Noor F (2013) 3D organotypic HepaRG cultures as in vitro model for acute and repeated dose toxicity studies. Toxicol In Vitro.

Nibourg GA, Chamuleau RA, van der Hoeven TV, Maas MA, Ruiter AF, Lamers WH, Oude Elferink RP, van Gulik TM, Hoekstra R (2012) Liver progenitor cell line HepaRG differentiated in a bioartificial liver effectively supplies liver support to rats with acute liver failure. PLoS One 7 (6):e38778.

Pal R, Mamidi MK, Das AK, Bhonde R (2012) Diverse effects of dimethyl sulfoxide (DMSO) on the differentiation potential of human embryonic stem cells. Arch Toxicol 86 (4):651-661.

Parent R, Marion MJ, Furio L, Trepo C, Petit MA (2004) Origin and characterization of a human bipotent liver progenitor cell line. Gastroenterology 126 (4):1147-1156.

Santos NC, Figueira-Coelho J, Martins-Silva J, Saldanha C (2003) Multidisciplinary utilization of dimethyl sulfoxide: pharmacological, cellular, and molecular aspects. Biochem Pharmacol 65 (7):1035-1041.

Schulze A, Mills K, Weiss TS, Urban S (2012) Hepatocyte polarization is essential for the productive entry of the hepatitis B virus. Hepatology 55 (2):373-383.

Su T, Waxman DJ (2004) Impact of dimethyl sulfoxide on expression of nuclear receptors and drug-inducible cytochromes P450 in primary rat hepatocytes. Arch Biochem Biophys 424 (2):226-234.

Sun AM, O'Shea GM, Goosen MF (1984) Injectable microencapsulated islet cells as a bioartificial pancreas. Appl Biochem Biotechnol 10:87-99

Takayama K, Kawabata K, Nagamoto Y, Kishimoto K, Tashiro K, Sakurai F, Tachibana M, Kanda K, Hayakawa T, Furue MK, Mizuguchi H (2013) 3D spheroid culture of hESC/hiPSC-derived hepatocyte-like cells for drug toxicity testing. Biomaterials 34 (7):1781-1789.

Torre C, Perret C, Colnot S (2010) Molecular determinants of liver zonation. Prog Mol Biol Transl Sci 97:127-150.

Tostoes RM, Leite SB, Miranda JP, Sousa M, Wang DI, Carrondo MJ, Alves PM (2011) Perfusion of 3D encapsulated hepatocytes--a synergistic effect enhancing long-term functionality in bioreactors. Biotechnol Bioeng 108 (1):41-49.

Tostoes RM, Leite SB, Serra M, Jensen J, Bjorquist P, Carrondo MJ, Brito C, Alves PM (2012) Human liver cell spheroids in extended perfusion bioreactor culture for repeated-dose drug testing. Hepatology (Baltimore, Md 55 (4):1227-1236

Wenzel C, Riefke B, Grundemann S, Krebs A, Christian S, Prinz F, Osterland M, Golfier S, Rase S, Ansari N, Esner M, Bickle M, Pampaloni F, Mattheyer C, Stelzer EH, Parczyk K, Prechtl S, Steigemann P (2014) 3D high-content screening for the identification of compounds that target cells in dormant tumor spheroid regions. Experimental cell research 323 (1):131-143

You J, Park SA, Shin DS, Patel D, Raghunathan VK, Kim M, Murphy CJ, Tae G, Revzin A (2013) Characterizing the Effects of Heparin Gel Stiffness on Function of Primary Hepatocytes. Tissue Eng Part A.

Zamek-Gliszczynski MJ, Xiong H, Patel NJ, Turncliff RZ, Pollack GM, Brouwer KL (2003) Pharmacokinetics of 5 (and 6)-carboxy-2',7'-dichlorofluorescein and its diacetate promoiety in the liver. J Pharmacol Exp Ther 304 (2):801-809.

CHAPTER 5

Discussion and perspectives

TABLE OF CONTENTS

1. Discussion and perspectives

Tremendous efforts have been made in the field of liver biology, tissue engineering and biotechnology in order to recapitulate hepatic functionality *in vitro* in the past years. Despite the particular requirements of each application, such as compatibility with high-throughput platforms for toxicological screening or GMP compliance for clinical applications, the global challenges and bottlenecks of hepatic tissue engineering are transversal: scarcity of functional cell sources and restoration and/or long-term maintenance of hepatic functionality. Thus, the development of culture systems and strategies capable of overcoming these bottlenecks while coping with the specific requirements of toxicology testing, cell therapy or extracorporeal liver support are the major hurdles in hepatic tissue engineering.

The work developed in this thesis aimed to develop culture strategies resulting in human hepatic cell models to recapitulate hepatic specific functions and predict drug metabolism and toxicity *in vitro*. With this purpose, both human hepatocytes and the hepatic cell line HepaRG were used combining 3D architecture, co-cultures and biomaterials with stirred culture in bioreactors using perfusion to attain relevant cell models. A panel of techniques was used to characterize the phenotype of the hepatic cellular models developed and to monitor the biosynthetic and xenobiotic metabolism and their applicability for toxicological applications. An overview of the work developed in this thesis is summarized in figure 5.1, where the aims, strategy and achievements of each chapter (2-5) are presented.

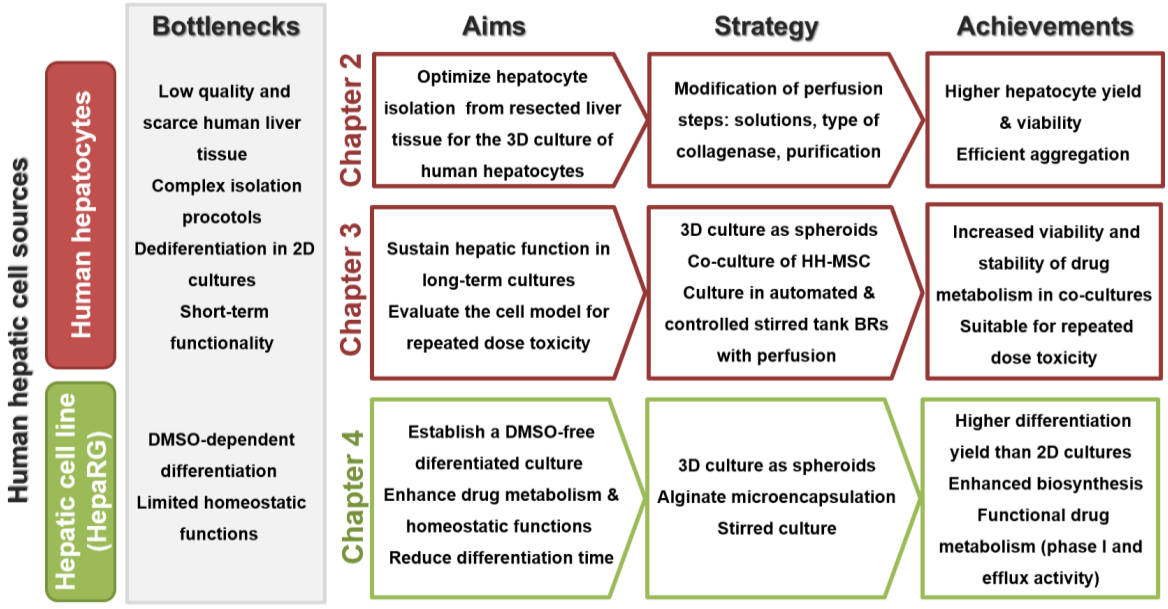

Figure 5.1 Schematic representation of the work performed in this thesis, comprising the cell sources and their bottlenecks as well as the aims, strategy and achievements of each chapter (2-5).

1.1 Hepatic cell sources: human hepatocytes and HepaRG cell line

As referred in the introductory section, widespread implementation of human hepatocyte culture is severely limited by the scarcity, dependence on donor characteristics, quality of the liver piece and isolation process (Godoy et al., 2013). Several studies using primary cultures reported in the literature have been developed with hepatocytes retrieved from rat or mice livers, with the aim of implementing and evaluating the technologies and methodologies. Human liver tissue, either recovered from whole organs or resected liver tissue from patients undergoing surgical hepatectomy, is usually at suboptimal conditions to perform perfusion when compared with animal tissue due to multiple factors (*e.g.* non-functional cardiovascular system, ischemia, histopathology, donor clinical history, etc.). Moreover, the protocols for isolation of hepatocytes from resected liver tissue are limited and were mostly developed for culture in monolayers. Thus, the isolation protocols from resected liver tissue still required optimization towards 3D culture and homogenization of procedures.

To optimize hepatocyte isolation and aggregation efficiency, in chapter 2, the variables affecting hepatocyte isolation were analyzed and two isolation methods were compared in terms of hepatocyte yield, viability and aggregation. By removing the calcium chelating solution HEPES-EGTA in the first perfusion step, modifying the type of collagenase used and refining the purification process, the average yield increased 3.7 fold, resulting in $4.4\pm1.4x10^6$ hepatocytes per gram of tissue with an approximate average viability of 55%. These results are comparable with what has been previously described in the literature for hepatocyte isolation from resected liver tissue (Bhogal et al., 2011; Hewes et al., 2006; Kawahara et al., 2010; Lee et al., 2014). Moreover, 91% of the cultures of freshly isolated hepatocytes aggregated in stirred culture systems, corresponding to a 3-fold improvement in the efficiency of aggregation. Thus, the protocol optimization resulted in an efficient aggregation process, as previously described for rat hepatocytes (Okubo et al., 2002), which is compatible with the 3D culture of hepatocytes in stirred conditions. The 3D culture of primary cultures of human hepatocytes was further combined with other strategies for optimization of the cell model, as described in chapter 3 and discussed below (section 1.2).

As alternative to human hepatocytes, HepaRG, a bipotent cell line that can be differentiated into hepatocyte-like cells and biliary-like cells (Gripon et al., 2002) was used during this thesis. HepaRG cells rely on DMSO to attain drug metabolic levels comparable with primary cultures of human hepatocytes. After 2 weeks of differentiation with 2% (v/v) of DMSO, HepaRG cells exhibit comparable expression levels of CYP3A4 to freshly isolated human hepatocytes and higher than cultured hepatocytes (Anthérieu et al., 2010; Hart et al., 2010). Other isoforms such as CYP2C9 and CYP1A2 have lower expression and activities when compared to either freshly isolated and cultured human hepatocytes but still higher than other cell lines such as HepG2 (Anthérieu et al., 2010; Hart et al., 2010). Thus, globally and when compared with other hepatic cellular sources, the high P450 complex expression and activity levels of HepaRG and the correct localization of hepatobiliary transporters in the apical and basolateral domains (Bachour-El Azzi et al., 2015) make this cell line an efficient model of liver function to pursue with toxicity studies in alternative to human hepatocytes. Despite these advantages, the high concentrations of DMSO used for differentiation

and its inherent toxicity and anti-apoptotic effects (Cerec et al., 2007) can reduce the biological relevance of toxicological studies and hamper its application for extracorporeal liver support. Moreover, HepaRG homeostatic functions, such as albumin production, glycogen storage and conversion of ammonia into urea (functions associated with periportal hepatocytes) are also repressed by DMSO supplementation (Hoekstra et al., 2011; Pal et al., 2012). To circumvent this, a 3D culture strategy to attain functional and mature hepatocyte-like cells in DMSO-free derived conditions was pursued and is described in chapter 4. The aggregation, microencapsulation and culture of HepaRG in stirred systems resulted in an improvement of approximately 36% in the hepatocyte differentiation, with a higher proportion of hepatocyte to biliary cells in 3D when compared to the 2D differentiation. The differentiated cells were functional in terms of drug metabolism, with CYP3A4 and CYP1A2 activities comparable to 2D differentiated cultures upon induction with prototypical inducers. In addition, biosynthetic metabolism was also enhanced, with a significant increase in albumin production and urea detoxification. This improvement is probably related with the higher number of hepatocyte-like cells in 3D and/or with the absence of DMSO and its repressive effects on biosynthetic functions. Thus, the novel 3D HepaRG model developed in this work is suitable for toxicological applications and its applicability can be broadened to liver physiology studies and for extracorporeal liver support, due to the xenobiotic metabolism and maintenance of biosynthetic functions.

As shown in this thesis, both human hepatocytes obtained from resected liver tissue and HepaRG cell line differentiated in 3D exhibit mature hepatic functions. Human hepatocytes are the cell source more representative of differentiated functions and of population diversity. Yet, the limited availability and inherent inter-donor variability favors the use of other more reproducible cell sources for method implementation and target screening, restricting the use of primary cultures for toxicological assays. The optimization of HepaRG culture has resulted in improvements regarding biosynthetic functionality, towards a more complete hepatic cell model. The differentiated functions, availability and reproducibility of HepaRG make it a strong candidate to be used in method implementation, large scale testing and to replace primary cultures from a single donor in toxicity testing. Nevertheless, hepatocyte cells derived from pluripotent stem cells are still the most promising cell source for hepatic replacement alternative. Its implementation depends on the improvement of differentiation protocols from PSC to deliver hepatocyte-like cells in higher quantities and better quality (improve differentiation yields and maturation of hepatocytes). This would solve the scarcity problem, allow the modeling of genetic-based hepatic diseases and include diversity in toxicological studies. Reaching this goal will enclose diverse approaches such as genetic engineering, rational selection and combined use of soluble factors and the improvement of culture strategies by the use of co-cultures, biomaterials and/or bioprocess optimization.

1.2 Approaches for the culture of human hepatic cell models

The 3D culture of hepatic cells in stirred conditions was a common approach used in this thesis for human hepatocytes and HepaRG cells. In addition to the 3D culture, other strategies were applied such as the use of biomaterials, co-cultures and environmentally controlled culture in stirred-tank bioreactors. Hepatic cells were cultured in 3D to potentiate cell-cell interactions and thereby prevent

hepatocyte dedifferentiation or induce hepatocyte differentiation, as reviewed in Godoy et al. (2013) and LeCluyse et al. (2012). This is due to the transcriptional regulation of cytoskeleton genes, key hepatic regulators and metabolic pathways in 3D (Chang and Hughes-Fulford, 2009; Chang and Hughes-Fulford, 2014). Cell aggregation was promoted by controlling culture hydrodynamics via tailoring of stirring rate, type of paddle and vessel to the cell source, resulting in different aggregation profiles for HepaRG and human hepatocytes. Stirring improves mass transfer, thereby increasing gas availability inside the culture system and enabling an efficient diffusion of nutrients through the tissue.

The porous and flexible alginate matrix was used to immobilize HepaRG spheroids in order to promote spatial constriction, thereby causing growth arrest and triggering differentiation (Cerec et al., 2007). Beyond the structural supportive function, the alginate matrix provides protection from the shear stress induced by hydrodynamic conditions, being important for stirred systems, and allows nutrient diffusion and gases exchange (Tostões et al., 2011). Moreover, the secreted ECM is retained within the alginate matrix, namely collagen type I and potentially other ECM fibrillar proteins (*e.g.* fibronectin), which may lead to the retention of soluble factors that would otherwise easily diffuse through the porous matrix. The prevention of soluble factors washout may preserve the cell spheroids microenvironment, thus enhancing the differentiation yield and hepatic phenotype.

Another strategy developed in thesis to support hepatic cells, by preserving the microenvironment and conferring protection from hydrodynamic-induced shear stress, was the co-culture of human hepatocytes with bone marrow-derived mesenchymal stem cells as spheroids in bioreactors. The improvements promoted by heterotypic interactions on hepatic functionality have been previously demonstrated by co-culture of non-parenchymal liver cells and other cellular types such as fibroblasts (Khetani et al., 2004; Kostadinova et al., 2013). Co-culture with mesenchymal stem cells had been mostly assessed as a therapeutic methodology to treat liver disease due to the widely described immunomodulatory properties of mesenchymal stem cells (Ghannam et al., 2010). Nevertheless, the co-culture of human hepatocytes and mesenchymal stem cells *in vitro* and its potential to develop a cellular model for toxicological applications has not been explored previously to this work.

In chapter 3, a dual step inoculation of human hepatocytes and mesenchymal stem cells is described, resulting in an overlay of MSC around the hepatic spheroid. The hepatic and mesenchymal phenotypes were maintained in long-term culture, with the mesenchymal stem cells acquiring a supportive stromal phenotype rather than differentiating into other terminally differentiated lineages. The biosynthetic and drug metabolism functionality were preserved for longer periods in co-cultures in comparison to mono-cultures, demonstrating the role of MSC in hepatocyte survival and maintenance of differentiated hepatic functions. The characterization performed showed evidence of paracrine signaling and ECM secretion, both contributing to the results observed.

A common feature of both cellular models developed (HH-MSC and HepaRG) was the existence of different cell types in co-culture, since differentiated HepaRG cells are a mixture of HLC and

other epithelial cells which have been associated with biliary phenotype (Parent et al., 2004). Although HepaRG's bipotent potential as well as its the differentiation into functional cholangiocytes have been clearly demonstrated (Dianat et al., 2014), the identity of the cells in co-culture with HLC has not been clarified. These cells resemble either undifferentiated progenitors or cells of the biliary lineage. It is also unclear whether the presence of these supportive cells is necessary for the maintenance of the highly differentiated phenotype of HLC or what their supportive role is exactly. Nevertheless, in the 2D DMSO-dependent differentiation protocol, more than 50% of the cells are BLC and, after purification of HLC through a dual step tripsinization method and cell re-seeding, the transdifferentiation into BLC occurs, suggesting their presence is needed for the culture (Cerec et al., 2007). In the 3D DMSO-free culture, there was an increase of the ratio of HLC to BLC, but the supportive cells were still present. Moreover, the 3D cellular spatial arrangement of the co-culture did not show preferential differentiation in any region of the spheroid and the formation of bile canalicular-like structures seemed to be homogenous across the spheroid, indicating a homogeneous differentiation and structural assembly.

The accumulation of the ECM component collagen type I surrounding the cell spheroids was demonstrated both in HH-MSC and HepaRG cultures, being attributed to the secretion of collagen by MSC and to retention of the collagen fibers within the alginate capsule, respectively. As previously mentioned, collagen type I is the most used biomaterial in hepatocyte culture and the one which effects on hepatic functionality have been mostly described both for differentiation and culture of mature hepatocytes (Jain et al., 2013). Both strategies developed in this thesis guaranteed the retention of the synthesized collagen in the adjacent regions of the spheroid. The polymerized ECM confers a network that most likely retains soluble factors and metabolic products, preserving important microenvironment factors in the periferic regions of the spheroid, which might have contributed for the high differentiation and hepatic functionality levels achieved.

The control of culture parameters such as pH, partial pressure of O_2 kept at 6% and temperature at 37ºC achieved in the work developed in chapter 3 also contribute to the preservation of hepatic microenvironment, as previously addressed by Tostões et al. (2011, 2012). Particularly, the control of O_2 tension, which was set as the average concentration between pericentral and periportal regions, might have had contributed to enhance the drug metabolism of cultured hepatocytes, as low oxygen tensions have been described to increase hepatic metabolism (polarization, gene expression, and drug clearance) (Allen et al., 2005; Kidambi et al., 2009). Importantly, stirred-tank bioreactors offer a tight control of the dissolved oxygen concentration through the use of probes that monitor the oxygen concentration inside the vessel and automatically inject gases to adjust into the set-up levels. Non-controlled studies establish the set-up in the air space and the oxygen concentration in the medium is undetermined. Moreover, the medium replenishment attained through perfusion operation mode allows the gradual supply of nutrients and removal of metabolic byproducts which may have a repressive impact on hepatic metabolism, (Tostões et al., 2011, 2012), contributing to create a nutritional gradient in the culture.

Altogether, evidence suggests that the preservation of hepatic microenvironment is critical to achieve high levels of hepatic functionality. Independently of the strategy chosen for the culture of

hepatic cells, the preservation of cell-cell interactions, cell-ECM interactions and the maintenance of the physiochemical environment seem to play a fundamental role in the development of cellular model (Figure 5.2).

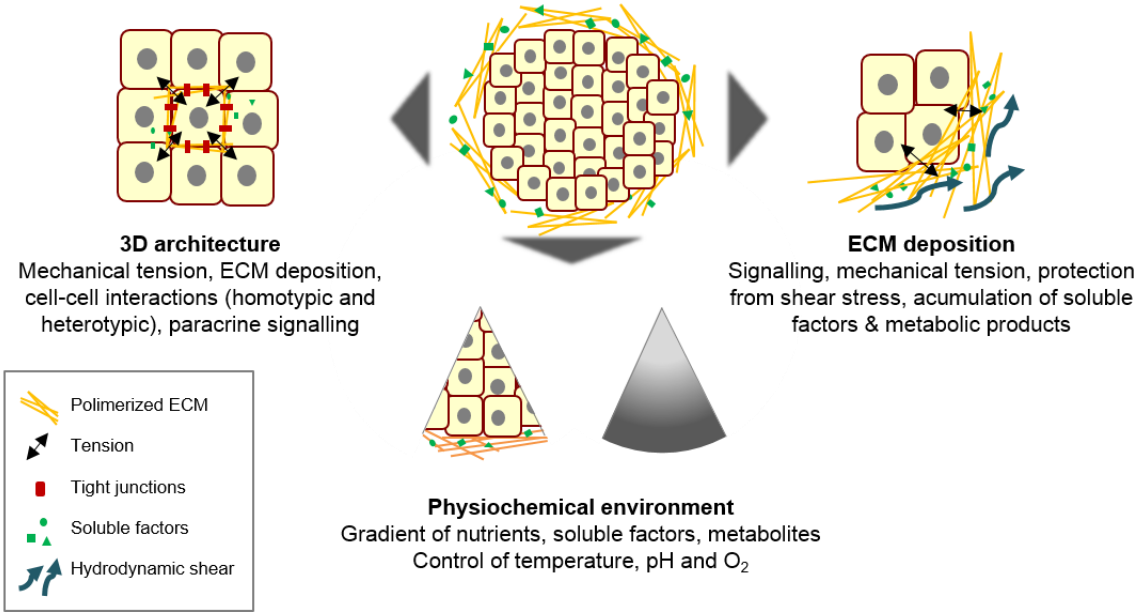

Figure 5.2 Schematic representation of the microenvironment features which have contributed to increase hepatic functionality, namely 3D architecture, ECM deposition and physiochemical environment, which were achieved by the combination of culture strategies applied (aggregation, microencapsulation, co-culture, automated BR with perfusion).

1.3 Tools to characterize human cell models

One of the major advantages of stirred-tank bioreactors is the non-destructive sampling, which allows the culture of a large volume of cells homogenously and cell monitoring along the culture period, being suitable for long-term cultures. Importantly, all the destructive/invasive endpoint characterization analytics may be performed with samples acquired along the culture while the culture is running in parallel in BR, allowing the assessment of multiple toxicological or physiological questions. In the work developed in this thesis, a panel of characterization tools was applied for spheroid characterization and hepatic performance evaluation.

Beyond routine culture sampling for monitoring cell number and viability, periodic sampling was performed for endpoint analytics including immunocytochemistry, gene expression, scanning electron microscopy and collagen quantification. This allowed the morphological characterization of the cultures with identification of the spatial distribution of the different cell types cultured. Regarding functional characterization, the analysis of activity upon induction with prototypical inducers was performed in multiwell plates, using the BR as a feeder system for multiplexed assays. Incubation with CYP450 substrates to evaluate enzyme inducibility and with ammonia to characterize ureagenesis were also performed in multiwell platforms while BR cultures were kept without exposure to external stimuli. Moreover, live imaging of efflux activity was performed immediately after sampling. Despite the possibility of using the BR as a feeder system for high throughput assays, there might be limitations on the culture of spheroids outside the BR, thus

sampling for assay development may only be suited for short-term assays (up to 48h), due to mass transfer limitations or difficulties in maintaining spheroid morphology in multiwells. This might be overcome using miniaturized systems with perfusion flow to perform assays. The culture medium collected in the BR outlet or throughout cell sampling allowed the detection of secreted albumin and urea levels and also the identification of secreted cytokines.

In addition to the characterization performed along the culture time through sampling, culture in BRs ensures a fully characterized process, by tracking oxygen uptake rate and pH fluctuations. Moreover, the controllable environmental parameters, as described above, allow the maintenance of reproducibility, which is critical for the minimization of variability of biological systems (particularly primary cultures). The rigorous and detailed process characterization, control and automation and the inherent reproducibility achieved, are critical for validation of cell models required for toxicological testing or cell-based therapeutics in the industry. In addition, novel on-line/non-invasive technologies may be coupled to BR, contributing to characterize the cultures even further in a rapid and integrated manner.

2. Final remarks

This PhD thesis contributes to the fields of hepatology, hepatic tissue engineering and toxicology by studying and developing strategies for the culture of human hepatic cell models, based on human hepatocytes and on the human derived cell line HepaRG, overcoming some of the inherent bottlenecks of these cell sources. Moreover, the characterization performed contributes to improve the knowledge on liver cell models.

Although cellular models cannot recapitulate the complexity of entire organs/organism, their easy manipulation, reproducibility, throughput and accessibility make them amenable to address particular questions through the manipulation of individual parameters. This is important for the acquisition of knowledge on the mechanisms underlying drug metabolism and toxicity, and also for understanding hepatic physiology and disease-related pathways. Its application in the drug development process is valuable for early pre-clinical development, being useful for target identification and validation and also for toxicological assessment in the later phases of pre-clinical development. Importantly, the strategies developed herein may be extended for other cell sources such as PSC.

Overall, this work improved the state-of-the art on cellular models and raised perspectives on how hepatic cultures, drug metabolism and toxicity screenings can be enhanced in the future.

3. References

Allen JW, Khetani SR, Bhatia SN. 2005. In vitro zonation and toxicity in a hepatocyte bioreactor. *Toxicol. Sci.* **84**:110–9.

Anthérieu S, Chesné C, Li R, Camus S, Lahoz A, Picazo L, Turpeinen M, Tolonen A, Uusitalo J, Guguen-Guillouzo C, Guillouzo A. 2010. Stable expression, activity, and inducibility of cytochromes P450 in differentiated HepaRG cells. *Drug Metab. Dispos.* **38**:516–525.

Bachour-El Azzi P, Sharanek A, Burban A, Li R, Le Guével R, Abdel-Razzak Z, Stieger B, Guguen-Guillouzo C, Guillouzo A. 2015. Comparative localization and functional activity of the main hepatobiliary transporters in HepaRG cells and primary human hepatocytes. *Toxicol. Sci.*

Bhogal RH, Hodson J, Bartlett DC, Weston CJ, Curbishley SM, Haughton E, Williams KT, Reynolds GM, Newsome PN, Adams DH, Afford SC. 2011. Isolation of primary human hepatocytes from normal and diseased liver tissue: a one hundred liver experience. *PLoS One* **6**:e18222.

Cerec V, Glaise D, Garnier D, Morosan S, Turlin B, Drenou B, Gripon P, Kremsdorf D, Guguen-Guillouzo C, Corlu A. 2007. Transdifferentiation of hepatocyte-like cells from the human hepatoma hepaRG cell line through bipotent progenitor. *Hepatology* **45**:957–967.

Chang TT, Hughes-Fulford M. 2009. Monolayer and spheroid culture of human liver hepatocellular carcinoma cell line cells demonstrate distinct global gene expression patterns and functional phenotypes. *Tissue Eng. Part A* **15**:559–567.

Chang TT, Hughes-Fulford M. 2014. Molecular mechanisms underlying the enhanced functions of three-dimensional hepatocyte aggregates. *Biomaterials* **35**:2162–71.

Dianat N, Dubois-Pot-Schneider H, Steichen C, Desterke C, Leclerc P, Raveux A, Combettes L, Weber A, Corlu A, Dubart-Kupperschmitt A. 2014. Generation of functional cholangiocyte-like cells from human pluripotent stem cells and HepaRG cells. *Hepatology* **60**:700–14.

Ghannam S, Bouffi C, Djouad F, Jorgensen C, Noël D. 2010. Immunosuppression by mesenchymal stem cells: mechanisms and clinical applications. *Stem Cell Res. Ther.* **1**:2.

Godoy P, Hewitt NJ, Albrecht U, Andersen ME, Ansari N, Bhattacharya S, Bode JG, Bolleyn J, Borner C, Böttger J, Braeuning A, Budinsky R a, Burkhardt B, Cameron NR, Camussi G, Cho C-S, Choi Y-J, Craig Rowlands J, Dahmen U, Damm G, Dirsch O, Donato MT, Dong J, Dooley S, Drasdo D, Eakins R, Ferreira KS, Fonsato V, Fraczek J, Gebhardt R, Gibson A, Glanemann M, Goldring CEP, Gómez-Lechón MJ, Groothuis GMM, Gustavsson L, Guyot C, Hallifax D, Hammad S, Hayward A, Häussinger D, Hellerbrand C, Hewitt P, Hoehme S, Holzhütter H-G, Houston JB, Hrach J, Ito K, Jaeschke H, Keitel V, Kelm JM, Kevin Park B, Kordes C, Kullak-Ublick G a, LeCluyse EL, Lu P, Luebke-Wheeler J, Lutz A, Maltman DJ, Matz-Soja M, McMullen P, Merfort I, Messner S, Meyer C, Mwinyi J, Naisbitt DJ, Nussler AK, Olinga P, Pampaloni F, Pi J, Pluta L, Przyborski S a, Ramachandran A, Rogiers V, Rowe C, Schelcher C, Schmich K, Schwarz M, Singh B, Stelzer EHK, Stieger B, Stöber R, Sugiyama Y, Tetta C, Thasler WE, Vanhaecke T, Vinken M, Weiss TS, Widera A, Woods CG, Xu JJ, Yarborough KM, Hengstler JG. 2013. Recent advances in 2D and 3D in vitro systems using primary hepatocytes, alternative hepatocyte sources and non-parenchymal liver cells and their use in investigating mechanisms of hepatotoxicity, cell signaling and ADME. *Arch. Toxicol.* Vol. 87 1315-530 p.

Gripon P, Rumin S, Urban S, Le Seyec J, Glaise D, Cannie I, Guyomard C, Lucas J, Trepo C, Guguen-Guillouzo C. 2002. Infection of a human hepatoma cell line by hepatitis B virus. *Proc. Natl. Acad. Sci. U. S. A.* **99**:15655–15660.

Hart SN, Li Y, Nakamoto K, Subileau E, Steen D, Zhong X. 2010. A comparison of whole genome gene expression profiles of HepaRG cells and HepG2 cells to primary human hepatocytes and human liver tissues. *Drug Metab. Dispos.* **38**:988–994.

Hewes JC, Riddy D, Morris RW, Woodrooffe AJ, Davidson BR, Fuller B. 2006. A prospective study of isolated human hepatocyte function following liver resection for colorectal liver metastases: the effects of prior exposure to chemotherapy. *J. Hepatol.* **45**:263–70.

Hoekstra R, Nibourg G a a, Van Der Hoeven T V., Ackermans MT, Hakvoort TBM, Van Gulik TM, Lamers WH, Elferink RPO, Chamuleau R a FM. 2011. The HepaRG cell line is suitable for bioartificial liver application. *Int. J. Biochem. Cell Biol.* **43**:1483–1489.

Jain E, Damania A, Kumar A. 2013. Biomaterials for liver tissue engineering. *Hepatol. Int.* **8**:185–197.

Kawahara T, Toso C, Douglas DN, Nourbakhsh M, Lewis JT, Tyrrell DL, Lund G a, Churchill T a, Kneteman NM. 2010. Factors affecting hepatocyte isolation, engraftment, and replication in an in vivo model. *Liver Transpl.* **16**:974–82.

Khetani SR, Szulgit G, Del Rio J a, Barlow C, Bhatia SN. 2004. Exploring interactions between rat hepatocytes and nonparenchymal cells using gene expression profiling. *Hepatology* **40**:545–54.

Kidambi S, Yarmush RS, Novik E, Chao P, Yarmush ML, Nahmias Y. 2009. Oxygen-mediated enhancement of primary hepatocyte metabolism, functional polarization, gene expression, and drug clearance. *Proc. Natl. Acad. Sci. U. S. A.* **106**:15714–9.

Kostadinova R, Boess F, Applegate D, Suter L, Weiser T, Singer T, Naughton B, Roth A. 2013. A long-term three dimensional liver co-culture system for improved prediction of clinically relevant drug-induced hepatotoxicity. *Toxicol. Appl. Pharmacol.* **268**:1–16.

LeCluyse EL, Witek RP, Andersen ME, Powers MJ. 2012. Organotypic liver culture models: Meeting current challenges in toxicity testing. *Crit. Rev. Toxicol.*

Lee SML, Schelcher C, Laubender RP, Fröse N, Thasler RMK, Schiergens TS, Mansmann U, Thasler WE. 2014. An algorithm that predicts the viability and the yield of human hepatocytes isolated from remnant liver pieces obtained from liver resections. *PLoS One* **9**:e107567.

Okubo H, Matsushita M, Kamachi H, Kawai T, Takahashi M, Fujimoto T, Nishikawa K, Todo S. 2002. A Novel Method for Faster Formation of Rat Liver Cell Spheroids. *Artif. Organs* **26**:497–505.

Pal R, Mamidi MK, Das AK, Bhonde R. 2012. Diverse effects of dimethyl sulfoxide (DMSO) on the differentiation potential of human embryonic stem cells. *Arch. Toxicol.* **86**:651–661.

Parent R, Marion M-J, Furio L, Trépo C, Petit M-A. 2004. Origin and characterization of a human bipotent liver progenitor cell line. *Gastroenterology* **126**:1147–56.

Tostões RM, Leite SB, Miranda JP, Sousa M, Wang DI, Carrondo MJ, Alves PM. 2011. Perfusion of 3D encapsulated hepatocytes--a synergistic effect enhancing long-term functionality in bioreactors. *Biotechnol. Bioeng.* **108**:41–49.

Tostões RM, Leite SB, Serra M, Jensen J, Bjorquist P, Carrondo MJ, Brito C, Alves PM. 2012. Human liver cell spheroids in extended perfusion bioreactor culture for repeated-dose drug testing. *Hepatology* **55**:1227–1236.